

HV 2023-45  
ISSN 2298-9137



## HAF- OG VATNARANNSÓKNIR

*MARINE AND FRESHWATER RESEARCH IN ICELAND*

Mat á ráðgjafareglum fyrir innfjarðarækjustofna  
í Arnarfirði og Ísafjarðardjúpi /

*Management strategy evaluation of harvest rates  
of the Northern shrimp *Pandalus borealis*  
in Arnarfjörður and Ísafjarðardjúp, Iceland*

*Pamela J. Woods, Bjarki Þ. Elvarsson og Ingibjörg G. Jónsdóttir*

HAFNARFJÖRÐUR – DESEMBER 2023

Mat á ráðgjafareglum fyrir innfjarðarækjustofna  
í Arnarfirði og Ísafjarðardjúpi /

*Management strategy evaluation of harvest rates  
of the Northern shrimp *Pandalus borealis*  
in Arnarfjörður and Ísafjarðardjúp, Iceland*

*Pamela J. Woods, Bjarki Þ. Elvarsson og Ingibjörg G. Jónsdóttir*



**HAFRANNSÓKNASTOFNUN**

Rannsókn- og ráðgjafarstofnun hafs og vatna

## Upplýsingablað

**Titill:** Mat á ráðgjafareglum fyrir innfjarðarækjustofna í Arnarfirði og Ísafjarðardjúpi.  
Management strategy evaluation of harvest rates of the Northern shrimp *Pandalus borealis* in Arnarfjörður and Ísafjarðardjúp, Iceland

**Höfundar:**

Pamela J. Woods, Bjarki Þ. Elvarsson, and Ingibjörg G. Jónsdóttir

**Skýrsla nr:**

HV 2023-45

**Verkefnisstjóri:**

Pamela J. Woods

**Verknúmer:**

9116

**ISSN**

2298-9137

**Fjöldi síðna:**

101

**Útgáfudagur:**

22. desember 2023

**Unnið fyrir:**

Hafrannsóknastofnun

**Dreifing:**

Opið

**Yfirlit af:**

William Butler

**Ágrip**

Ráðgjöf fyrir innfjarðarækjustofna í Arnarfirði og Ísafjarðardjúpi byggir á því að nota fast veiðihlutfall af vísitölu veiðistofns nema í þeim tillfellum þegar vísitalan mælist undir aðgerðarmörkum eru veiðar ekki heimilaðar. Afrán þorsks og ýsu hefur aukist á þessari öld og hefur vísitala veiðistofns mælist undir aðgerðarmörkum í nokkur ár sem leiddi til þess að veiðar voru ekki heimilaðar þau ár. Því var þörf á að meta hvort ráðgjafareglurnar sem notaðar eru í þessum stofnum stæðust varúðarsjónarmið og samræmdust markmiðum um hámarksafkasturs til lengri tíma litið. Í þessari skýrslu er grunnur ráðgjafar kannaður fyrir þessa stofna með aldurs-lengdarháðu hermilíkani (GADGET) sem byggir á gögnum úr stofnmælingarleiðöngrum innfjarðarækju auk aflasýna. Áhrif helstu afræningja voru einnig metin svo unnt væri að kanna áhrif þeirra í framreikningum. Breytingar á veiðihlutfalli og aðgerðarmörkum voru auk þess prófaðar til að meta bæði núverandi og önnur hugsanleg aðgerðarmörk. Niðurstöður gefa til kynna að núverandi ráðgjafaregla samræmist varúðarsjónarmiðum við núverandi afránsstöðu. Þær gefa einnig til kynna að hægt væri annaðhvort að auka veiðihlutfallið eða lækka aðgerðarmörk lítilega en þó ekki bæði í Ísafjarðardjúpi. Breytingar á núverandi ráðgjafareglum eru þó ekki taldar æskilegar vegna óvissu bæði í líkaninu og á magni afræningja. Vert er að benda á að núverandi ráðgjafareglur eru taldar uppfylla varúðarsjónarmið að því gefnu að magn afræningja aukist ekki meir en 25 %, og því nauðsynlegt að fylgjast með stöðu afræningja.

**Abstract**

*Two inshore stocks of Northern shrimp *Pandalus borealis*, one in Arnarfjörður and the other in Ísafjarðardjúp in the Westfjords region of Iceland, are currently managed using a constant harvest rate that is reduced to 0 when the survey index drops below a trigger index value. Predation by gadoids appears to have increased over the past two decades,*

*and shrimp survey index values have dropped below the trigger in several years, leading to fishery closures. This has prompted the need for an evaluation of the decision rules applied to these stocks. In this study, a management strategy evaluation was performed for both stocks using a Gadget-based operating model fitted to autumn and winter inshore shrimp survey data, as well as commercial data. Predation was included in the model, and scenarios were explored in which future predation levels were varied. A range of harvest rates and alternative index limit values were tested to evaluate current and potential harvest strategies. Results indicated that MSY-based harvest rate reference points were slightly higher than those currently implemented as target harvest rates in management. Therefore, current decision rules are sufficiently precautionary according to ICES guidelines, although either the harvest rates could be increased or the trigger index lowered slightly. Changes are not advised, however, because of high uncertainty in the model and in future predator population sizes. The current harvest rate can tolerate a 25% increase in predation levels, so predator population indices should be taken into account when providing advice.*

**Lykilorð:** stock assessment, management strategy evaluation, Northern shrimp, *Pandalus borealis*, Gadget

**Undirskrift verkefnisstjóra:**



**Undirskrift forstöðumanns sviðs:**





# Management strategy evaluation of harvest rates of the Northern shrimp *Pandalus borealis* in Arnarfjörður and Ísafjarðardjúp, Iceland

Pamela J. Woods, Bjarki Þ. Elvarsson, and Ingibjörg G. Jónsdóttir

Marine and Freshwater Research Institute, Hafnarfjörður, Iceland

## Contents

<b>1</b>	<b>Executive summaries</b>	<b>11</b>
1.1	Yfirlit á íslensku . . . . .	11
1.2	Executive Summary in English . . . . .	12
<b>2</b>	<b>Introduction</b>	<b>15</b>
<b>3</b>	<b>Methods</b>	<b>17</b>
3.1	Study systems . . . . .	17
3.2	Operating model . . . . .	17
3.3	Population dynamics in Gadget . . . . .	20
3.4	Maturation . . . . .	21
3.5	Growth . . . . .	21
3.6	Recruitment and initial abundances . . . . .	22
3.7	Fishing . . . . .	23
3.8	Predation . . . . .	23
3.9	Fitting to data . . . . .	24
3.10	Management strategy evaluation . . . . .	28
<b>4</b>	<b>Base model results</b>	<b>30</b>
<b>5</b>	<b>Parametric bootstrap results</b>	<b>45</b>
5.1	Fits to parametric bootstrap series . . . . .	45
5.2	Estimates derived from base models and parametric bootstrap uncertainty . . . . .	65
<b>6</b>	<b>Projections</b>	<b>66</b>
6.1	Estimating a stock-recruitment relationship . . . . .	72
6.2	Management procedure in forward projections . . . . .	72

<b>7</b>	<b>Management strategy evaluation results</b>	<b>75</b>
7.1	Status quo . . . . .	75
7.2	Predation scenarios . . . . .	81
7.3	Trigger value scenarios . . . . .	89
<b>8</b>	<b>Conclusions</b>	<b>100</b>
<b>9</b>	<b>Acknowledgments</b>	<b>101</b>

## List of Figures

1	Relationship between index trigger level and median harvest rates that either reflect the maximum harvest rate that can also achieve a spawning stock biomass that does not drop below a level with increased risk of recruitment impairment ( $P < 5\%$ of $SSB < B_{lim}$ ) or harvest rates that maximise yield. Five scenarios were explored where the index trigger values were set to 50%, 75%, 100%, 125%, and 150% of the current level. Vertical dashed lines show current trigger values (100%) and horizontal dashed lines indicate the median harvest rate at the 100% trigger value that achieves $P < 5\%$ of $SSB < B_{lim}$ . Green dots represent currently implemented values. . . . .	14
2	Relationship between index trigger level and median yield as a proportion of $B_{lim}$ that can also achieve a spawning stock biomass that does not drop below a level with increased risk of recruitment impairment ( $B_{loss}$ ). Relationships are depicted by base model, 5 trigger scenarios set to 50%, 75%, 100%, 125%, and 150% of the current level. Vertical dashed lines show the status quo scenario values (100% predation level). . . . .	14
3	Relationship between index trigger level and probability of 0 catches resulting from the survey index falling below the trigger. Relationships are depicted by base model, 5 trigger scenarios set to 50%, 75%, 100%, 125%, and 150% of the current level. Vertical dashed lines show the status quo scenario values (100% predation level). . . . .	15
4	Arnarfjörður (blue polygon) and Ísafjarðardjúp (red polygon) in the westfjords region of Iceland.	18
5	Time series of shrimp indices reflecting harvestable biomass and used for management by fjord.	19
6	Yellow and white alternating vertical bands demonstrate length ranges of the five survey indices used to fit the Gadget model. Years were arbitrarily chosen as examples of how length ranges line up with typical length distributions. . . . .	25
7	Results of the optimisation grid search over combinations of natural mortality ('M', x-axis) and recruitment upper bound ('up', log-scaled y-axis, in units of $1e10$ ). Colors indicate that the score value for a model optimised with a certain combination of M and up. Models with scores less than 9696 are shown with circles, the size of which are inversely related to the score, and values with stars were retained in the subset of 10 models used in the management strategy evaluation. . . . .	30
8	Total consumption estimates (biomass removals in 000s of tonnes) of shrimp in Arnarfjörður and Ísafjarðardjúp from each of the 10 best models. Each panel row corresponds with a model, labelled on the right by its implemented natural mortality value (0.27–0.33) and its recruitment upper bound (-0.54–1.25, log-scaled and in units of $1e10$ ). Predator removals are summed over all predator groups implemented. . . . .	31

9	Spawning stock biomass and recruitment estimates of shrimp in Arnarfjörður and Ísafjarðardjúp from each of the 10 best models. Each panel row corresponds with a model, labelled on the right by its implemented natural mortality value (0.27–0.33) and its recruitment upper bound (-0.54–1.25, log-scaled and in units of $1e10$ ). . . . .	32
10	Fit of the best-fit model to autumn and winter length based survey indices from the autumn and winter surveys in each area. Panel rows show indices in order of increasing length ranges moving downward. Panel columns indicate a specific survey within a given fjord. . . . .	34
11	Fit of the best-fit model to Autumn survey length distributions in Arnarfjörður. Grey lines indicate observations, black lines are predictions. . . . .	35
12	Fit of the best-fit model to Autumn survey length distributions in Ísafjarðardjúp. Grey lines indicate observations, black lines are predictions. . . . .	36
13	Fit of the best-fit model to Winter survey length distributions in Arnarfjörður. Grey lines indicate observations, black lines are predictions. . . . .	37
14	Fit of the best-fit model to Winter survey length distributions in Ísafjarðardjúp. Grey lines indicate observations, black lines are predictions. . . . .	38
15	Fit of the best-fit model to commercial length distribution samples in Arnarfjörður. Labels indicate years and quarters. Grey lines indicate observations, black lines are predictions. . . .	39
16	Fit of the best-fit model to commercial length distribution samples in Ísafjarðardjúp. Labels indicate years and quarters. Grey lines indicate observations, black lines are predictions. . . .	39
17	Fit of the best-fit model to gut content length distribution samples from predators < 45 cm (cod, haddock, and whiting). Labels indicate years and areas. Grey lines indicate observations, black lines are predictions. . . . .	40
18	Fit of the best-fit model to gut content length distribution samples from predators 45 - 75 cm (cod, haddock, and whiting). Labels indicate years and areas. Grey lines indicate observations, black lines are predictions. . . . .	41
19	Fit of the best-fit model to gut content length distribution samples from predators > 45 cm (cod and haddock). Labels indicate years and areas. Grey lines indicate observations, black lines are predictions. . . . .	42
20	Total and harvestable biomass estimates by fjord across base models represented by colors. . .	43
21	Fishing mortality and predation mortality estimates by fjord across base models represented by colors. . . . .	44
22	Recruitment estimates by fjord across base models represented by colors. . . . .	45
23	Biomass removals in the form of reported commercial catches by fjord and predation removal estimates, each with proportions estimated between mature and immature stock components, based on the best-fit model (base 1, top), or the model with the highest estimated absolute biomass levels within Arnarfjörður (base 7, bottom). . . . .	46
24	Observed survey index frequencies across years (black lines) are compared with those generated as parametric bootstrap replicates (colored lines) for each of the 10 base models (10 replicates each). . . . .	47
25	Proportions on the log scale of shrimp carapace lengths observed across years in autumn surveys compared with those generated as parametric bootstrap replicates for each base model. Actual data, which are the same across baselines, are represented by the black line (median) and yellow ribbons. Inner ribbons represent the 50th percentile range and outer edges represent the 95th percentile range. Blue lines represent the median (dashed), 50th percentile range (inner solid lines), and 95th percentile range (outer blue lines), calculated across years and the 10 replicates per base. . . . .	48

26	Proportions on the log scale of shrimp carapace lengths observed across years in winter surveys compared with those generated as parametric bootstrap replicates for each base model. Actual data, which are the same across baselines, are represented by the black line (median) and yellow ribbons. Inner ribbons represent the 50th percentile range and outer edges represent the 95th percentile range. Blue lines represent the median (dashed), 50th percentile range (inner solid lines), and 95th percentile range (outer blue lines), calculated across years and the 10 replicates per base. . . . .	49
27	Proportions on the log scale by year of shrimp carapace lengths observed in autumn surveys in Arnarfjörður compared with those generated as parametric bootstrap replicates for base model 1 only. Actual data are represented by the black line (median) and yellow ribbons. Inner ribbons represent the 50th percentile range and outer edges represent the 95th percentile range. Blue lines represent the median of parametric bootstrap replicates (dashed), 50th percentile range (inner solid lines), and 95th percentile range (outer blue lines). . . . .	50
28	Proportions on the log scale by year of shrimp carapace lengths observed in autumn surveys in Ísafjarðardjúp compared with those generated as parametric bootstrap replicates for base model 1 only. Actual data are represented by the black line and yellow ribbons. Inner ribbons represent the 50th percentile range and outer edges represent the 95th percentile range. Blue lines represent the median of parametric bootstrap replicates, 50th percentile range (inner solid lines), and 95th percentile range (outer blue lines). . . . .	51
29	Proportions on the log scale by year of shrimp carapace lengths observed in winter surveys in Arnarfjörður compared with those generated as parametric bootstrap replicates for base model 1 only. Actual data are represented by the black line and yellow ribbons. Inner ribbons represent the 50th percentile range and outer edges represent the 95th percentile range. Blue lines represent the median of parametric bootstrap replicates, 50th percentile range (inner solid lines), and 95th percentile range (outer blue lines). . . . .	52
30	Proportions on the log scale by year of shrimp carapace lengths observed in winter surveys in Ísafjarðardjúp compared with those generated as parametric bootstrap replicates for base model 1 only. Actual data are represented by the black line and yellow ribbons. Inner ribbons represent the 50th percentile range and outer edges represent the 95th percentile range. Blue lines represent the median of parametric bootstrap replicates, 50th percentile range (inner solid lines), and 95th percentile range (outer blue lines). . . . .	53
31	Fits to the parametric bootstrap survey index data replicates from the Autumn survey in Arnarfjörður. Columns correspond with survey indices and the 10 rows correspond with bases. Original data are represented by black lines and points. Original model fits are represented by the red lines. The black line is the bootstrap median and the yellow area is the 5 and 95% percentiles of the parametric bootstrapped indices. The blue solid line is the median of the predicted indices from the bootstrap runs; the blue dotted lines are the 5 and 95% percentiles. . . . .	54
32	Fits to the parametric bootstrap survey index data replicates from the Autumn survey in Ísafjarðardjúp. Columns correspond with survey indices and the 10 rows correspond bases. Original data are represented by the black lines and points. Original model fits are represented by the red lines. The black line is the bootstrap median and the yellow area is the 5 and 95% percentiles of the parametric bootstrapped indices. The blue solid line is the median of the predicted indices from the bootstrap runs; the blue dotted lines are the 5 and 95% percentiles. . . . .	55
33	Fits to the parametric bootstrap survey index data replicates from the Winter survey in Arnarfjörður. Columns corresponds with survey indices and the 10 rows correspond with bases. Original survey index data are represented by black lines and points. Original model fits are represented by the red lines. The black line is the bootstrap median and the yellow area is the 5 and 95% percentiles of the parametric bootstrapped indices. The blue solid line is the median of the predicted indices from the bootstrap runs; the blue dotted lines are the 5 and 95% percentiles. . . . .	56

34	Fits to the parametric bootstrap survey index data replicates from the Winter survey in Ísafjarðardjúp. Columns correspond with survey indices and the 10 rows correspond with bases. Original survey index data are represented by the black lines and points. Original model fits to these data are represented by red lines. The black line is the bootstrap median and the yellow area is the 5 and 95% percentiles of the parametric bootstrapped indices. The blue solid line is the median of the predicted indices from the bootstrap runs; the blue dotted lines are the 5 and 95% percentiles. . . . .	57
35	Example of a fit to a parametric bootstrap generated length distribution from the Autumn survey samples compared with model estimates to the parametric bootstrap data (from 2017, step 4, base model 1). Green points and vertical bars denote the median and 95% interval of the parametric bootstrap distribution of observed values, while the solid lines and golden ribbon the median and 95% intervals of the predictions by the model after fitting to the bootstrapped data. The black line with points indicates the original data and the solid red line indicates the fit to these data from the baseline model. . . . .	58
36	Histogram of parameter estimates from 100 bootstrap samples. The red line indicates the estimates from the base runs. The $\beta_0$ and $\beta_1$ originate from the beta-binomial distributions reflecting growth of immature (s=0) or mature (s=1) shrimp, whereas $\beta_b$ and $\beta_s$ indicate coefficients controlling growth rate in immature shrimp related to bottom (b) or surface (s) water temperatures. Subscripts 1 and 2 reflect $r = \text{Arnarfjörður}$ and $r = \text{Ísafjarðardjúp}$ , in area $r$ -specific parameters such as $\lambda$ (which controls steepness of the logistic maturation function), intercept of immature growth rate ( $\alpha_k$ ), initial length at recruitment $l_0$ , and catchability of shrimp by predators $q_{pred}$ . For logistic suitability parameters $b$ and $l_{50}$ , where subscripts indicate either selectivity of the survey and commercial fleets ( $f$ ), all predators (cod, haddock, and whiting) above 45 cm ( $h = 45$ ), or all predators above 75 cm ( $h = 75$ ). Constant suitability estimated for predators below 45 cm length was represented by $c_0$ . . . . .	59
37	Histogram of $l_{50}$ annual maturity parameter estimates from 100 bootstrap samples. Parameters are labeled by area and year . . . . .	60
38	Boxplots of annual recruitment (age 0) bootstrap estimates, the red line indicates the estimate from the base run. . . . .	61
39	Boxplots of initial age structure bootstrap estimates, the red line indicates the estimate from the base run. . . . .	62
40	Boxplot of estimated catchability parameters from the autumn survey, $q_g$ , as a function of the survey index length group. . . . .	63
41	Boxplot of estimated catchability parameters from the winter survey, $q_g$ , as a function of the survey index length group. . . . .	64
42	Estimates of growth from parametric bootstrap replicates. Medians are represented by the black lines and 95th percentile ranges are represented by blue (Arnarfjörður) or yellow (Ísafjarðardjúp) ribbons. . . . .	65
43	Estimates of selectivity across all fleets from parametric bootstrap replicates. Medians are represented by the black lines and 95th percentile ranges are represented by yellow ribbons. . . . .	66
44	Bootstrap model total biomass results. Colors represent the 10 base models. Each set of solid, dashed, and dotted colored lines represents the median, 50, and 95% intervals of the bootstrapped estimates for a certain base model, as derived from 10 replicates per base model. The solid black lines indicate fits from the 10 base models. . . . .	67
45	Bootstrap model harvestable biomass results. Colors represent the 10 base models. Each set of solid, dashed, and dotted colored lines represents the median, 50, and 95% intervals of the bootstrapped estimates for a certain base model, as derived from 10 replicates per base model. The solid black lines indicate fits from the 10 base models. . . . .	68

46	Bootstrap model recruitment results. Colors represent the 10 base models. Each set of solid, dashed, and dotted colored lines represents the median, 50, and 95% intervals of the bootstrapped estimates for a certain base model, as derived from 10 replicates per base model. The solid black lines indicate fits from the 10 base models. . . . .	69
47	Bootstrap model fishing mortality (F) results. Colors represent the 10 base models. Each set of solid, dashed, and dotted colored lines represents the median, 50, and 95% intervals of the bootstrapped estimates for a certain base model, as derived from 10 replicates per base model. The solid black lines indicate fits from the 10 base models. . . . .	70
48	Bootstrap model predation mortality results. Colors represent the 10 base models. Each set of solid, dashed, and dotted colored lines represents the median, 50, and 95% intervals of the bootstrapped estimates for a certain base model, as derived from 10 replicates per base model. The solid black lines indicate fits from the 10 base models. . . . .	71
49	Spawning stock biomass (SSB) and recruitment relationship. Uncertainty in recruitment and SSB is indicated with 95% quantile intervals. Error bars missing from points range beyond the limits of the figure. The yellow vertical bar represents the 95% inter-quantile range of $B_{loss}$ . All quantiles are calculated across all 10 replicates x 10 base model run. $B_{loss}$ values do not match annual estimates exactly as the medians of minimum SSB levels over several years are used to calculate $B_{loss}$ , whereas medians are calculated within years to indicate SSB levels. . . . .	73
50	Equilibrium catch curves of Northern shrimp in Arnarfjörður and Ísafjarðardjúp according to 10 base models, shown as a function of $H$ , under status quo predation and without the survey index limit implemented. The black solid curves indicate the median projected catch and the shaded yellow regions the 25% – 75% and 5% – 95% ranges. Vertical lines indicate the harvest rate generating the greatest yield in the long term. In this case, these harvest rates caused the annual probability of SSB dropping below $B_{lim}$ to exceed 5%, and cannot be used to reflect $H_{msy}$ according to ICES guidelines. . . . .	76
51	Equilibrium catch curves of Northern shrimp in Arnarfjörður and Ísafjarðardjúp across the 10 base models, shown as a function of $H$ , under status quo predation and with the fishery closing below the implemented survey index limit. The black solid curves indicate the median projected catch and the shaded yellow regions the 25% – 75% and 5% – 95% ranges. Vertical lines indicate the harvest rate generating the greatest yield in the long term. In this case, these harvest rates caused the annual probability of SSB dropping below $B_{lim}$ to exceed 5%, and cannot be used to reflect $H_{msy}$ according to ICES guidelines. . . . .	77
52	Equilibrium spawning stock biomass curves of Northern shrimp in Arnarfjörður and Ísafjarðardjúp according to 10 base models, shown as a function of $H$ , under status quo predation and with the fishery closing below the implemented survey index limit. The black solid curves indicate the median projected harvestable biomass and the shaded yellow regions the 25% – 75%, 15% – 85%, and 5% – 95% ranges. $B_{lim}$ is shown by the red solid horizontal line, set as minimum spawning stock biomass level observed since 1989, and set to as $B_{loss}$ in the hockey stick recruitment function. The solid red vertical lines indicate harvest rates producing maximum yield in the long term. The dashed red vertical lines indicate the harvest rates below which the population dropped below $B_{lim}$ over 5% of the time annually, and are used to define $H_{msy}$ according to ICES guidelines. . . . .	78
53	Results of harvestable biomass levels from a single simulation used as an example from each of the 10 base models (indicated by color) under status quo predation. Harvest rate is indicated by $H$ . All colors overlap during the base model years (< 2020), but uncertainty implemented in recruitment and management procedures causes variability in future years. All simulations show slight population growth under no fishing ( $H = 0$ ) versus a rapid decrease under high fishing rates. . . . .	79

54	Results of catch (solid) and predation (dashed) levels from a single simulation used as an example from each of the 10 base models (indicated by color) under status quo predation. Note that predation levels scale with biomass levels across base models in Arnarfjörður. Harvest rate is indicated by $H$ . All colors overlap during the base model years ( $< 2020$ ), but uncertainty implemented in recruitment and management procedures causes variability in future years. All simulations show high catch at intermediate harvest rates versus a rapid decrease under high fishing rates. . . . .	80
55	Equilibrium catch curves of Northern shrimp in Arnarfjörður and Ísafjarðardjúp according to 10 base models, shown as a function of $H$ , under 25% current predation levels and with the fishery closing below the implemented survey index limit. The black solid curves indicate the median projected catch and the shaded yellow regions the 25% – 75% and 5% – 95% ranges. Vertical lines indicate the harvest rate generating the greatest yield in the long term. In Arnarfjörður, these harvest rates caused the annual probability of SSB dropping below $B_{lim}$ to exceed 5%, and cannot be used to reflect $H_{msy}$ according to ICES guidelines. . . . .	81
56	Equilibrium spawning stock biomass curves of Northern shrimp in Arnarfjörður and Ísafjarðardjúp across 10 base models, shown as a function of $H$ , under 25% current predation levels and with the fishery closing below the implemented survey index limit. The black solid curves indicate the median projected harvestable biomass and the shaded yellow regions the 25% – 75%, 15% – 85%, and 5% – 95% ranges. $B_{lim}$ is shown by the red solid horizontal line, set as minimum spawning stock biomass level observed since 1989, and set to as $B_{loss}$ in the hockey stick recruitment function. The dashed red vertical lines indicate the harvest rates below which the population dropped below $B_{lim}$ over 5% of the time, and the solid red vertical lines indicate the harvest rates that generate maximum yield. Therefore, $H_{msy}$ is represented by the red dashed line for Arnarfjörður and the red solid line for Ísafjarðardjúp. .	82
57	Results of harvestable biomass levels from a single simulation used as an example from each of the 10 base models (indicated by color) under 25% current predation levels and with the fishery closing below the implemented survey index limit. Harvest rate is indicated by $H$ . All colors overlap during the base model years ( $< 2020$ ), but uncertainty implemented in recruitment and management procedures causes variability in future years. All simulations show slight population growth under no fishing ( $H = 0$ ) versus a rapid decrease under high fishing rates.	83
58	Results of catch (solid) and predation (dashed) levels from a single simulation used as an example from each of the 10 base models (indicated by color) under 25% current predation levels and with the fishery closing below the implemented survey index limit. Harvest rate is indicated by $H$ . Note that predation levels scale with biomass levels across base models. All colors overlap during the base model years, but uncertainty implemented in recruitment and management procedures causes variability in future years. All simulations show high catch at intermediate harvest rates versus a rapid decrease under high fishing rates. . . . .	84
59	Equilibrium catch curves of Northern shrimp in Arnarfjörður and Ísafjarðardjúp across 10 base models, shown as a function of $H$ , under 125% current predation levels and with the fishery closing below the implemented survey index limit. The black solid curves indicate the median projected catch and the shaded yellow regions the 25% – 75% and 5% – 95% ranges. Vertical lines indicate the harvest rate generating the greatest yield in the long term. In this case, these harvest rates caused the annual probability of SSB dropping below $B_{lim}$ to exceed 5%, and cannot be used to reflect $H_{msy}$ according to ICES guidelines. . . . .	85

60	Equilibrium spawning stock biomass curves of Northern shrimp in Arnarfjörður and Ísafjarðardjúp across 10 base models, shown as a function of $H$ , under 125% current predation levels and with the fishery closing below the implemented survey index limit. The black solid curves indicate the median projected harvestable biomass and the shaded yellow regions the 25% – 75%, 15% – 85%, and 5% – 95% ranges. $B_{lim}$ is shown by the red solid horizontal line, set as minimum spawning stock biomass level observed since 1989, and set to as $B_{loss}$ in the hockey stick recruitment function. The solid red vertical lines indicate harvest rates producing maximum yield in the long term. The dashed red vertical lines indicate the harvest rates below which the population dropped below $B_{lim}$ over 5% of the time annually, and are used to define $H_{msy}$ according to ICES guidelines. . . . .	86
61	Results of harvestable biomass levels from a single simulation used as an example from each of the 10 base models (indicated by color) under 125% current predation levels. Harvest rate is indicated by $H$ . All colors overlap during the base model years, but uncertainty implemented in recruitment and management procedures causes variability in future years. All simulations show slight population growth under no fishing ( $H = 0$ ) versus a rapid decrease under high fishing rates. . . . .	87
62	Results of catch (solid) and predation (dashed) levels from a single simulation used as an example from each of the 10 base models (indicated by color) under 125% current predation levels. Note that predation levels scale with biomass levels across base models. Harvest rate is indicated by $H$ . All colors overlap during the base model years, but uncertainty implemented in recruitment and management procedures causes variability in future years. All simulations show high catch at intermediate harvest rates versus a rapid decrease under high fishing rates. . . . .	88
63	Relationship between predation level and median of the maximum harvest rate that can also achieve a spawning stock biomass that does not drop below a level with increased risk of recruitment impairment ( $B_{lim}$ ). Relationships are depicted across base models, across 5 future predation scenarios: 25%, 50%, 75%, 100%, and 125% of the mean level experienced during the last three years of data. Vertical dashed lines show the status quo scenario values (100% predation level), and horizontal dashed lines indicate the median harvest rate at the 100% trigger value that achieves $P < 5\%$ of $SSB < B_{lim}$ . Green dots represent currently implemented values. . . . .	89
64	Equilibrium catch curves of Northern shrimp in Arnarfjörður and Ísafjarðardjúp across 10 base models, shown as a function of $H$ , under status quo predation and with the fishery closing below the implemented survey index limit. The index trigger is set at 75% of the current level. The black solid curve indicates the median projected catch and the shaded yellow regions the 25% – 75% and 5% – 95% ranges. Vertical lines indicate the harvest rate generating the greatest yield in the long term. In this case, these harvest rates caused the annual probability of $SSB$ dropping below $B_{lim}$ to exceed 5%, and cannot be used to reflect $H_{msy}$ according to ICES guidelines. . . . .	90
65	Equilibrium spawning stock biomass curves of Northern shrimp in Arnarfjörður and Ísafjarðardjúp according to 10 base models, shown as a function of $H$ , under status quo predation and with the fishery closing below the implemented survey index limit. The index trigger is set at 75% of the current level. The black solid curves indicate the median projected harvestable biomass and the shaded yellow regions the 25% – 75%, 15% – 85%, and 5% – 95% ranges. $B_{lim}$ is shown by the red solid horizontal line, set as minimum spawning stock biomass level observed since 1989, and set to as $B_{loss}$ in the hockey stick recruitment function. The solid red vertical lines indicate harvest rates producing maximum yield in the long term. The dashed red vertical lines indicate the harvest rates below which the population dropped below $B_{lim}$ over 5% of the time annually. In this case, these harvest rates caused the annual probability of $SSB$ dropping below $B_{lim}$ to exceed 5%, and cannot be used to reflect $H_{msy}$ according to ICES guidelines. . . . .	91



66	Results of harvestable biomass levels from a single simulation used as an example from each of the 10 base models (indicated by color) under status quo predation. Harvest rate is indicated by $H$ . All colors overlap during the base model years, but uncertainty implemented in recruitment and management procedures causes variability in future years. The index trigger is set at 75% of the current level. All simulations show slight population growth under no fishing ( $H = 0$ ) versus a rapid decrease under high fishing rates. . . . .	92
67	Results of catch (solid) and predation (dashed) levels from a single simulation used as an example from each of the 10 base models (indicated by color) under status quo predation. Harvest rate is indicated by $H$ . Note that predation levels scale with biomass levels across base models. The index trigger is set at 75% of the current level. All colors overlap during the base model years, but uncertainty implemented in recruitment and management procedures causes variability in future years. All simulations show high catch at intermediate harvest rates versus a rapid decrease under high fishing rates. . . . .	93
68	Equilibrium catch curves of Northern shrimp in Arnarfjörður and Ísafjarðardjúp according to 10 base models, shown as a function of $H$ , under status quo predation and with the fishery closing below the implemented survey index limit. The index trigger is set at 125% of the current level. The black solid curves indicate the median projected catch and the shaded yellow regions the 25% – 75% and 5% – 95% ranges. Vertical lines indicate the harvest rate generating the greatest yield in the long term. For Arnarfjörður, these harvest rates caused the annual probability of SSB dropping below $B_{lim}$ to exceed 5%, and cannot be used to reflect $H_{msy}$ according to ICES guidelines. . . . .	94
69	Equilibrium spawning stock biomass curves of Northern shrimp in Arnarfjörður and Ísafjarðardjúp according to 10 base models, shown as a function of $H$ , under status quo predation and with the fishery closing below the implemented survey index limit. The index trigger is set at 125% of the current level. The black solid curves indicate the median projected harvestable biomass and the shaded yellow regions the 25% – 75%, 15% – 85%, and 5% – 95% ranges. $B_{lim}$ is shown by the red solid horizontal line, set as minimum spawning stock biomass level observed since 1989, and set to as $B_{loss}$ in the hockey stick recruitment function. The solid red vertical lines indicate harvest rates producing maximum yield in the long term. The dashed red vertical lines indicate the harvest rates below which the population dropped below $B_{lim}$ over 5% of the time, and the solid red vertical lines indicate the harvest rates that generate maximum yield. Therefore, $H_{msy}$ is represented by the red dashed line for Arnarfjörður and the red solid line for Ísafjarðardjúp. . . . .	95
70	Results of harvestable biomass levels from a single simulation used as an example from each of the 10 base models (indicated by color) under status quo predation. Harvest rate is indicated by $H$ . All colors overlap during the base model years, but uncertainty implemented in recruitment and management procedures causes variability in future years. The index trigger is set at 125% of the current level. All simulations show slight population growth under no fishing ( $H = 0$ ) versus a rapid decrease under high fishing rates. . . . .	96
71	Results of catch (solid) and predation (dashed) levels from a single simulation used as an example from each of the 10 base models (indicated by color) under status quo predation. Harvest rate is indicated by $H$ . Note that predation levels scale with biomass levels across base models. The index trigger is set at 125% of the current level. All colors overlap during the base model years, but uncertainty implemented in recruitment and management procedures causes variability in future years. All simulations show high catch at intermediate harvest rates versus a rapid decrease under high fishing rates. . . . .	97

72	Relationship between index trigger level and median harvest rates that either reflect the maximum harvest rate that can also achieve a spawning stock biomass that does not drop below a level with increased risk of recruitment impairment ( $P < 5\%$ of $SSB < B_{lim}$ ) or harvest rates that maximise yield. Five scenarios were explored where the index trigger values were set to 50%, 75%, 100%, 125%, and 150% of the current level. Vertical dashed lines show current trigger values (100%) and horizontal dashed lines indicate the median harvest rate at the 100% trigger value that achieves $P < 5\%$ of $SSB < B_{lim}$ . Green dots represent currently implemented values. . . . .	98
73	Relationship between index trigger level and median harvest rates that reflect the maximum harvest rate that can also achieve a spawning stock biomass that does not drop below a level with increased risk of recruitment impairment ( $B_{loss}$ ). Relationships are depicted by base model, 5 trigger scenarios set to 50%, 75%, 100%, 125%, and 150% of the current level. Vertical dashed lines show the status quo scenario values (100% predation level). Green dots represent currently implemented values. . . . .	99
74	Relationship between index trigger level and probability of 0 catches resulting from the survey index falling below the trigger. Relationships are depicted by base model, 5 trigger scenarios set to 50%, 75%, 100%, 125%, and 150% of the current level. Vertical dashed lines show the status quo scenario values (100% predation level). Green dots represent currently implemented values. . . . .	100

# 1 Executive summaries

## 1.1 Yfirlit á íslensku

**Inngangur:** Varúðarnálgun hefur verið beitt við ráðgjöf rækju í Arnarfirði og Ísafjarðardjúpi. Ráðgjöfin byggir á því að nota fast veiðihlutfall af vísitölu veiðistofns nema í þeim tilfellum sem vísitalan er undir skilgreindum aðgerðarmörkum. Í þeim tilfellum eru veiðar ekki heimilaðar. Veiðihlutfallið var ákvarðað út frá sögulegum aflagögnum frá því tímabili þar sem afrán á rækju var lítið og veiðar virtust ekki hafa mikil áhrif á vísitölu veiðistofns. Hins vegar þá hefur afrán þorsks og ýsu aukist og á þessari öld hefur vísitala veiðistofns nokkrum sinnum verið undir aðgerðarmörkum sem leiddi til þess að veiðar voru ekki heimilaðar. Þörf er því að meta ráðgjafareglurnar sem notaðar eru í þessum stofnum.

**Aðferðir:** Í þessari skýrslu er farið yfir grunn ráðgjafar fyrir þessa tvo rækjustofna með aldurs-lengdarháðu líkani (GADGET) sem tekur tillit til helstu afræningja. Notuð voru gögn úr stofnmælingu rækju að hausti en farið hefur verið í stofnmælingu rækju á hverju ári frá árinu 1988. Einnig voru notuð gögn úr stofnmælingu rækju í febrúar, en sú mæling fór fram árlega til ársins 2004 en síðan þá hefur aðeins verið farið nokkrum sinnum, og að lokum voru notaðar lengdarmælingar úr afla rækjubáta. Afránsþáttur var tekinn inn í líkanið en hann byggðist á vísitölu afræningja (þorsks, ýsu og lýsu) í stofnmælingu rækju að hausti. Metin voru áhrif afræningja miðað við 25%, 50%, 75%, 100% og 125% af meðallífmassa þeirra síðustu þriggja ára. Mismunandi hlutfall (50%, 75%, 100%, 125% og 150%) af núverandi aðgerðarmörkum var prófað til að meta bæði núverandi og önnur hugsanleg aðgerðarmörk. Sérstaklega var horft til 75% af núverandi gildi þar sem að í leiðbeiningum Norðvestur Atlantshafs fiskveiðistofnunarinnar (NAFO) frá árinu 2004 segir að ef ekki er hægt að byggja ráðgjöf á tölfræðilegu stofnmati og hægt að túlka hæsta gildi vísitölu sem ígildi hámarksstofnstærðar, skuli miða við 15% því gildi (04/12 2004). Að auki voru skoðuð áhrif mismunandi afráns á veiðihlutfall. Fylgt var leiðbeiningum Alþjóðahafrannsóknaráðsins (ICES) fyrir ráðgjöf og stofnmat fyrir stofna þar sem gögn eru rýr og fyrir tegundir með stuttan lífsferil (ICES [8]). Einnig var stuðst við leiðbeiningar Alþjóðahafrannsóknaráðsins fyrir stofna þar sem tölfræðilegt stofnmat er til að setja varúðar- og gátmörk. Þar á meðal voru varúðarmörk ( $B_{lim}$ ), sú stærð þar sem ef hrygningarstofn mælist undir henni má vænta skertrar nýliðunar, og kjörsókn ( $HR_{MSY}$ ), sem er það veiðihlutfall sem leiðir til hámarksafkasturs (ICES [7]).

**Veiðihlutfall ( $H_{proxy,msy}$ ):** Til að uppfylla skilyrði Alþjóðahafrannsóknaráðsins um að veiðihlutfall myndi leiða til minna en 5% líkum á að hrygningarstofn fari undir Blim þá mætti veiðihlutfallið ekki vera hærra en 0,6 miðað við núverandi aðgerðarmörk (604) í Ísafjarðardjúpi og 0,42 (núverandi aðgerðarmörk 390) í Arnarfirði. Þetta er aðeins hærra en núverandi veiðihlutfall (0,5 í Ísafjarðardjúpi og 0,346 í Arnarfirði) og því er núverandi veiðihlutfall í samræmi við varúðarsjónamið samkvæmt leiðbeiningum Alþjóðahafrannsóknaráðsins. Afránsforsendur hafa hins vegar umtalsverð áhrif á þessar niðurstöður. Ef lífmassi afræningja myndi minnka eða aukast um 25% til lengri tíma þá myndi það hafa talsverð áhrif á niðurstöðurnar. Kjörsókn yrði metin við 0,5 ef lífmassi afræningja myndi aukast í Ísafjarðardjúpi en 0,76 ef hann minnkar. Í Arnarfirði myndi kjörsókn sveiflast frá 0,24 í 0,6.

**Aðgerðarmörk ( $I_{trigger}$ ):** Sé aðgerðarmörkum ráðgjafareglanna breytt (50%, 75%, 100%, 125% og 150% af núverandi gildi) eru áhrifin mismunandi milli stofnanna tveggja. Í Arnarfirði eru áhrifin óveruleg og höfðu ekki teljandi áhrif á mat á kjörsókn. Í Ísafjarðardjúpi hinsvegar, væru áhrifin meiri. Væru aðgerðarmörkin færð niður lækkar mat á kjörsókn vegna varúðarsjónarmiða þar sem lækkingun aðgerðarmarkna myndi auka líkurnar á því að stofninn færi niður fyrir varúðarmörk. Væru aðgerðarmörkin hækkuð hins vegar mætti hækka veiðihlutfallið en væntur heildaraffi myndi lækka vegna þess að veiðar væru oftar stöðvaðar í Djúpinu.

Það er því lítið sem réttlætir breytingar á aðgerðarmörkum í núverandi ráðgjafareglunum þar sem affi myndi vera mjög svipaður miðað við þau aðgerðarmörk sem voru prófuð, nema að væntur affi myndi lækka við hærri aðgerðarmörk í Ísafjarðardjúpi. Breyting á aðgerðarmörkum hafði ekki mikil áhrif á niðurstöðurnar í Arnarfirði. Í Ísafjarðardjúpi væri möguleiki að lækka aðgerðarmörk (miðað við 75% af núverandi gildi) en halda sama veiðihlutfalli. Þessi breyting myndi ekki fela í sér breytingar í afla en myndi leiða til þess að líklegra væri að rækjuveiðar yrðu heimilari þar sem líklegra væri að vísitala veiðistofns væri yfir aðgerðarmörkum. Nauðsynlegt er þó að taka þessum niðurstöðum með fyrirvara. Í fyrsta lagi er töluverð óvissa í líkaninu. Ekki

er hægt að ákvarða aldur rækju, náttúrulegur dauði er ekki þekktur og er líklega hár, vöxtur er breytilegur og tengdur umhverfinu, og breytileiki í vísitölum er mikill. Í öðru lagi er ekki tekið tillit til tengsla þessara stofna við úthafs rækju, en þau tengsl eru ekki þekkt, né er tekið tillit til hækkandi afla á sóknareiningu (vegna þéttingar rækju innst á svæðunum) þrátt fyrir lækkingu vísitölu. Í þriðja lagi er líkurnar á því að vísitalan falli niður fyrir aðgerðamörk vegna mæliskekkju illa metnar, og byggir nú á einföldum. Að lokum var notað tvílinulegt samband milli hrygningarstofns og nýliðunar en í þess konar líkani er nýliðun lækkuð línulega þegar hrygningarstofn fer undir gátmörk ( $B_{lim}$ ). Blim var valið sem lægsta gildi á tímabili sem var talið áreiðanlegast. Vísitalan hefur lækkað mikið í Ísafjarðardjúpi og nýliðun hefur verið mjög lítil síðustu 5 ár. Ef nýliðun helst lág á næstu árum þá gæti þurft að endurskoða  $B_{lim}$ .

## 1.2 Executive Summary in English

**Introduction:** Two inshore stocks of Northern shrimp *Pandalus borealis*, one found in Arnarfjörður and the other in Ísafjarðardjúp in the Westfjords region of Iceland, are currently managed using a constant harvest rate that is reduced to 0 when the survey index drops below a trigger index value. Harvest rates were set in the past based on historical patterns of harvest rates that led to generally stable survey index patterns, as 20% of the average of the highest 3 index values. However, predation by gadoids in these fjords appears to have increased, and in several years over the past 2 decades, survey index values have dropped below the trigger, leading to 0 advised catches and fishery closures. This situation has prompted the need for an evaluation of the decision rule applied to these stocks.

**Methods:** In this study, a management strategy evaluation was performed for both stocks using a Gadget-based operating model fitted to autumn and winter inshore shrimp survey data, as well as commercial data. The model also included an effect of predation that scaled with the indices of predators calculated from the autumn shrimp surveys. Predation was included in the model, and scenarios were explored in which future predation levels were varied to be 25 %, 50%, 75%, 100%, or 125% mean levels observed over the last 3 years of the model. A range of harvest rates and 50%, 75%, 100%, 125% and 150% of the current index limit values were tested to evaluate current and potential harvest strategies. In particular, 75% of the index limit was chosen as an alternative to the current index limit as this value corresponds with NAFO guidelines that indicate setting trigger index values as 15% of the mean of the highest 3 index values would be a sufficient strategy (04/12 [1]). In addition, a range of predation levels were tested to explore the effect of predation levels on sustainable harvest levels. This evaluation followed ICES technical guidance for decision rules and stock assessments for stocks in categories 2 and 3 (ICES [8]), Method 3.2 for short-lived stocks (2022 [2] and 2022 [3]). ICES technical guidance for category 1 stocks were also used for guidance in setting reference points. These reference points included  $B_{lim}$  values, levels below which recruitment impairment could be expected, and  $H_{msy}$  values, which are considered maximal options for a target harvest rate (ICES [7]).

**Harvest rates ( $H_{proxy,msy}$ ):** Results indicate that in order to fulfill ICES criteria that a target harvest rate should maximize yield while maintaining less than a 5% annual probability of spawning stock biomass (SSB) falling below a level that could exhibit recruitment impairment ( $B_{lim}$ ), the target harvest rate should not exceed 0.6 with the current survey index limit implemented (604) in Ísafjarðardjúp, and the target harvest rate should not exceed 0.42 with the current survey index limit implemented (390) in Arnarfjörður. These harvest rate values are slightly higher than the currently implemented harvest rates (0.5 for Ísafjarðardjúp and 0.346 for Arnarfjörður), indicating that the currently implemented decision rules are sufficiently precautionary according to ICES guidelines.

Predation levels had an effect on harvest rates that meet this criterion, which limited definition of  $H_{msy}$  according to ICES guidelines in all predation scenarios. With the current survey index limits implemented, a decrease in predation by 25% versus an increase in predation by 25% led to harvest rates in Ísafjarðardjúp of 0.76 versus 0.5. A 25% decrease versus increase in predation in Arnarfjörður led to harvest rates of 0.6 versus 0.24 (Figure 1).

**Trigger reference points ( $I_{trigger}$ ):** In scenarios involving changes in trigger values, similar harvest rates that would satisfy ICES guidelines for defining  $H_{msy}$  were generated at a wide variety of trigger values for Arnarfjörður. However, lower harvest rates were needed for both lower and higher survey index limits

implemented in Ísafjarðardjúp. This difference is partly due to the pattern that in Arnarfjörður, harvest rates were limited by the requirement that the probability of spawning stock biomass falling below  $B_{lim}$  should not exceed 5% across all tested values of the survey trigger. That is, median values along the red line in Figure 1 were always lower than those along the blue line for Arnarfjörður. As a result, both a 25% decrease and 25% increase in trigger values for Arnarfjörður would lead to the same approximate harvest rate of 0.42 and 0.42 (Figure 1). In Ísafjarðardjúp however, this probability only limits the harvest rate at trigger values lower than that currently set (red line is lower than blue line in Figure 1). When trigger values are implemented at a higher value, the resulting increase in the frequency of 0 catches, due to an increase in the frequency of survey indices falling below the trigger, causes an overall reduction in median yield (Figure 2). As a result, harvest rates generating maximum sustainable yield decrease, as decreased harvest rates will lead to higher survey indices and a lower probability of the survey trigger being crossed. Lower harvest rates therefore maximise yield under these conditions, but mainly as a function of the trigger itself (by avoiding 0 catches), as the frequency 0 catches increases very quickly for Ísafjarðardjúp when higher trigger values are implemented (Figure 3). As a result, the median yield resulting from harvest rates under a 25% reduction versus a 25% increase in the survey index trigger would lead again to the same  $H_{msy}$  in Ísafjarðardjúp, of 0.51.

In both locations, there is little justification for suggesting a change in harvest rates, as there is little change in yield among harvest rates chosen in this range of potential trigger values, except a downward trend at higher trigger values for Ísafjarðardjúp (Figure 2). Uncertainty is also high in this modeling framework. Changing trigger values had little impact on results for Arnarfjörður, but for Ísafjarðardjúp, an alternative decision rule to the current one could be to maintain the current harvest rate but set the trigger value to 75% of the current level. This alternative is expected to have similar results to the current decision rule but with a lower probability of catches being set to 0 due to the survey index falling below the index limit.

Results from this study should be taken with a series of caveats. First, this management strategy evaluation is based on results of a highly uncertain operating model. As is often the case with invertebrate stocks, no age data are available for these stocks, natural mortality is unknown but may be high, growth can be variable and related to environmental factors, and survey indices are highly variable. Second, the model does not take into account either connections with offshore shrimp populations (which are unclear) or a potential increase in catchability with population decline due to aggregation (MFRI [19]). Third, results regarding probability of the survey index falling below the index limit will be dependent on assumed assessment uncertainty, which in this case is not well understood. Finally, in performing forward simulations, a hockey-stick recruitment function was used to simulate recruitment based on spawning stock biomass levels. In the hockey-stick model, recruitment was reduced when spawning stock biomass dropped below a certain level ( $B_{lim}$ ), at a rate proportionate to the ratio of spawning stock biomass to  $B_{lim}$ . For both stocks,  $B_{lim}$  was chosen to be the minimum spawning stock biomass levels estimated to have occurred historically within a period representing the most reliable period of the model time series. As Ísafjarðardjúp has experienced a large historical decline, and the past 5 years of recruitment estimates have been rather low, the choice of  $B_{lim}$  may need to be revisited if a pattern of decreasing recruitment levels continues into the future.

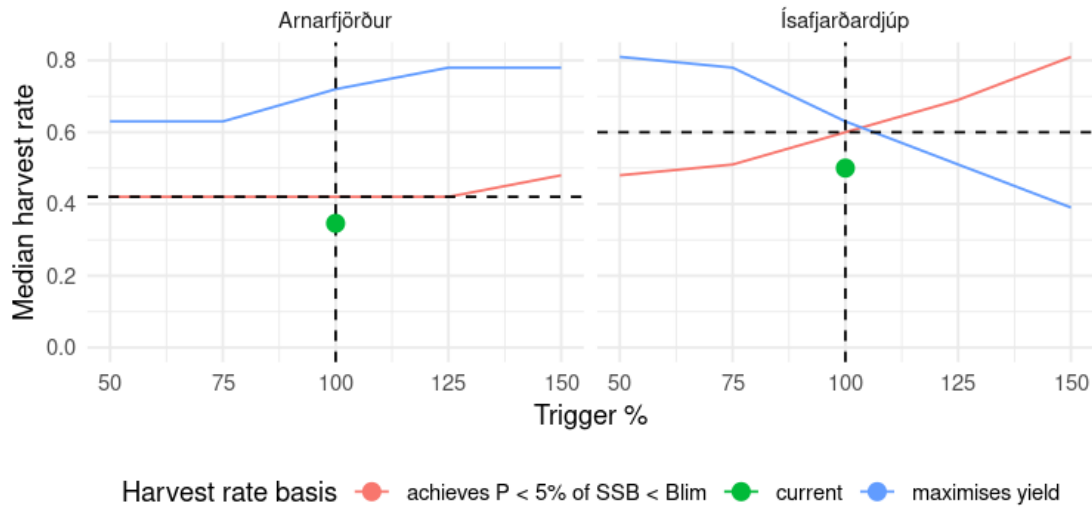


Figure 1: Relationship between index trigger level and median harvest rates that either reflect the maximum harvest rate that can also achieve a spawning stock biomass that does not drop below a level with increased risk of recruitment impairment ( $P < 5\%$  of  $SSB < B_{lim}$ ) or harvest rates that maximise yield. Five scenarios were explored where the index trigger values were set to 50%, 75%, 100%, 125%, and 150% of the current level. Vertical dashed lines show current trigger values (100%) and horizontal dashed lines indicate the median harvest rate at the 100% trigger value that achieves  $P < 5\%$  of  $SSB < B_{lim}$ . Green dots represent currently implemented values.

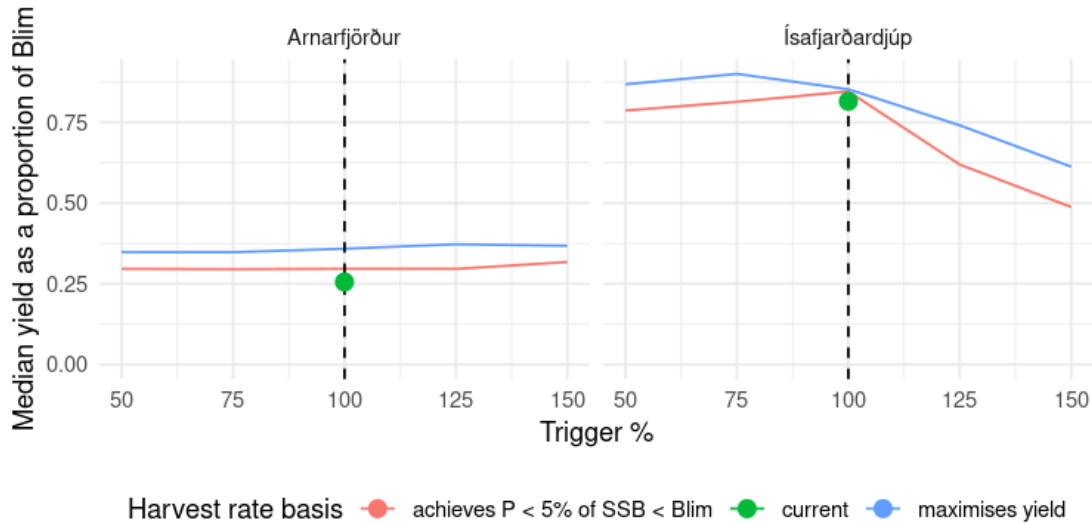


Figure 2: Relationship between index trigger level and median yield as a proportion of  $B_{lim}$  that can also achieve a spawning stock biomass that does not drop below a level with increased risk of recruitment impairment ( $B_{loss}$ ). Relationships are depicted by base model, 5 trigger scenarios set to 50%, 75%, 100%, 125%, and 150% of the current level. Vertical dashed lines show the status quo scenario values (100% predation level).

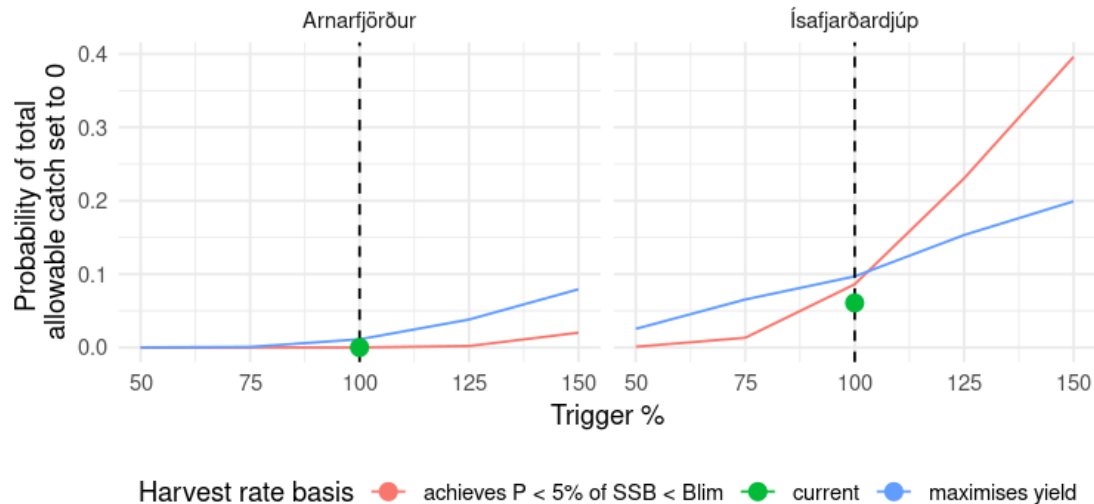


Figure 3: Relationship between index trigger level and probability of 0 catches resulting from the survey index falling below the trigger. Relationships are depicted by base model, 5 trigger scenarios set to 50%, 75%, 100%, 125%, and 150% of the current level. Vertical dashed lines show the status quo scenario values (100% predation level).

## 2 Introduction

In Iceland, the Northern shrimp *Pandalus borealis* is mainly fished within fjords in the west and northwest, or as a fishery offshore of the same regions. Northern shrimp are split into inshore and offshore stocks, and inshore stocks are further split into a series of fjord- or area- specific stocks, based on its life history and genetics, which suggests that the species may form local populations. There is also some evidence suggesting that temperature and local predation by resident or transitory gadoids could affect population dynamics (Björnsson et al. [5], Jónsdóttir, Bakka, and Elvarsson [11]).

Advice for setting fishing limits on shrimp stocks is currently based on multiplying a target proxy fishing rate against stock survey indices. However, target proxy fishing rates are not well-justified, as they are based on historical survey index patterns as they relate to fishing levels. This approach is similar to the Fproxy-based methods once used for Category 3 (data-limited) stocks in ICES assessment guidelines (ICES [8]), but which has been discontinued. Survey indices are also rather variable, and are sometimes not available; therefore, translation of these stock indices into fisheries advice can be difficult, and in recent years has gained criticism from stakeholders as being arbitrary. Stakeholders in this system are mainly small-scale independent fishers (rather than large companies), resident to communities adjacent to the fjords. Within-fjord shrimp fishing is especially suited to small-scale fishers because it is one of the only quota-controlled fisheries that can be performed within fjords in Iceland, due to a ban on trawling within 3 - 12 nm of the coast (12 nm around the Westfjords region). Shrimp fishing is also performed with smaller trawls relative to many industrial fishing trawls, and has a long history of commercial capture in Icelandic fjords, dating back to 1935 (Sigurðardóttir and Jónsdóttir [24]). Processing of shrimp is performed in shrimp factories that are mainly located within towns adjacent to fjords; however, due to a shortage of shrimp in recent years, shrimp factories have reduced in number and those left have needed to rely on imported shrimp to maintain viability. Patterns in community structure within fjords in the north of Iceland also suggests a possible regime shift around the year of 2003 (Jónsdóttir, Bakka, and Elvarsson [11]), and inshore shrimp stocks have likewise undergone reductions in maturity at age (Jónsdóttir, Thórarinsdóttir, and Jonasson [14], Jónsdóttir [9]), indicating that productivity of species as a fishable resource may have decreased after this period (Jónsdóttir, Magnússon, and Skúladóttir [13], Jónsdóttir [9]). This potential change coupled with high demand for shrimp fishing warrants more detailed assessment of the inshore northern shrimp stock

management to determine whether current fishing advisory processes are sustainable, or whether the stocks can sustain more or less fishing than is currently targeted.

The Northern shrimp is a widely distributed stock in the north Atlantic and is fished commercially by virtually all nearby territories (Canada, Greenland, Norway, and Russia). The species reaches a maximum carapace length of roughly 3 cm, but is generally fished after reaching roughly 1.5 cm. Northern shrimp are sequential hermaphrodites, turning into females at approximately 1.5 – 2.0 cm carapace length, depending on the location and fishing pressure experienced (Jónsdóttir, Thórarinsdóttir, and Jonasson [14]). However, for a variety of reasons, stock assessment of the species is problematic. First, age data for these shrimp are not available as is the case for many invertebrates, precluding the use of common age-structured methods (Punt, Huang, and Maunder [23], Punt, Haddon, and McGarvey [22]). Although ageing methods are under development and hold promise at least for the first few years of life, they are not yet usable (Kilada et al. [18]). A cohort analysis of inshore shrimp length distributions in Iceland, shows that they likely grow to at least eight years old and that growth rates differ between areas (Jónsdóttir et al. [15]). Second, like all invertebrates, growth occurs by molting, and both growth and recruitment patterns can depend on local conditions, particularly temperature (Jónsdóttir, Magnússon, and Skúladóttir [13], Jónsdóttir et al. [15]). Third, it is unclear how connected the shrimp are to offshore shrimp populations. Survey indices of many inshore shrimp stocks are not obviously related to shrimp in offshore areas and mixing of individuals appears limited spatially over small scales (~40 - 150 km). Therefore, the inshore shrimp stocks analyzed in this study are considered separate in management. Fourth, shrimp have been known to aggregate spatially, possibly as a behavioral response to a recent increase in gadoids within fjords. Aggregation has led to level or increasing trends in catch per unit effort in certain areas, even as survey indices, when taken across an entire fjord, indicate a decrease in biomass levels (Sigurðardóttir and Jónsdóttir [24], Jónsdóttir et al. [16], MFRI [19], MFRI [20]). Fifth, shrimp are consumed in high numbers by a variety of predatory species, including small-sized cod (*Gadus morhua*), haddock (*Melanogrammus aeglefinus*), and whiting (*Merlangius merlangus*) that are often transient or resident in fjords (Jónsdóttir, Björnsson, and Skúladóttir [12], Jónsdóttir [10]) and may influence recruitment (Jónsdóttir, Magnússon, and Skúladóttir [13], Björnsson et al. [5]). Finally, natural mortality in invertebrates is not well known and could be quite variable, even among different locations of the same stock (Jørgensen et al. [17]). Because many invertebrates tend to be prey for other marine species, trophic dynamics can also be important for understanding sustainable utilization of it and other fished predator stocks (Pérez-Rodríguez et al. [21]).

This project will respond to the need for greater justification in shrimp stock assessment methods by creating an operating model of shrimp population dynamics based on the best available data, and applying the model to reflect local populations within fjords. It focuses on two inshore regions within the Westfjords, Arnarfjörður and Ísafjarðardjúp, that have historically had viable shrimp fisheries, management using target F-proxies, and consistent sampling regimes. Northern shrimp in the two areas have different growth patterns: shrimp in Arnarfjörður tend to grow faster than those in Ísafjarðardjúp (Jónsdóttir et al. [15]). Previous attempts at assessing stock biomass levels have used methods based on surplus production models (Skúladóttir [25], Barua, Thordarson, and Jonsdottir [4]). In this study, we used length-based models, which have the ability to capture more specific stock dynamics and have been used for various other invertebrate species (Punt, Huang, and Maunder [23]). Within the operating model, relationships are tested with temperature and predation to determine whether these could increase the predictive capability of the model. Finally, the model will be used in a management strategy evaluation to evaluate current decision rules for translating shrimp survey indices into management advice, given natural variability in the stock dynamics and uncertainty in biomass estimates. In addition, reference points, defined according to ICES guidelines (ICES [7]) are generated under two sets of scenarios, one set in which future predation levels are varied and another in which index trigger levels are varied, to analyse the effect of predation and trigger values and potential target harvest rates and resulting yield patterns.



## 3 Methods

### 3.1 Study systems

#### 3.1.1 Ísafjarðardjúp

Ísafjarðardjúp is a long and deep, major fjord in the Westfjords region of Iceland with a series of smaller fjords lining its periphery (Figure 4). It is home to the major fishing ports of Bólungarvík, Hnífsdalur and Ísafjarðarbæ (pops. 958 for Bólungarvík and 3794 for the latter two in 2021, Statistics Iceland, [hagstofa.is](http://hagstofa.is)). In the past, shrimp fishing has yielded substantial catches in Ísafjarðardjúp, ranging roughly 1000 - 3000 kg between 1978 and 2002, with the number of vessels using shrimp gear dropping from 52 in 1972 to 22 in 2000 and only 5 in 2020. More recent decades have been subject to periods of extended fishery closure (2003 – 2010) followed by relatively lower catches (~300 - 1100, MFRI [20]). Currently, the decision rule used in calculating the advice on total allowable catch for Ísafjarðardjúp is to multiply the survey index obtained in the fall by 0.5, but to close the fishery when the survey index drops below 604 (MFRI [20]).

#### 3.1.2 Arnarfjörður

Arnarfjörður is a rather smaller fjord in the Westfjords region of Iceland, south of Ísafjarðardjúp, with two major branches at its innermost end with some smaller sub-branches, and a rather constricted mouth at its outermost end, due to a shallow submerged ledge (Figure 4). It is home to the fishing ports of Bildudalur (pop. 208 in 2019, Statistics Iceland, [hagstofa.is](http://hagstofa.is)), which is within the Vesturbyggð municipality (pop. 1064 in 2021, [hagstofa.is](http://hagstofa.is)). From 1960 - 2015, shrimp fishing has yielded substantial but variable catches in Arnarfjörður, ranging roughly 100 – 850 tonnes, but the fishery was closed for two fishing seasons (2006 – 2007) due to low biomass levels, and currently is thought to sustain rather low catch values (~100 – 200 tonnes, MFRI [19]). The number of vessels using shrimp gear is substantially lower than in Ísafjarðardjúp, but has experienced a similar decline from 16 in 1974 to 9 in 2000 and only 3 in 2020. Currently, the decision rule used in calculating the advice on total allowable catch for Arnarfjörður is to multiply the survey index obtained in the fall by 0.346, but to close the fishery when the survey index drops below 390 (MFRI [19]).

### 3.2 Operating model

#### 3.2.1 Northern shrimp population dynamics

A two-area, two-stock, length-based Gadget model was used to represent shrimp populations in Ísafjarðardjúp and Arnarfjörður. A preliminary model was first developed based on a single-stock, single-area model only including Arnarfjörður (which had more complete data available) to determine realistic parameter boundaries and the best model-fitting approach, while final results and a management strategy evaluation were based on the model containing both areas and stocks. The Gadget model is described in the next section.

#### 3.2.2 Data available

Area-specific catch data in kg are available from all inshore Northern shrimp stocks, including Arnarfjörður and Ísafjarðardjúp. Typically, two different gears are used in the shrimp fishery: a shrimp trawl with a Nordmøre grid exclusion device to reduce bycatch, and the same shrimp trawl but with a collection bag attached, which was designed to retain the portion of fish bycatch above minimum landing sizes (Einarsson et al. [6]). Although they may have slightly different selectivities for shrimp, commercial gears were not distinguished here due to possible inconsistencies in data recording. An annual shrimp survey has been conducted by the Marine and Freshwater Research Institute (MFRI) roughly in October every year since the 1970s; however, due to standardization issues, only data from 1988 are used as input to fit the operating model (Sigurðardóttir and Jónsdóttir [24]). An industry-sponsored survey has also taken place annually in

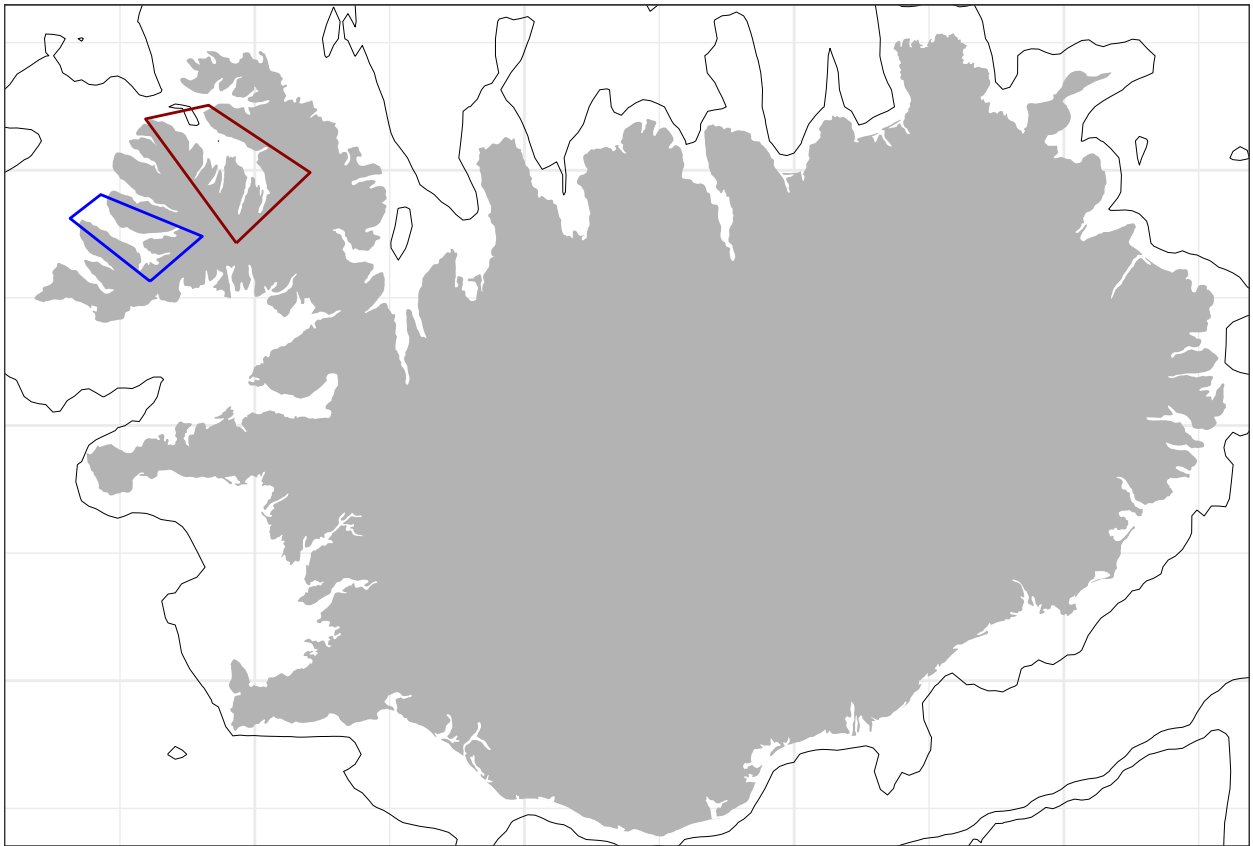


Figure 4: Arnarfjörður (blue polygon) and Ísafjarðardjúp (red polygon) in the westfjords region of Iceland.

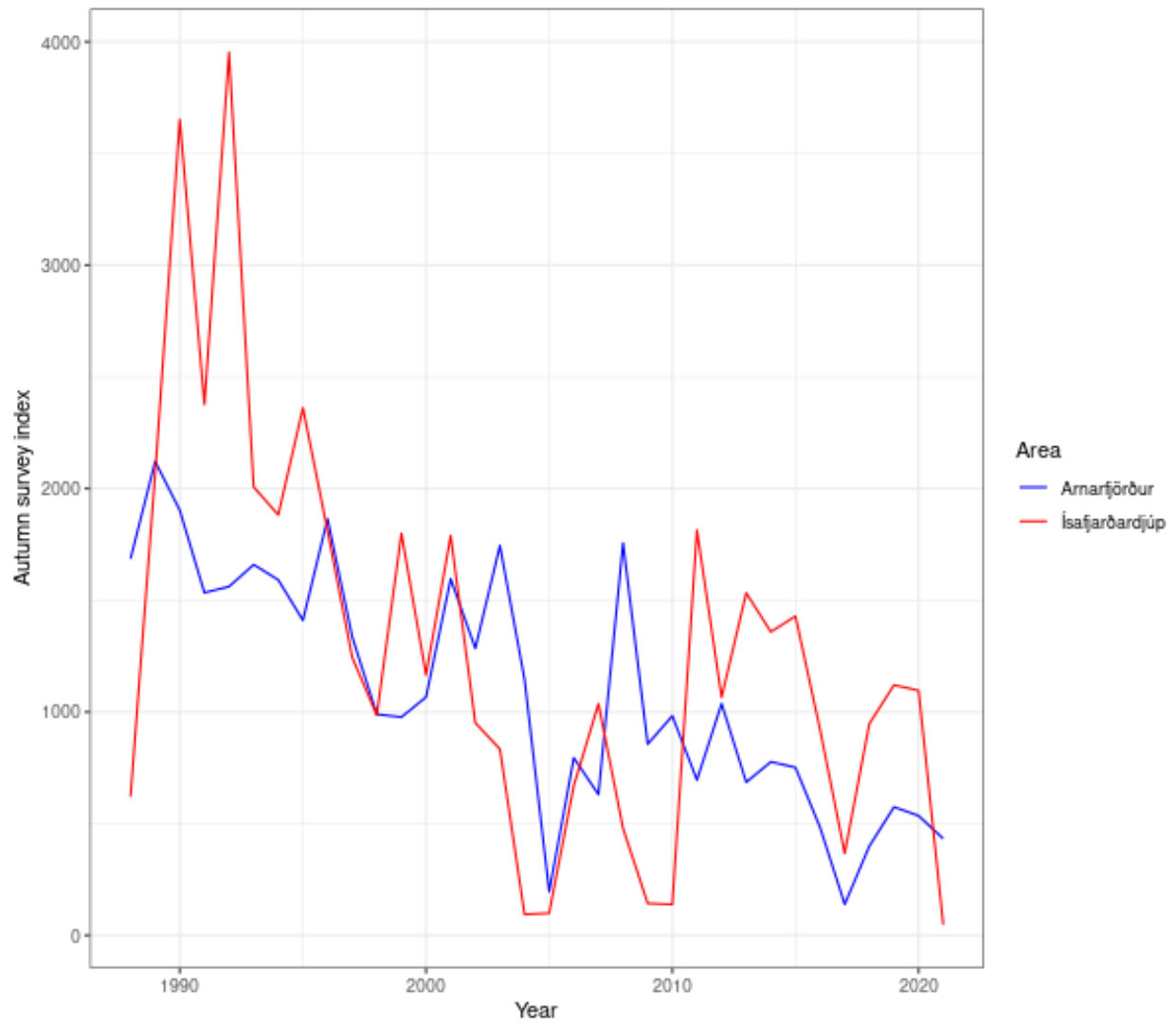


Figure 5: Time series of shrimp indices reflecting harvestable biomass and used for management by fjord.

late January to early February since 1989 (Jónsdóttir et al. [16]). Survey data were split into five length slices to create five carapace-length-based biomass indices from each survey: <1.3, 1.3 - 1.55, 1.55 - 1.7, 1.7 - 1.9, and >1.9 (latter number inclusive). Biomass indices were taken as the raw sum of biomass across stations within an area, without stratification. Length distribution data were also included from both surveys and from commercial samples, although the latter were only available in Arnarfjörður from 4 years and in Ísafjarðardjúp from 17 years over the period 1984 - 2018. Maturity composition data were included only from the fall survey. Because this species is a sequential hermaphrodite, maturation is reflected by a change in sex from male to female, and the proportions of males to females at a certain length reflects maturity proportions. As a result, spawning stock biomass in this species is a measure of the female biomass, which is thought to be the limiting factor in the quantity of spawning possible at any time. However, most analyses are conducted in terms of harvestable biomass, which is calculated as the biomass available for shrimp with lengths 1.55+ cm, plus a linearly increasing proportion of biomass of shrimp lengthed 1.3 - 1.55 (with 0 being included at length 1.3). This definition of harvestable biomass corresponds with calculation of survey indices used in management procedures. Temperature and predation index information were also taken from the fall and winter shrimp surveys. Temperature was taken as the simple mean across stations recorded from CTDs attached to the survey shrimp trawls in the fall and winter surveys. These series were then used for each quarter of that calendar year, centered at 0. Predation indices were formed by first splitting the three main predator species (cod, haddock, and whiting) within three length slices: 0 - 44 cm, 45 - 74 cm, and 75 cm or greater. Preliminary analyses on gut content data showed that the size of the predator affected the size of the shrimp consumed, but very few trends among species could be seen among species could be seen (e.g., in frequency of shrimp eaten). In preliminary analyses, three types of indices were created and compared, one that reflected simple total biomass of predators within species and length slices (raw sum of counts x mean weights across stations without stratification), an index of biomass indices adjusted for the expected amount of shrimp consumed given the predator length and species (predictions from a delta-gamma model fit to gut content data, Stefánsson and Pálsson [28]), and a similar index of biomass indices as that based on the delta-gamma model, but based only on data with shrimp present (i.e., the gamma model only, Stefánsson and Pálsson [28]). However, comparing these results showed very similar trends across the time series; therefore, the simplest index (raw biomass index) was chosen to include as an indicator of predation effort in the operating model.

### 3.3 Population dynamics in Gadget

The simulated quantity is the number of individuals,  $N_{alrsyt}$ , at age  $a = a_{min} \dots a_{max}$ , in a length-group  $l$ , representing lengths ranging between  $l_{min}$  and  $l_{max}$  cm in  $\Delta l$  cm length-groups, in area  $r$ , stock  $s$  and year  $y$  which is divided into time steps, in this case quarters,  $t = 1 \dots T$ . The length of the time step is denoted  $\Delta t$ . The population is described by the following equations:

$$\begin{aligned}
N_{alrsy,t+1} &= \sum_{l'} G_{l'}^l \left[ (N_{al'rsyt} - \sum_f C_{fal'rst})e^{-M_a \Delta t} + I_{al'lrst} \right] && \text{if } t < T \\
N_{a,lrs,y+1,1} &= \sum_{l'} G_{l'}^l \left[ (N_{a-1,l'rsy,T} - \sum_f C_{fa-1,l'rs,T})e^{-M_{a-1} \Delta t} + I_{a-1,l'lrst} \right] && \text{if } t = T \text{ and } a < a_{max} \\
N_{a,lrs,y+1,1} &= \sum_{l'} G_{l'}^l (N_{al'rsy,T} - \sum_f C_{fal'rsy,T} + \\
&\quad N_{a-1,l'rsy,T} - \sum_f C_{f,a-1,l'rsy,T})e^{-M_a \Delta t} && \text{if } t = T \text{ and } a = a_{max}
\end{aligned} \tag{1}$$

where  $G_{l'}^l$  is the proportion in length-group  $l$  that has grown  $l - l'$  length-groups in  $\Delta t$ ,  $C_{falrsyt}$  denotes the catches by the commercial fleet  $f \in \{C\}$  (as there is only a single commercial fleet in this case),  $M_a$  the natural mortality at age  $a$  and  $I_{al'lrst}$  denotes the movement of fish at length  $l'$  from the immature to the mature stock component at length  $l$ . The survey fleet catches are given a nominal catch (1 kg) to

allow for survey age and length distribution predictions. Note that here  $l$  is used interchangeably as either the length-group or the midpoint of the length interval for that particular length-group, depending on the context.

In the case of northern shrimp within fjords in Iceland, stocks are considered to differ by fjord. Therefore,  $r$  distinguishes shrimp stocks in Ísafjarðardjúp from those in Arnarfjörður in this study, whereas  $s$  will be used in the next section to denote mature versus immature stock components, which do not overlap among fjords. The model is structured in length bins with 0.05 cm intervals, as this is the highest data resolution available.

### 3.4 Maturation

Maturation is modeled as a transition between two stock components, from the immature to mature stock. First, the movement from immature to the mature stock is formulated as

$$I_{al'lrst} = \begin{cases} N_{al'r0y,t-1} \times m_{l'}^l & \text{if } s = 1 \text{ and } t > 1 \\ N_{al'r0y-1,T} \times m_{l'}^l & \text{if } s = 1 \text{ and } t = 1 \\ -N_{al'r0y,t-1} \times m_{l'}^l & \text{if } s = 0 \text{ and } t > 1 \\ -N_{al'r0y-1,T} \times m_{l'}^l & \text{if } s = 0 \text{ and } t = 1 \end{cases} \quad (2)$$

where  $s = 0$  denotes the immature stock component and  $s = 1$  denotes the mature stock. The proportion of immatures  $m_{l'}^l$ , that mature between the lengths  $l$  and  $l'$  are defined as:

$$m_{l'}^l = \frac{\lambda_r(l-l')}{1 + e^{-\lambda_r(l-l_{50ry})}} \quad (3)$$

The parameter representing the length at which 50% of individuals are expected to be mature ( $l_{50ty}$ ) were allowed to vary annually by fjord across all years that contained maturity data, i.e., 1995 and later. All years prior to 1995 were parameterized with the 1995 values.

During the same time step when individuals of the immature stock component reach a certain maturity according to their lengths, they move to the mature stock. Those who have not matured by the maximal age in the immature stock are all moved to the same age in the mature stock component in the last step of the year.

### 3.5 Growth

Growth in length is modeled as a two-stage process, an average length update in  $\Delta t$  and a growth dispersion around the mean update [as described by 26]. Lengths are updated by calculating the mean growth for each length group at each time step, using a simplified form of the Von Bertalanffy function:

$$\Delta l = (l_\infty - l)(1 - e^{-k_{rsy}(\tau)\Delta t}) \quad (4)$$

where  $l_\infty$  is the terminal length and  $k$  is the annual growth rate. In this model we allow the growth rate parameter to vary by area and be partially controlled by bottom temperature in the immature stock components only. The annual growth rate of an immature stock ( $s = 0$ ) in area  $r$  is the product of an intercept growth rate  $k_{r0}$  and the multiplicative effects (estimated by coefficients  $\beta_b$  and  $\beta_s$ ) of two temperature time series from the shrimp surveys, the bottom temperature  $\tau_{b,ry}$  and the surface temperature  $\tau_{s,ry}$ :

$$k_{r0y}(\tau) = k_{r0} \exp(\beta_b \tau_{b,ry} + \beta_s \tau_{s,ry}) \quad (5)$$

The annual growth rate of the mature stocks found in both areas  $r$  are instead controlled by the same growth rate parameter  $k_{r1y} = k_1$  with no dependency on temperature or region. Only a single  $l_\infty$  is implemented across areas, stocks, and time.

The length distributions are updated by taking the mean growth as the most frequent length update, but also allowing some portion of the fish to have no growth, a proportion grown by one length group, a proportion grown by two length groups, etc. How these proportions are selected affects the spread of the length distributions, but these two equations must be satisfied:

$$\sum_i p_{il} = 1$$

and

$$\sum_i i p_{il} = \Delta l$$

Here  $\Delta l$  is the mean growth and  $p_{il}$  is the proportion of fish in length group  $l$  growing  $i$  length groups. Here the growth is dispersed according to a beta-binomial distribution parameterized by the following equation:

$$G_l^{l'} = \frac{\Gamma(n+1)}{\Gamma((l'-l)+1)} \frac{\Gamma((l'-l)+\alpha)\Gamma(n-(l'-l)+\beta)}{\Gamma(n-(l'-l)+1)\Gamma(n+\alpha+\beta)} \frac{\Gamma(\alpha+\beta)}{\Gamma(\alpha)\Gamma(\beta)} \quad (6)$$

where  $\alpha$  is subject to

$$\alpha = \frac{\beta \Delta l}{n - \Delta l} \quad (7)$$

where  $n$  denotes the maximum length group growth and where  $(l' - l)$  the number of length-groups grown. In this case, the maximum length group growth was set to a rather low value (2) to prevent a large amount of variation in predicted growth, which can be difficult to estimate in a model with no age data included.

The weight,  $W_{sl}$ , at length-group  $l$  is calculated according to the following general length-weight relationship, estimated *a priori*:

$$W_l = \mu l^\omega \quad (8)$$

### 3.6 Recruitment and initial abundances

In this model the number of recruits per area each year,  $R_{ry}$ , is estimated directly within the model as a series of recruitment parameters.

Recruitment enters the population in the immature stock  $s = 0$  at the minimum age of 0 and with initial area-specific length  $l_{0,r}$  according to:

$$N_{a_{min}l_{0,r}0yt'} = R_{ry} p_l \quad (9)$$

where  $t'$  denotes the recruitment time-step and  $p_l$  is the proportion in length-group  $l$  that is recruited. The Proportions  $p_l$  are determined by a normal density with mean length set according to eq. (4) and variance  $\sigma_{l_0}^2$  (variance is the same among areas). The initial length  $l_{0,r}$  can be interpreted the same as the  $t_0$  used in a typical von Bertalanffy growth model.

A simple formulation of initial abundance in numbers is used for each age group  $a$  in length-group  $l$ :

$$N_{alrs11} = \nu_{ars} q_{al} \quad (10)$$

where  $\nu_{ars}$  is the initial number at age  $a$  in the initial year of stock  $s$  in area  $r$  and  $q_l$  the proportion at length-group  $l$  which is determined by a normal density with a mean calculated according to the growth model in equation (according to the  $l_0$  value, length at age 0) (4) and variance  $\sigma_a^2$  (which was fixed in all cases to a value of 0.25).

### 3.7 Fishing

Catches are implemented based on reported total landings and a length- based suitability function (also known as the ‘selectivity’ function) for each of the commercial and survey fleets). Total landings are assumed to be known and the total biomass of the population is simply offset by the landed catch, according to the expected length distribution described by the suitability function. The catches for length-group  $l$ , fleet  $f$  at year  $y$  and time-step  $t$  are calculated as

$$C_{falrsyt} = E_{fryt} \frac{S_f(l)N_{alrsyt}W_{ls}}{\sum_{s'} \sum_{l'} \sum_{a'} S_f(l')N_{al'rs'yt}W_{l's'}} \quad (11)$$

where  $E_{fryt}$  is the effort needed to produce landed biomass  $C_{falrsyt}$  at time  $t$  and  $S_f(l)$  is the suitability of length-group  $l$  by fleet  $f$  defined as:

$$S_f(l) = \frac{1}{1 + e^{(-b_f(l-l_{50,f}))}} \quad (12)$$

It was assumed that survey and commercial fleets were the same, so there is only one designation of fleet  $f$ , which we simply set to  $f$ .

Fishing mortality is calculated as a harvest rate in terms of the reference biomass is calculated as:

$$F_{ry} = \frac{C_{ry}}{B_{ref,ry}} \quad (13)$$

where  $C_{ry} = \sum_{falst} C_{falrsyt}$  and  $B_{ref,ry} = \sum_{alst} p_{ref,l} N_{alrsyt} W_{s,l}$ , where  $p_{ref,l}$  reflects the proportion of individuals at a certain length group that are included in the  $B_{ref,ry}$ . Reference biomass is chosen here to correspond with the reference survey index calculation currently used for management. This reference biomass of calculated as all shrimp larger than 1.55 cm plus the biomass of shrimp 1.3 - 1.55 cm included according to a proportion that increases linearly from 0 at lengths  $< 1.3$  to 1 at length  $> 1.55$  cm ( $p_{ref,l < 1.3} = 0$ ,  $p_{ref,l=1.3} = 0.143$ ,  $p_{ref,l=1.35} = 0.286$ ,  $p_{ref,l=1.4} = 0.429$ ,  $p_{ref,l=1.45} = 0.571$ ,  $p_{ref,l=1.5} = 0.714$ ,  $p_{ref,l=1.55} = 0.857$ ,  $p_{ref,l > 1.55} = 1$ ).

### 3.8 Predation

Predation by cod, haddock and whiting in three length ranges (0 - 44 cm, 45 - 74 cm, and 75 cm or above) was implemented here similarly to a commercial fleet, except that predators fleets are parameterized as a series of effort fleets. Therefore, instead of catch being a known quantity removed from the population each quarter as is the case for commercial fleets, an annual indicator of effort was applied. Each fleet was distinguished by the predator species  $p$  and length range  $h$  as a certain combination denoted  $ph$ . This yielded 9 possible combinations, but only 8 implemented because no whiting predators existed in the largest size group. However, note that subscript  $f$  for fleet designations can be used interchangeably with predator-length combination  $ph$  because both represent sources of removals from shrimp population. This will be done in later equations. The designation  $ph$  is used here to emphasize that suitability (or selectivity) is only specific to size ( $h$ ), not predator-size group ( $ph$ ). Predation removals from the shrimp population  $C_{phalrsyt}$  were represented as:

$$C_{phalrsyt} = q_{pred,r} E_{phrt} S_h(l) N_{alrsyt} W_{ls} \quad (14)$$

where  $q_{pred,r}$  is an area-specific catchability,  $E_{phrt}$  is the effort exhibited by predator group  $ph$  in area  $r$  at time  $t$  and  $S_h(l)$  is the suitability (a.k.a. selectivity) of prey length-group  $l$  to a particular predator size group  $h$ . Suitabilities were defined as a constant  $S_h(l) = c_h$  for the smallest predator size group (0 - 45 cm,  $h = 0$ ) or a logistic equation otherwise ( $h = 45$  for the predator size group 45 - 75 cm, and  $h = 75$  for the predator size group  $> 75$  cm):

$$S_h(l) = \frac{1}{1 + e^{(-b_h(l-l_{50,h}))}} \quad (15)$$

Effort  $E_{phrt}$  was assumed here to be proportionate to the survey indices of numbers belonging to each predator group ( $I_{phrt}$ ) calculated from the same surveys as the shrimp indices were calculated. All other parameters were estimated ( $q_{pred,r}$ ,  $c_h$ ,  $b_h$  and  $l_{50,h}$ ).

### 3.9 Fitting to data

A significant advantage of using an length- and age- structured model is that the modeled output can be compared directly against a wide variety of different data sources. It is not necessary to convert length into age data before comparisons. Gadget can use various types of data that can be included in the objective function. Importantly this ability to handle length data directly means that the model can be used for stocks such as shrimp where age data are absent. Length data can be used directly for model comparison. The model is able to combine a wide selection of the available data by using a maximum sum of squares approach to find the best fit to a weighted sum of the data sets.

In Gadget, data are assimilated using a weighted log-sum-of-squares function. Here three types of data enter the likelihood: length-based survey indices, maturity at length from the surveys, and length distributions from survey, commercial, and predator fleets.

In formulations below it is assumed that the compositional data are sampled at random, both from the fishery and surveys, as this is how the sampling protocol for the Icelandic shrimp surveys and commercial data collections are designed.

#### 3.9.1 Model settings

The maximum age of Northern shrimp was set at 8 which also acted as a plus group, as cohort analyses suggested that Northern shrimp within these fjords may attain 8 years of aged at least if unfished (Jónsdóttir et al. [15]). The length range in the model was between 0.3 and 2.5 cm, in 0.5 cm length intervals, representing carapace lengths as they are usually measured. Recruitment to the immature stock component occurs at age 0, at the end of the 3<sup>rd</sup> quarter. To better align the main timing of data collection (surveys) with the model time structures, quarters have been offset by a month, so that quarter  $t = 1$  in year  $y$  actually corresponds with December in year  $y - 1$  through February in year  $y$ . Quarter  $t = 2$  therefore corresponds with March - May of the same year, quarter  $t = 3$  is June - August of the same year, and quarter  $t = 4$  is September - November of the same year.

#### 3.9.2 Survey indices

For each length range  $g$  the survey index is compared to the modeled abundance at year  $y$  and time-step  $t$  in area  $r$  using:

$$l_g^{SI} = \sum_y \sum_t (\log I_{gry} - (\log q_g r + b_g r \log \widehat{N}_{gryt}))^2 \quad (16)$$

where

$$\widehat{N}_{gryt} = \sum_{l \in g} \sum_a \sum_s N_{alrsyt}$$

The five index length groups were chosen as  $< 1.3$  cm, 1.3–1.55 cm, 1.55–1.7 cm, 1.7–1.9 cm, and  $> 1.9$  cm.



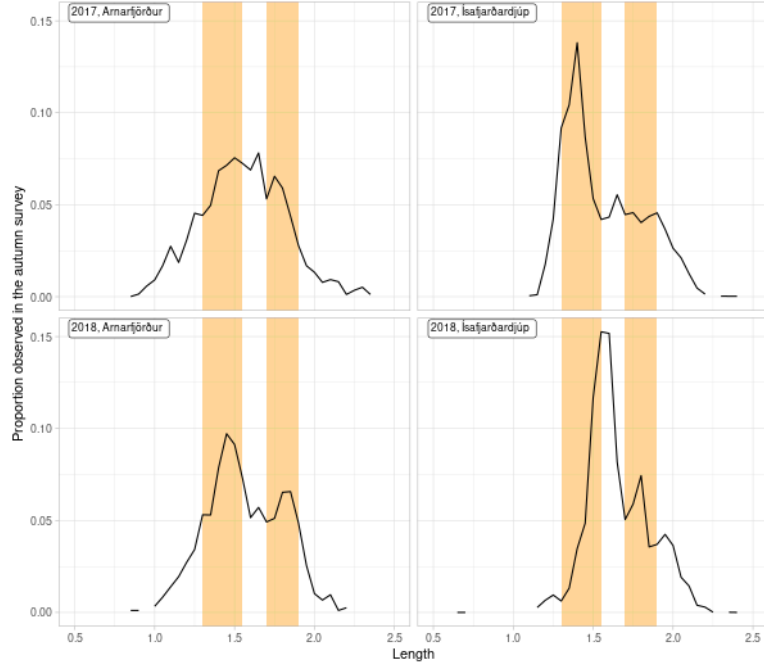


Figure 6: Yellow and white alternating vertical bands demonstrate length ranges of the five survey indices used to fit the Gadget model. Years were arbitrarily chosen as examples of how length ranges line up with typical length distributions.

### 3.9.3 Distributional data

Length distributions are compared to predictions using

$$l_f^{\text{LD}} = \sum_y \sum_t \sum_l (\pi_{flryt} - \hat{\pi}_{flryt})^2 \quad (17)$$

where  $f$  denotes the fleet where data was sampled from and

$$\pi_{flryt} = \frac{\sum_a \sum_s O_{falrsyt}}{\sum_{a'} \sum_{l'} \sum_s O_{fa'l'rsyt}}$$

and

$$\hat{\pi}_{flryt} = \frac{\sum_a \sum_s C_{falrsyt}}{\sum_{a'} \sum_{l'} \sum_s C_{fa'l'rsyt}}$$

i.e the observed and modeled proportions in length-group  $l$  respectively at year  $y$  and time-step  $t$  in area  $r$ . In this case, fleet  $f$  could refer to either the survey, commercial, or predator fleets, in which case the observed proportions were generated from survey length distribution data, commercial samples, or gut content data respectively. When fleet  $f$  referred to a predator species-size combination,  $f$  can be replaced with  $ph$ , and the observed proportions are derived from shrimp length distributions observed in predator guts collected during the shrimp surveys. Very few gut content data were available. Length distributions from commercial data were only available for some years.

Length at maturity comparisons use the number of shrimp of which maturity status has been assigned that are observed in the shrimp survey. As the Northern shrimp is a sequential hermaphrodite, maturity is

signified by becoming female, so the ratio of mature to immature in the model is compared to the sex ratio of females to males in survey data. The observed proportions are compared to the modeled proportion using sum of squares:

$$l_f^M = \sum_y \sum_t \sum_l (\pi_{flryt} - \hat{\pi}_{flryt})^2 \quad (18)$$

where

$$\pi_{flryt} = \frac{\sum_a O_{falr1yt}}{\sum_{a'} \sum_{l'} \sum_s O_{fa'l'rsyt}}$$

and

$$\hat{\pi}_{flryt} = \frac{\sum_a C_{falr1yt}}{\sum_{a'} \sum_{l'} \sum_s C_{fa'l'rsyt}}$$

i.e. the observed and modelled proportions of shrimp in length group  $l$  and mature, in year  $y$  and time-step  $t$  and area  $r$ , and where the fleet  $f$  corresponds to the survey.

### 3.9.4 Likelihood component weights

The total objective function used the modeling process combines equations (16), (17), and (18) using the following formula:

$$l^\Gamma = \sum_g w_g^{\text{SI}} l_g^{\text{SI}} + \sum_{f \in \{s, c, ph\}} (w_f^{\text{LD}} l_f^{\text{LD}}) + w^{\text{M}} l^{\text{M}} \quad (19)$$

where  $f = s, c$  or a  $ph$  combination denotes the survey, commercial, or predator fleets respectively. The  $w$ 's are the weights assigned to each likelihood components.

The weights,  $w_i$ , are necessary for several reasons. For instance, they prevent particular components from dominating the likelihood function, as well as reduce the effect of low data quality. The weights,  $w_i$ , can be used as an *a priori* set of estimates of the variance in each subset of the data.

Assigning likelihood weights is not a trivial matter; it has in the past been the most time consuming part of a Gadget model. Commonly this has been done using some form of 'expert judgement'. General heuristics have recently been developed to estimate these weights objectively. Here the iterative re-weighting heuristic introduced by (Stefánsson [27]), and subsequently implemented in (Taylor et al. [29]), is used.

The general idea behind the iterative re-weighting is to assign the inverse variance of the fitted residuals as component weights. The variances, and hence the final weights, are calculated according the following algorithm:

1. Calculate the initial sums of squares (SS) given the initial parameterization for all likelihood components. Assign the inverse SS as the initial weight for all likelihood components, resulting in a total initial score of 1 for each component.
2. For each likelihood component, do an optimization run with the initial weighted SS for that component set to 10000. Then estimate the residual variance using the resulting SS of that component divided by the degrees of freedom ( $df^*$ ), i.e.  $\hat{\sigma}^2 = \frac{SS}{df^*}$ .
3. After the optimization set the final weight for that all components as the inverse of the estimated variance from the step above (weight =  $1/\hat{\sigma}^2$ ).

The number of non-zero data-points ( $df^*$ ) is used as a proxy for the degrees of freedom. While this may be a satisfactory proxy for larger data-sets it could be a gross overestimate of the degrees of freedom for smaller data-sets. In particular, if the survey indices are weighed on their own while the yearly recruitment is estimated they could be over-fitted. In general, problems such as these can be solved with component grouping, that is in step 2 the likelihood components that should behave similarly, such as survey indices representing similar age ranges, should be upweighted and optimized together. The grouping used in the present model included 4 groups of survey indices: the two containing the two indices representing the smallest size ranges, one for each survey, and two containing the indices representing the largest size ranges, again by survey.

### 3.9.5 Optimization

The Gadget model was fit by running an iterative reweighting routine to determine the weightings that were applied to the likelihood score of each data source, or group of data sources, before summing in the objective function of the model search. In the case presented here, the model implemented may be overparameterised given the amount of data available. In addition, because the total objective function to be minimised is a weighted sum of the different components, the estimation can be difficult because of some or groups of parameters are correlated and therefore the possibility of multiple optima cannot be excluded. The optimization routine implemented here began with the more robust simulated annealing algorithm to make the results less sensitive to the initial (starting) values, and then proceeded to the more local Hooke and Jeeves search algorithm (relative tolerance of  $1e-6$ ) in the neighborhood of the global optima. The simulated annealing algorithm used in the model fitting process had 2,000,000 iterations with parameter settings initial temperature = 12000, temperature reduction factor = 0.95, number of loops before temperature adjusted = 2, number of loops before step length adjusted = 5, initial value for maximum step length = 1, step length adjustment factor = 2, lower limit for the ratio when adjusting step length = 0.1, and upper limit for ratio when adjusting step length = 0.9, and number of temperature loops to check = 12. The following Hooke and Jeeves algorithm had a maximum of 40,000 iterations of the Hook and Jeeves algorithm (minimum epsilon controlling halt criteria = 0.0001, resizing multiplier = 0.5, and initial value for the step length = 0). The BFGS algorithm was not implemented because exploratory model runs suggested that quasi-Newton optimisation methods may not be effective due to a discontinuous search gradient.

Results from the preliminary model run, which included only the Arnarfjörður shrimp stock, suggested that the optimization routine tended to converge when an upper bound of an annual recruitment parameter was reached, even though better values for the objective function (i.e., lower negative log likelihood scores) could be reached at lower values of that recruitment parameter. As this upper recruitment bound scaled the resulting biomass levels obtained by the model, a key result of these analyses, it was deemed necessary to try a variety of recruitment upper bounds to narrow the range of realistic biomass levels. However, as appropriate levels of natural mortality are also unknown for this species, and natural mortality likewise determines realistic biomass levels obtained by the model, it was also deemed appropriate to try a variety of fixed natural mortality values. Therefore, after obtaining weights an initial run of the iterative reweighting routine for a model including both fjords, weights were held constant and a grid search was additionally implemented, over all combinations of natural mortality within the range 0.15 to 0.67 (in steps of 0.01) and recruitment values at 15 values within the range of 0.2 - 30 (in log-scaled steps of roughly 0.35). For each combination of recruitment upper bound and natural mortality, the initial data grouping and weighting scheme were applied in the objective function, as well as the same optimization routine (simulated annealing followed by the Hooke and Jeeves algorithm). Many model fits within this grid search resulted in highly similar model fits, likely as a result of many parameters being fit to rather sparse data sources. Therefore, a subset of models containing a set of 10 best models were chosen from this set, distinguished as having the lowest likelihood scores (best fits to the data), to include in the following management strategy evaluation.

### 3.10 Management strategy evaluation

The goal of the management strategy evaluation was to test decision rules that aim to sustainably harvest shrimp based on the population dynamics within the operating model. To do so requires first characterizing and simulating uncertainty expected in the system, choosing a single test decision rule, then projecting the shrimp populations under this uncertainty and whilst implementing the decision rule to obtain a set encompassing a variety of plausible future scenarios that could arise after implementing that decision rule for a number of years. To test a single decision rule, for example, 1000 models of the shrimp population were run, each of which differ slightly due to the incorporation of a single combination of the errors implemented; that is, a single combination of expected 1) natural mortality levels and biomass levels resulting from imprecise structure of the stock assessment, 2) observation error, 3) future recruitment variability, 4) implementation error of the decision rule, and 5) bias derived from running the same assessment year after year (autocorrelation).

#### 3.10.1 Operating model uncertainty and observation error

Uncertainty in natural mortality rates and biomass levels (1 above) was represented by including a subset of ten of the best-fit models, from the grid search described above. Model uncertainty due to the fitting procedure and observation error were then simulated by repeating the model-fitting procedure (with the same fixed likelihood score weights) on 10 sets of simulated data for each of the 10 operating models. For each set of simulated data, observation error was simulated by performing a parametric bootstrap of the residuals obtained in the operating model (2 above). In the parametric bootstrap, parametric distributions were fit to residuals of a single model, after which the sets of simulated data were created as 10 random draws from the parametric distributions. In all cases, to prevent negative value generation in simulated data, residuals were calculated as the log of predictions from the operating model divided by observations, and therefore error was applied multiplicatively to the original data. A normal distribution was fitted to each set of residuals of survey indices from a length slice and survey. A multivariate normal distribution was fitted to length distribution proportions from the fall survey. Because data were too sparse to fit a multivariate normal distribution to other length distribution residuals (e.g., from commercial data and the winter survey), the variance-covariance matrix obtained from the multivariate normal distribution fitted to fall survey length distribution residuals was borrowed to generate data for commercial and winter survey data. Length distributions from gut content data, however, were replicated in simulations with no modification. Maturity proportion data were generated by fitting a logit model in each year and fjord, then drawing random draws from that predicted relationship. All other data sets were left as-is. Gadget models were then optimized for each of the 100 simulated data sets (although a few parameters were fixed before optimizations, see results for details).

#### 3.10.2 Projections

The model fits obtained from the 100 simulated data sets (10 per each of 10 operating models) were then forward projected for 50 years under a decision rule. An assumption regarding future recruitment levels must be made for this projection, which per ICES procedures is done either by fitting a stock-recruitment relationship to model estimates or using guidelines to determine a suspected spawning stock level below which recruitment impairment may be expected ( $B_{loss}$ , ICES [7]). No recruitment impairment was obvious in the stock-recruitment pattern in Arnarfjörður, and although impairment could be observed in Ísafjardardjúp, this shift could likewise be interpreted as a regime shift (see further discussion under **Base model results**, and Figure 9). As a result, because there is a wide dynamic range in SSB values for both stocks, these stocks were considered to best resemble an ICES Category Type 5 stock (ICES [7]). According to this guidelines, a hockey-stick recruitment function can be used to generate recruits in the next times step from the current spawning stock biomass and account for recruitment variability (3 above), with the breakpoint of the hockey-stick function ( $B_{loss}$ ), defined as the minimum spawning stock biomass value observed after 1990 ( $B_{lim}$ ). According to the hockey-stick model, if a spawning stock biomass level dropped below this, then recruitment would be linearly reduced. Otherwise, above this breakpoint, recruitment was generated

by a 7-year block bootstrap sample from the recruitment series. Only recruitment values after 1999 were sampled as they appear more lower and more stable than values earlier in the time series, especially for Ísafjarðardjúp, and therefore are more likely to represent future conditions. In addition, to account for error in the stock assessment and effort implementation process (4 and 5 above), random draws of assessment error from a lognormal distribution with mean 1 and standard deviation of 0.2 and an AR1 value of 0.2 was multiplied against the mature biomass value against which the harvest rate is multiplied in the decision rule.

### 3.10.3 Decision rule

A decision rule was implemented to closely represent the procedure currently employed in management. However, as the survey index used for management in reality is not calculated in the modeling procedure, a proxy was used. The known survey index used in management is meant to represent an unknown harvestable biomass, so an unknown value for catchability translates these values and needs to be assumed in this modeling procedure. To do this, for each simulation, the survey index time series observed in reality was divided by the comparable series of harvestable biomass values generated by Gadget model predictions, and an average catchability for each simulation over all years was calculated. These catchabilities were then used to translate the actual trigger survey index values used in management, below which fisheries within a fjord have been closed, into a constant, simulation-specific harvestable biomass trigger used in the projected decision rule. Similarly, harvest rates implemented were applied as a proportion of the harvestable biomass, multiplied by this catchability, so that it is applied on the scale of the survey index.

## 4 Base model results

The 10 base models retained for further analysis varied very little in scores, and can be considered to have similar fits. These included combinations of  $M$  that ranged 0.27 – 0.33 and log recruitment upper bounds of  $-0.54 – 1.25$ , in units of  $1e10$ . The optimization search space was rather flat in the vicinity of the best models (Figure 7), but jumps to other local minimum are possible (see abrupt change in score values at values of the log upper bound less than 1 and  $M$  greater than 0.3).

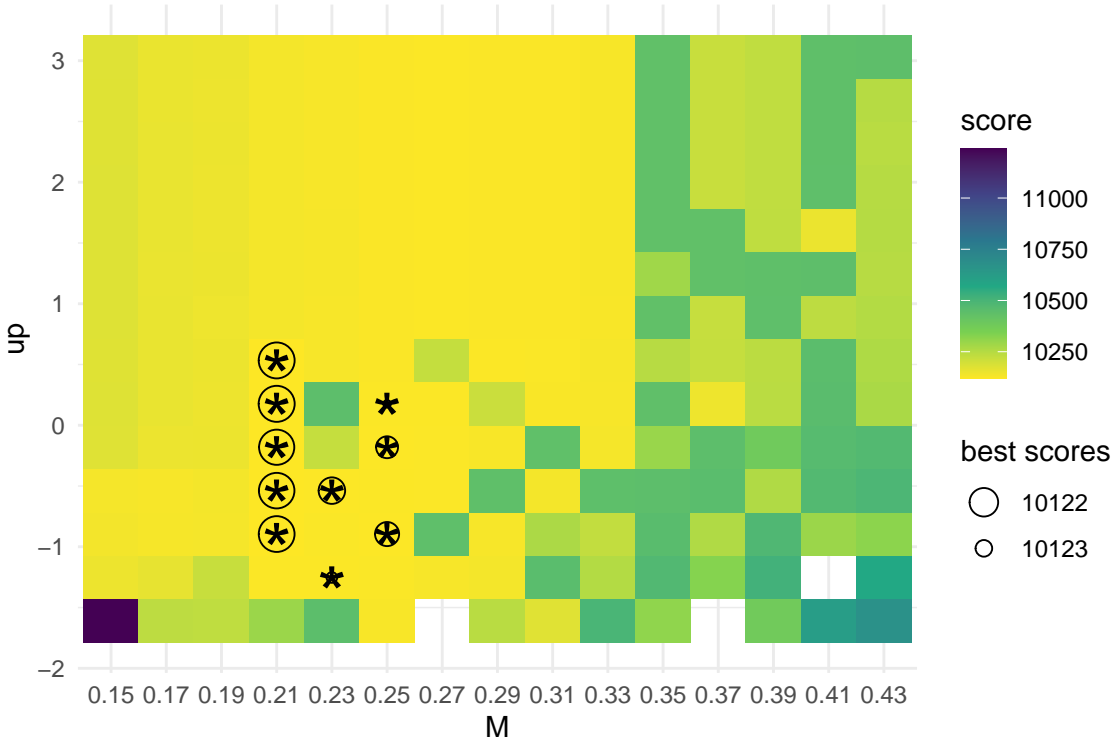


Figure 7: Results of the optimisation grid search over combinations of natural mortality ( $M$ , x-axis) and recruitment upper bound ( $up$ , log-scaled y-axis, in units of  $1e10$ ). Colors indicate that the score value for a model optimised with a certain combination of  $M$  and  $up$ . Models with scores less than 9696 are shown with circles, the size of which are inversely related to the score, and values with stars were retained in the subset of 10 models used in the management strategy evaluation.

The 10 retained best models showed similar patterns in SSB and recruitment, except that the scale of biomass levels in Arnarfjörður was sometimes estimated much higher than the majority of the models (in 4 / 10 cases, Figure 9). Differences in biomass levels across the 10 best models also translated to different views of predation levels, with a relatively high contribution of predation to total biomass removals from shrimp populations as biomass levels increased across models (Figure 8). Plots of spawning stock biomass (SSB) and recruitment estimates showed only very flat relationships without a clear decrease in recruitment despite large decreases in SSB over time (Figure 9).

### 4.0.1 Fits to individual data sets

Fits to individual data sets were also similar, so only results based on the best-fit model are shown here ( $M = 0.29$ , recruitment upper bound is  $\exp(0.18) \cdot 1e10$ ).

Fits to survey indices are reasonably good given the high variability in index values and little obvious movement of cohorts through survey index length slices over time (Figure 10). Length distributions show

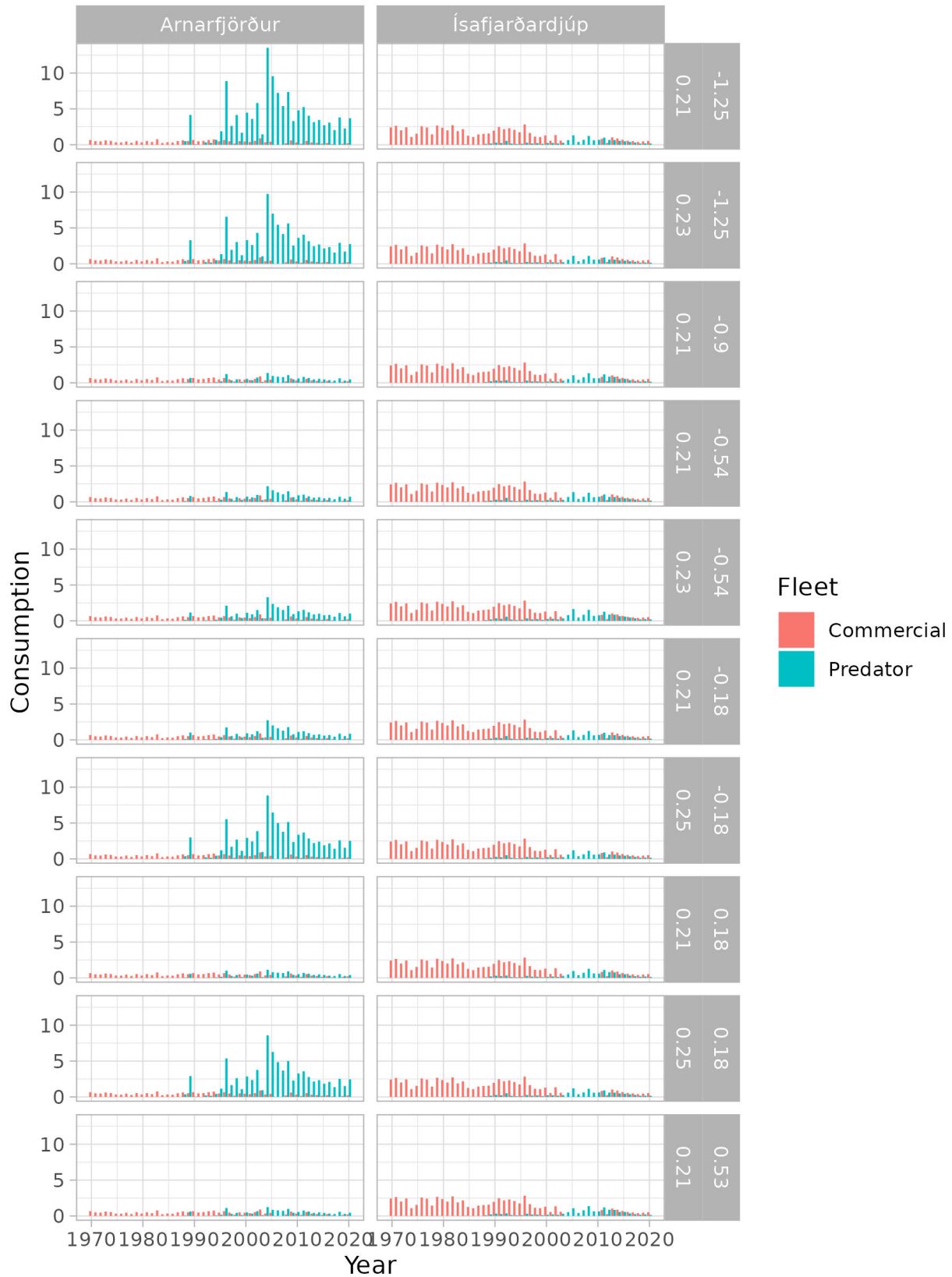


Figure 8: Total consumption estimates (biomass removals in 000s of tonnes) of shrimp in Arnarfjörður and Ísafjarðardjúp from each of the 10 best models. Each panel row corresponds with a model, labelled on the right by its implemented natural mortality value (0.27–0.33) and its recruitment upper bound (-0.54–1.25, log-scaled and in units of  $1e10$ ). Predator removals are summed over all predator groups implemented.

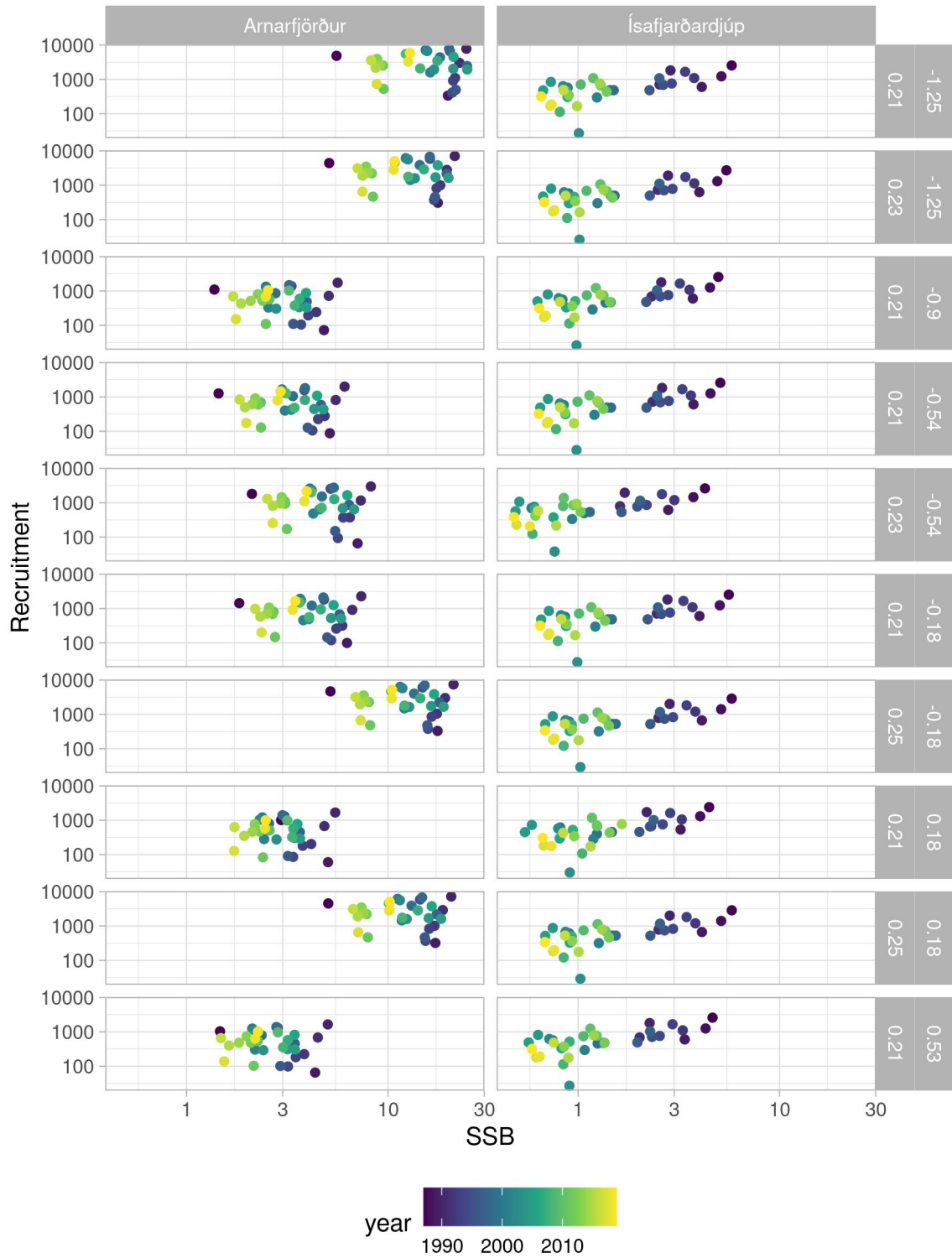


Figure 9: Spawning stock biomass and recruitment estimates of shrimp in Arnarfjörður and Ísafjarðardjúp from each of the 10 best models. Each panel row corresponds with a model, labelled on the right by its implemented natural mortality value (0.27–0.33) and its recruitment upper bound (–0.54–1.25, log-scaled and in units of  $1e10$ ).



good fits to the data in both surveys and fjords, except where more extreme picks are not captured. More extreme peaks may be caused by correlations among length groups not accounted for in the model (Figures 11, 12, 13, 14), perhaps as a result of shrimp aggregating by size classes.

Predictions of commercial samples of length distributions did not fit data as well as survey data except during the earliest time periods where fewer survey data had a lesser influence on length distributions. Samples were not taken consistently from commercial samples, so these data may not fully represent the shrimp stock for a variety of reasons (Figures 15 and 16).

Gut content data used to inform selectivity patterns of predation by the size groups of cod, haddock and whiting predators were particularly sparse, so predictions were not very accurate. However, they still give a general view of predation patterns in the data (Figures 17, 18, and 19).

#### 4.0.2 Base model results

Results are shown for all base models, differing by color. Only results from 1990 and later are analyzed because they span a period of more reliable data (Figure 20). Earlier years in the data set can be thought of as a burn-in period to allow the model to fit the data better in years after 1990. Base models differed greatly in predicted biomass levels of shrimp in Arnarfjörður, due to difficulties in estimating catchability, likely as a result of low contrast in the data (Figure 20). Ísafjarðardjúp had more stable biomass levels among base models, and indicate that biomass levels are currently around 13% of what they were in 1990. The stock in Arnarfjörður has also experienced declines, but less dramatic, and is estimated to have slightly higher biomass levels (Figure 20). The differences in biomass levels could be related to a greater historical fishing mortality in Ísafjarðardjúp (Figure 21) in addition to very high levels of predation (Figure 21). Estimates of biomass removals from the populations due to predation versus commercial fishing indicate high predation in both fjords (Figure 23), but the combination with historically high fishing levels may have reduced biomass levels more substantially in Ísafjarðardjúp. Lower recent recruitment estimates (Figure 22) may have resulted from high historical fishing pressure, causing recruitment impairment, but this pattern is difficult to distinguish from known environmental changes (Jónsdóttir, Bakka, and Elvarsson [11]), also reflected by high recent predation levels. It is possible that Ísafjarðardjúp is already in a state of recruitment impairment, rendering this method to yield underestimates of  $B_{lim}$ . However, the data is variable enough that potential recruitment impairment has also not obviously occurred, and instead resembles an ICES Category 5 Stock, for which choosing the  $B_{lim}$  based on a minimum in the SSB series is appropriate (ICES [7]). Choosing a higher  $B_{lim}$  based on estimating a breakpoint is likely to be highly uncertain and not very accurate. Observed changes may instead be due to environmental changes, which are indicated to have occurred in these same fjords soon after the turn of the century (Jónsdóttir, Bakka, and Elvarsson [11]). Instead, choosing recent recruitment estimates (from 2000 onwards) to reflect future expected recruitment, as was done in this study, is more justifiable than assuming a state of recruitment impairment.

Note that biomass levels in Ísafjarðardjúp were more stable among base model runs than in Arnarfjörður. This is likely a result of greater contrast in the data (i.e., Ísafjarðardjúp has experienced higher fishing rates). Therefore, this model cannot be used to produce an analytical stock assessment for these shrimp stocks with reliable estimates of biomass, especially for the Arnarfjörður stock. However, using general knowledge can help narrow down the range of believable biomass levels. For example, survey indices from both Ísafjarðardjúp and Arnarfjörður have the same general magnitude, and both mostly cover the main shrimp fishing grounds in each area. Therefore they should not be hugely different. It is also apparent that despite biomass level estimates varying greatly among base lines, predation rates were more stable (Figure 21) due to higher absolute biomass removals increasing with population biomass levels (Figure 23). This association was likely necessary to fit the same observed catch levels across base models. Therefore, in order to believe models with very high biomass levels, it must also be believable that very large quantities of biomass have been removed by predation. In the case of base model 5, for example, which exhibited the highest fitted biomass levels (Figure 20), biomass removals by predation would need to exceed commercial removals by roughly three times (Figure 23, bottom panels). Even in the best model, predation was estimated as roughly ten times that of commercial removals (Figure 23, bottom panels) in Arnarfjörður. Although this may not be biologically unreasonable, it is very different from the Ísafjarðardjúp scenario of predation removing the same

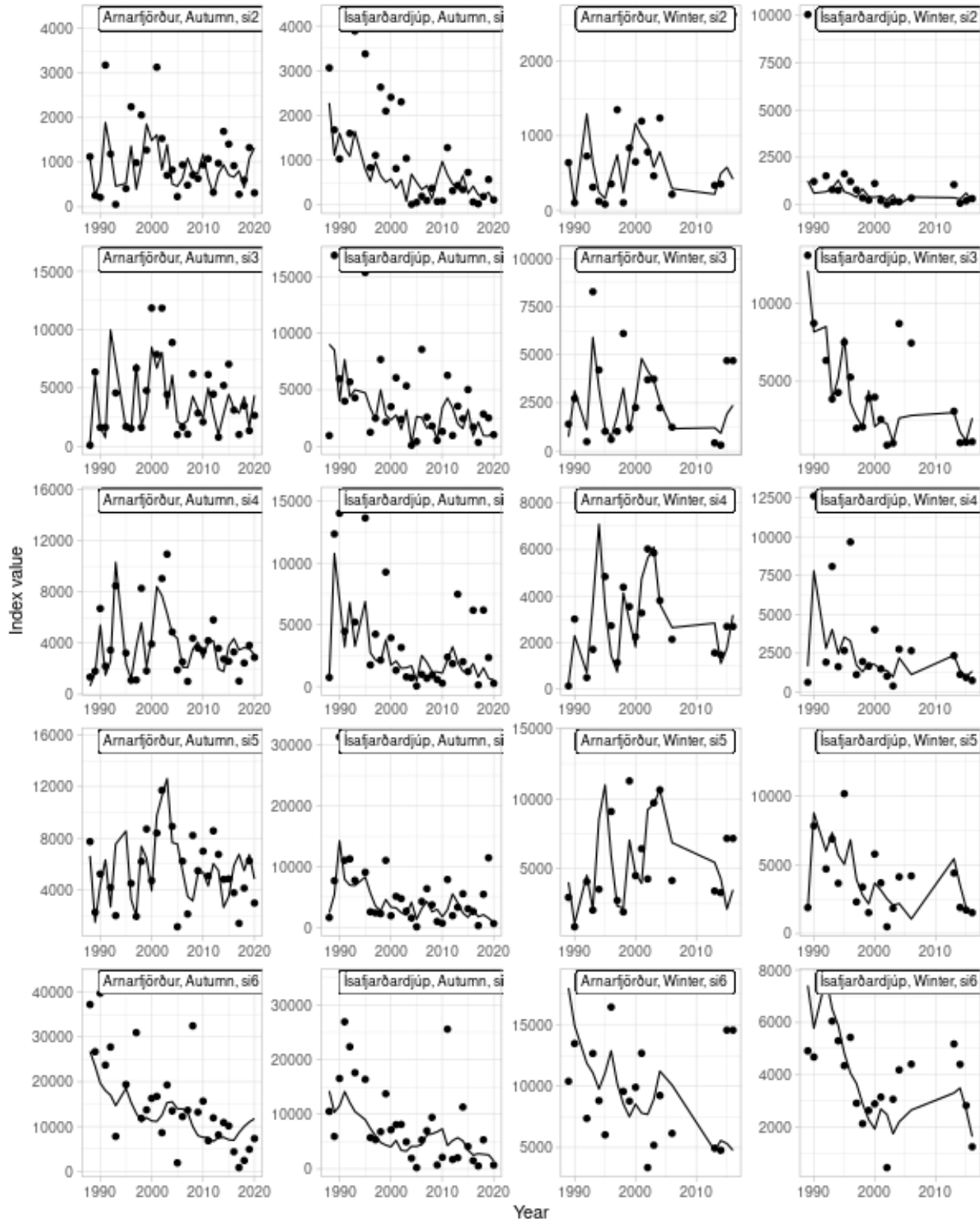


Figure 10: Fit of the best-fit model to autumn and winter length based survey indices from the autumn and winter surveys in each area. Panel rows show indices in order of increasing length ranges moving downward. Panel columns indicate a specific survey within a given fjord.



Figure 11: Fit of the best-fit model to Autumn survey length distributions in Arnarfjörður. Grey lines indicate observations, black lines are predictions.

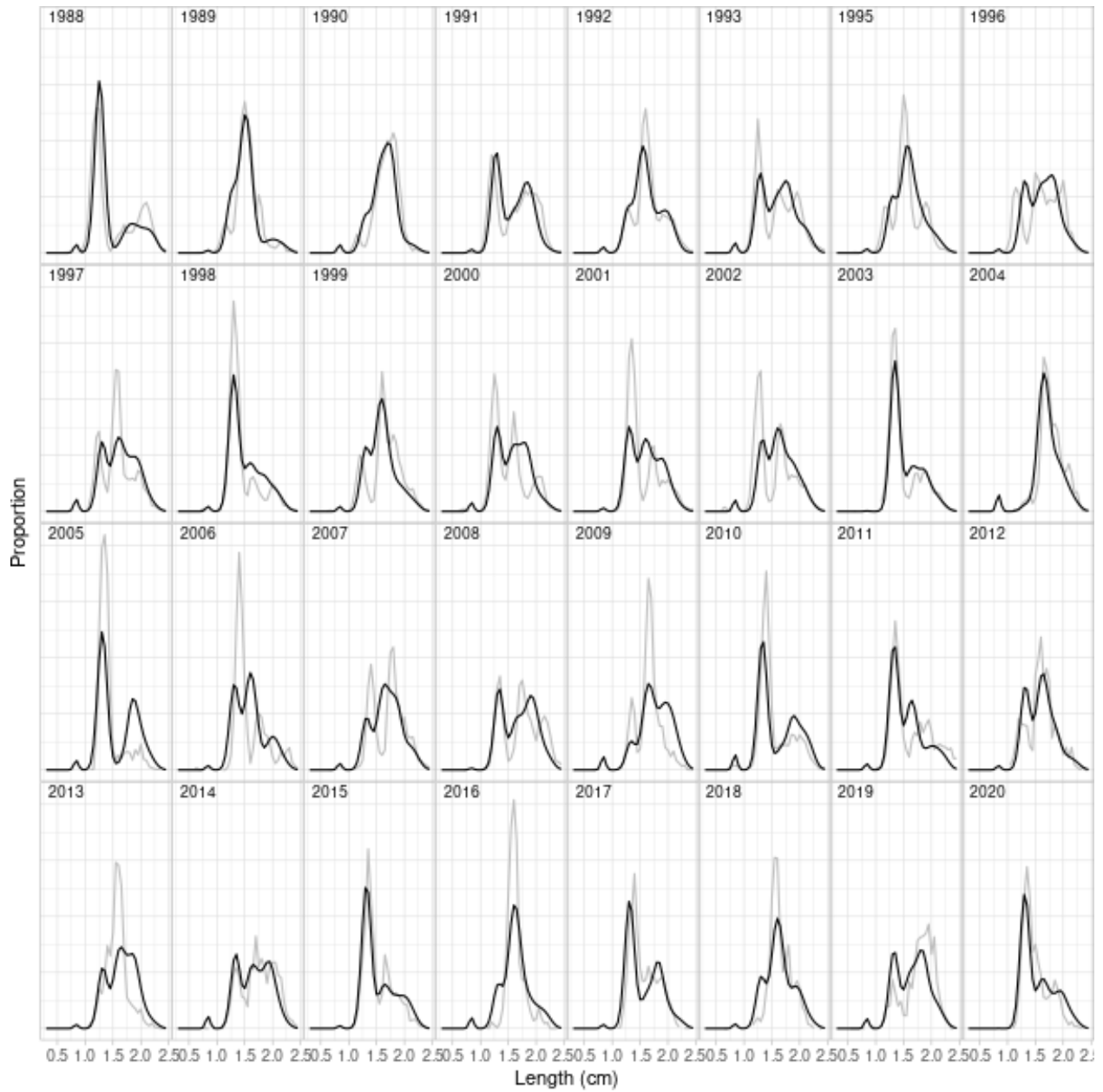


Figure 12: Fit of the best-fit model to Autumn survey length distributions in Ísafjarðardjúp. Grey lines indicate observations, black lines are predictions.

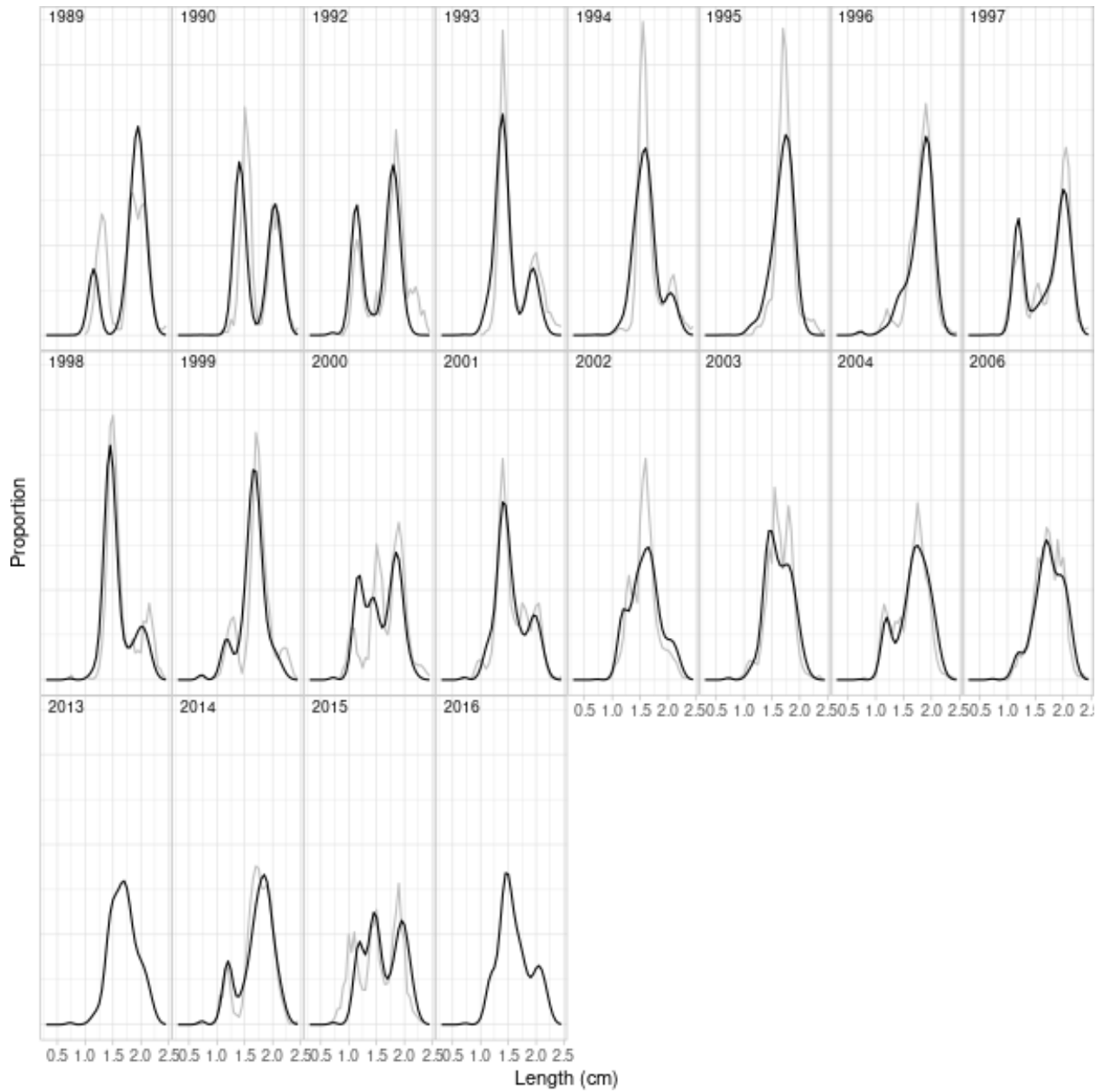


Figure 13: Fit of the best-fit model to Winter survey length distributions in Arnarfjörður. Grey lines indicate observations, black lines are predictions.

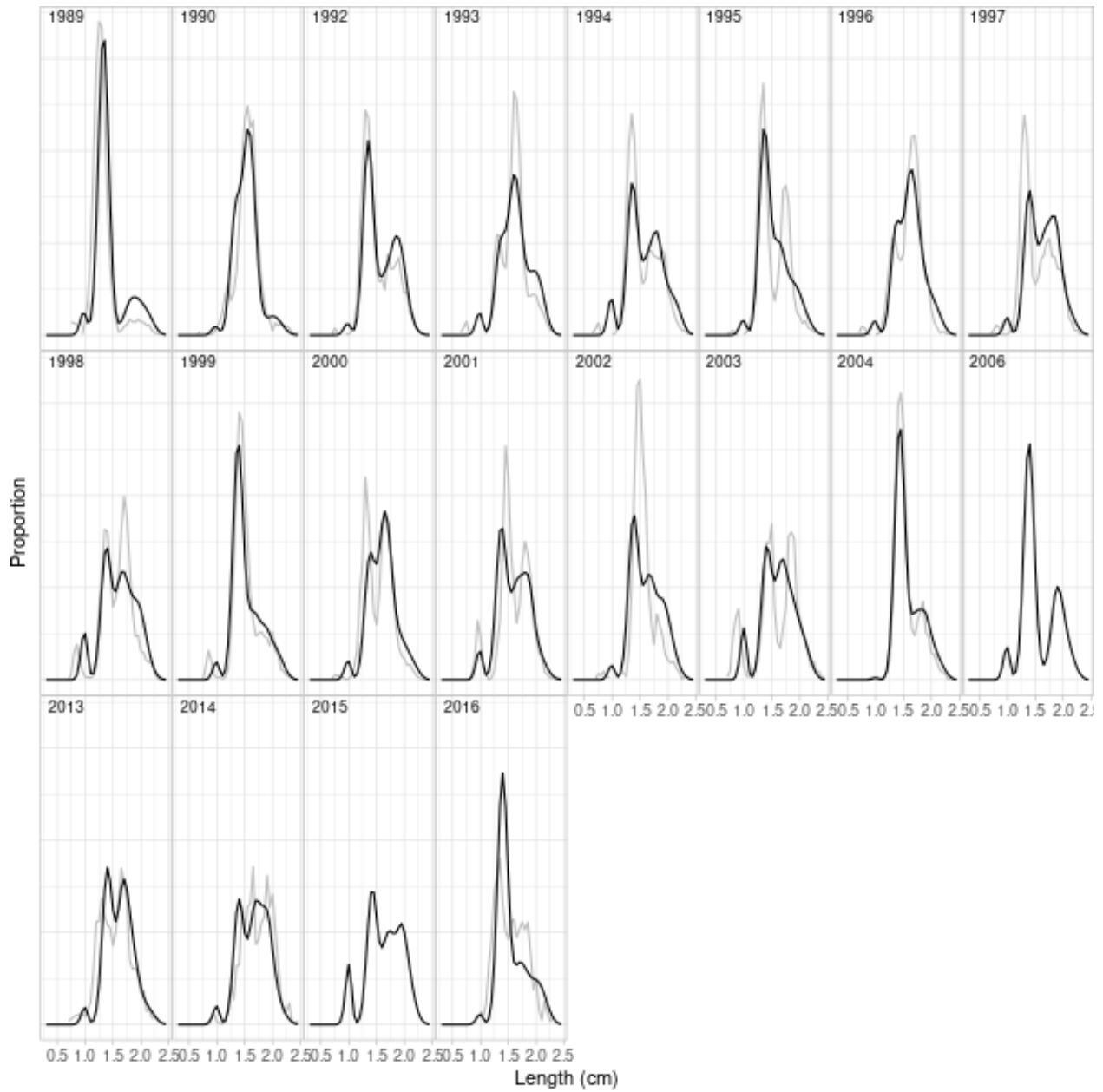


Figure 14: Fit of the best-fit model to Winter survey length distributions in Ísafjarðardjúp. Grey lines indicate observations, black lines are predictions.

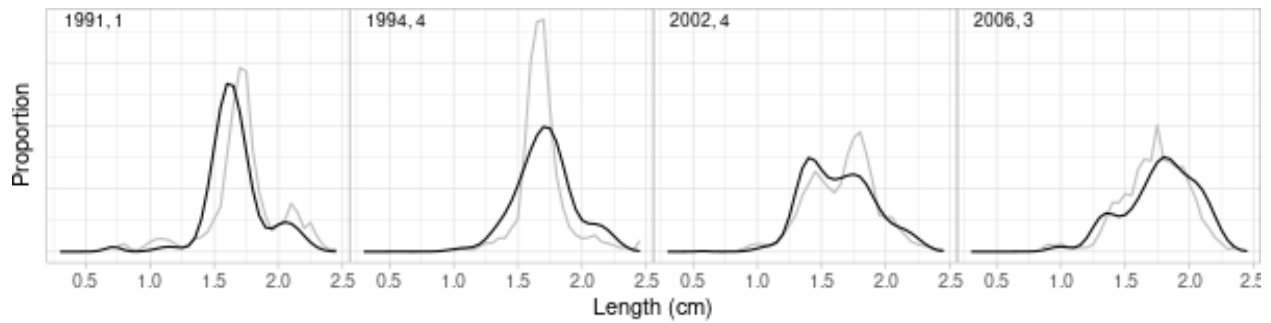


Figure 15: Fit of the best-fit model to commercial length distribution samples in Arnarfjörður. Labels indicate years and quarters. Grey lines indicate observations, black lines are predictions.

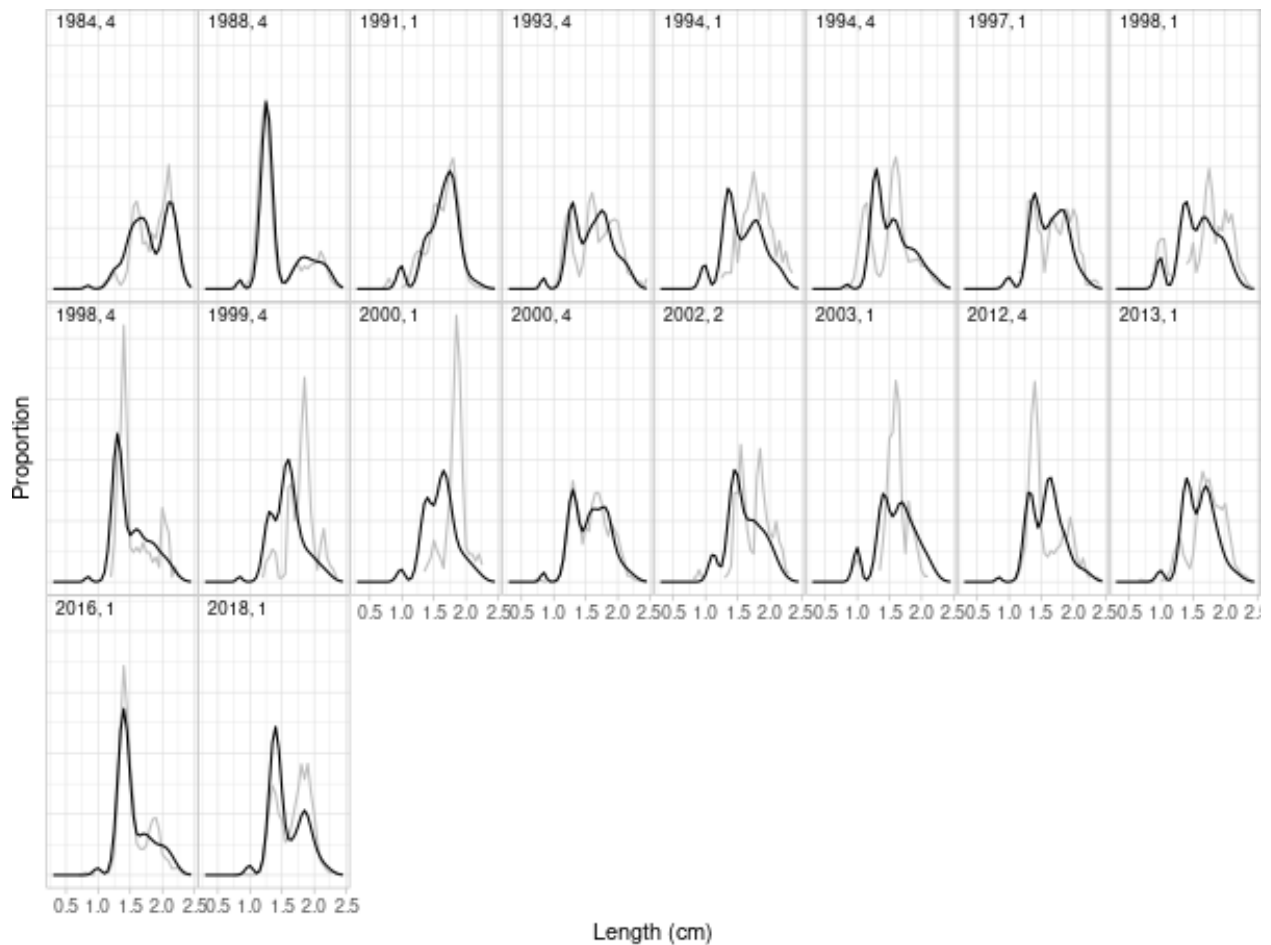


Figure 16: Fit of the best-fit model to commercial length distribution samples in Ísafjarðardjúp. Labels indicate years and quarters. Grey lines indicate observations, black lines are predictions.

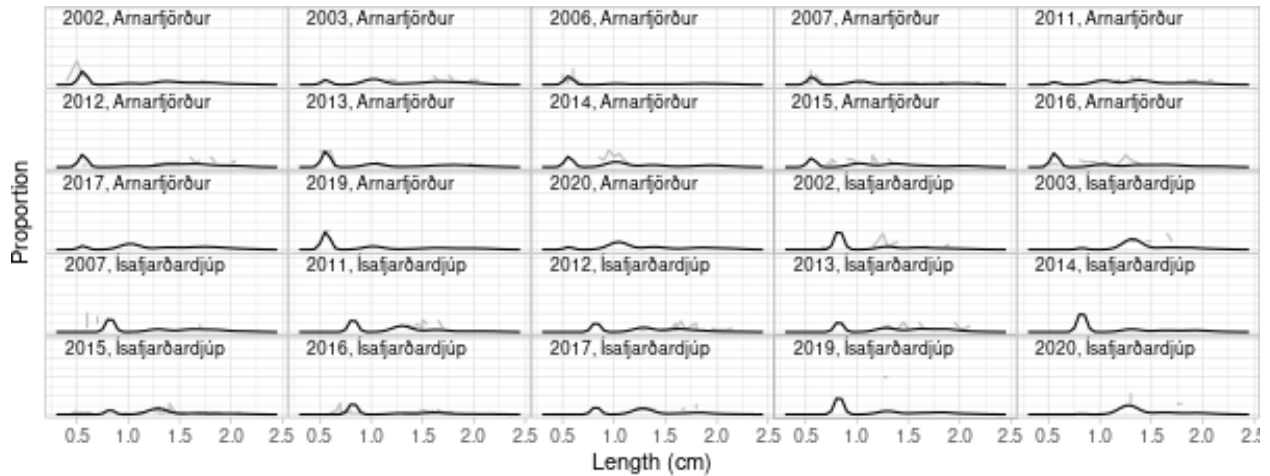


Figure 17: Fit of the best-fit model to gut content length distribution samples from predators < 45 cm (cod, haddock, and whiting). Labels indicate years and areas. Grey lines indicate observations, black lines are predictions.

order of magnitude of biomass as commercial fleets. Because commercial fleet removals are so much higher in total in Ísafjarðardjúp, however, the total removals across both fjords are more similar in the best-fit model case (Figure 23, top panels) than higher-biomass base models (Figure, 23, bottom panels). As survey indices for both shrimp and predators are not hugely different in magnitude among fjords, we suspect that the base models that exhibited the highest absolute biomass levels and predation (i.e., base models 7 and 9) to be less likely to accurately represent true biomass levels within Arnarfjörður than those with lower absolute biomass levels. Furthermore, because biomass estimates are especially poor and total predation removals are especially high in Arnarfjörður, it should be kept in mind that even the lowest-biomass base model results may be overestimates. That is, if it is reasonable to assume that the total amount of biomass removals due to predation are similar between the two fjords, then the biomass removals due to predation depicted in the best-fit base model (Figure, 23, top panels) would need to be roughly halved in Arnarfjörður, and so would the total population biomass estimates, thereby resulting in similar biomass levels as in Ísafjarðardjúp (Figure 20).



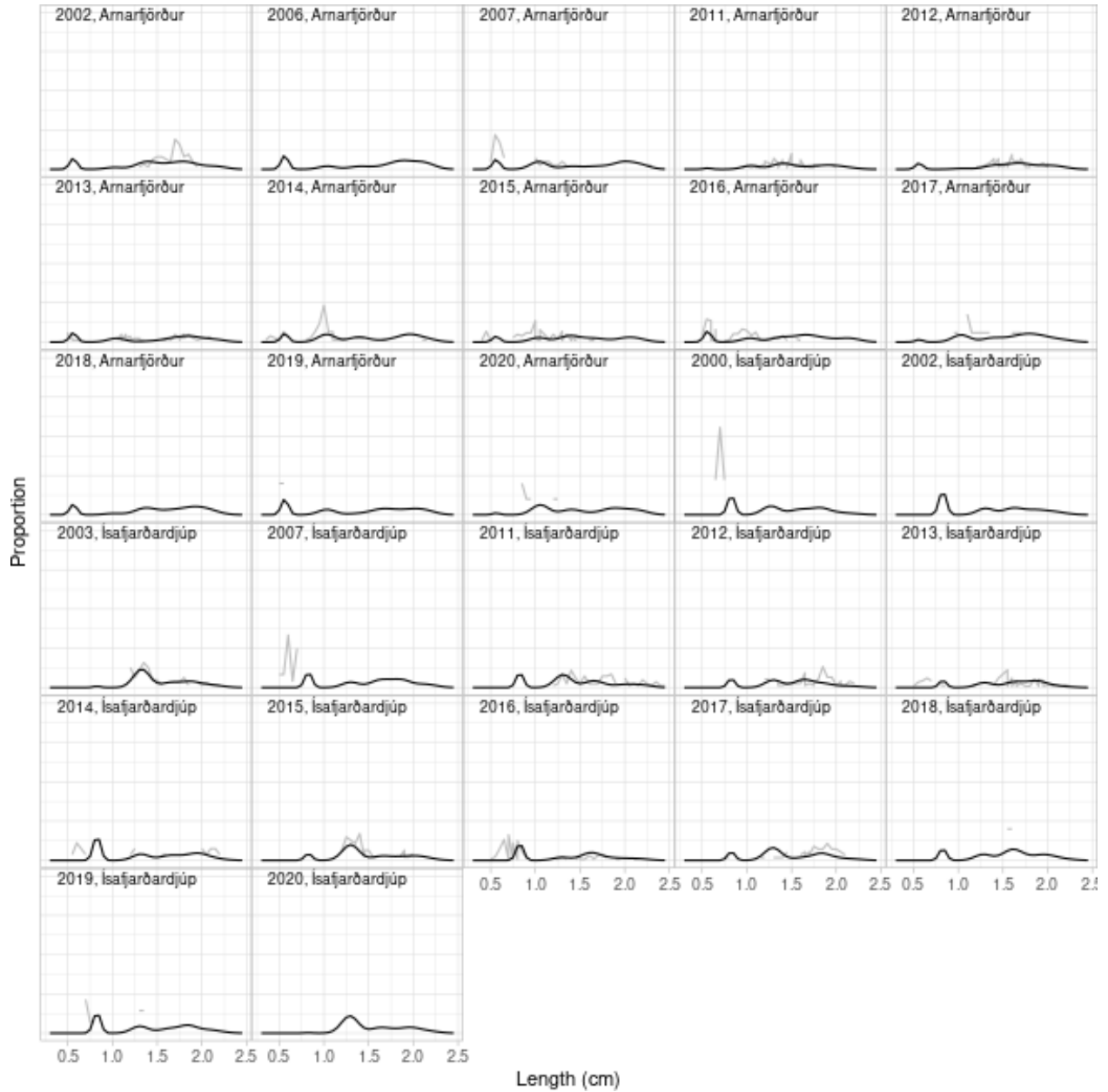


Figure 18: Fit of the best-fit model to gut content length distribution samples from predators 45 - 75 cm (cod, haddock, and whiting). Labels indicate years and areas. Grey lines indicate observations, black lines are predictions.

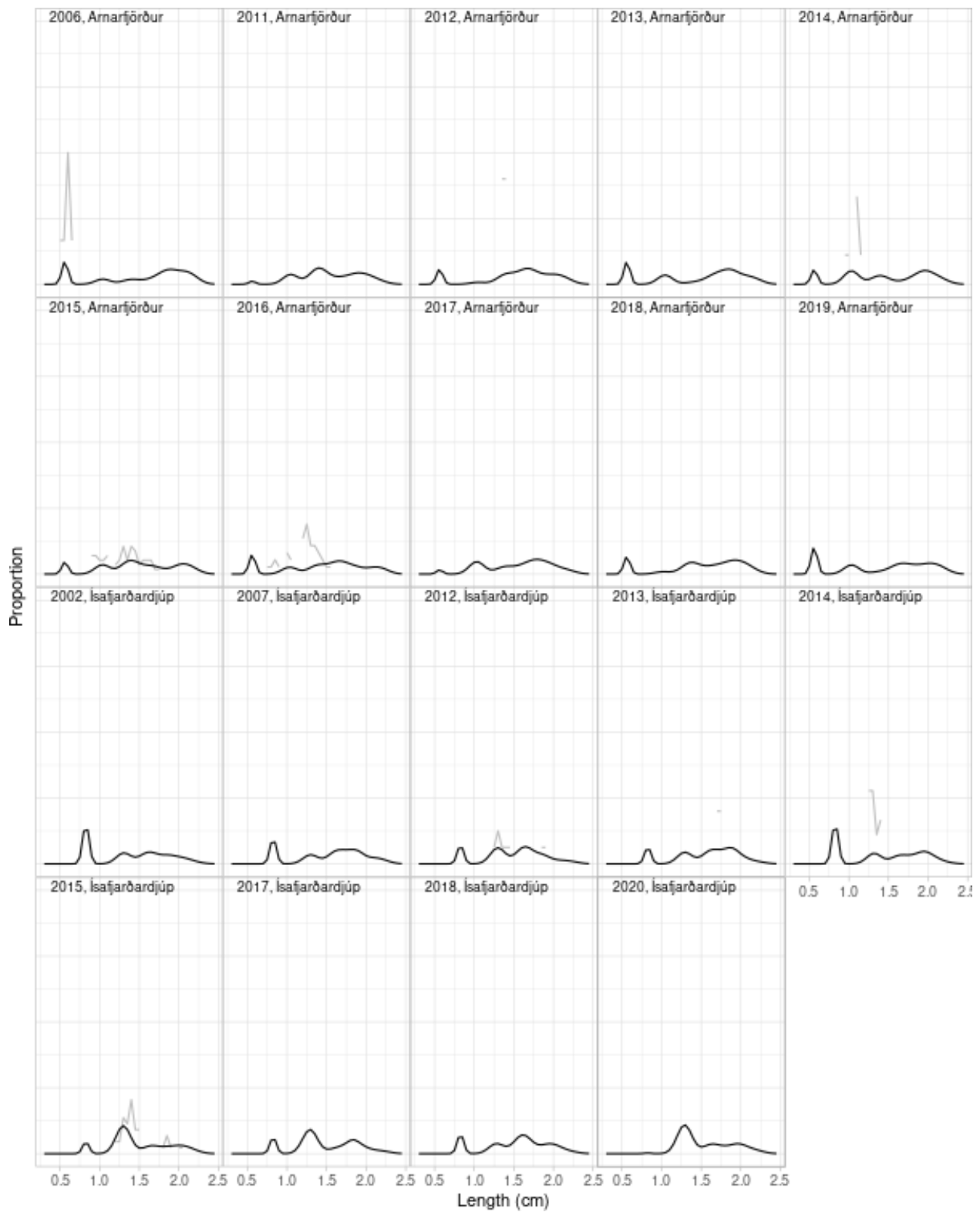


Figure 19: Fit of the best-fit model to gut content length distribution samples from predators > 45 cm (cod and haddock). Labels indicate years and areas. Grey lines indicate observations, black lines are predictions.

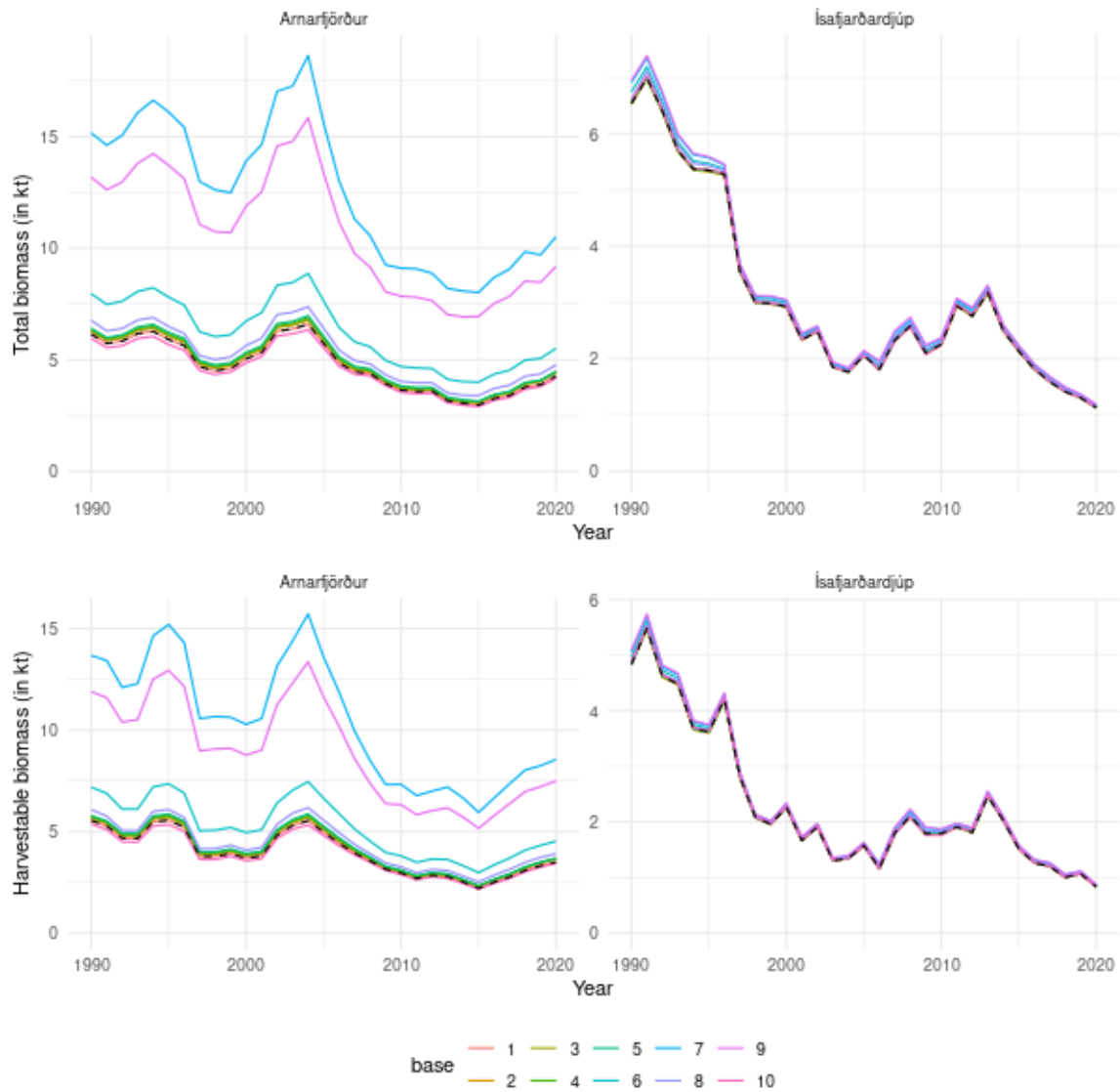


Figure 20: Total and harvestable biomass estimates by fjord across base models represented by colors.

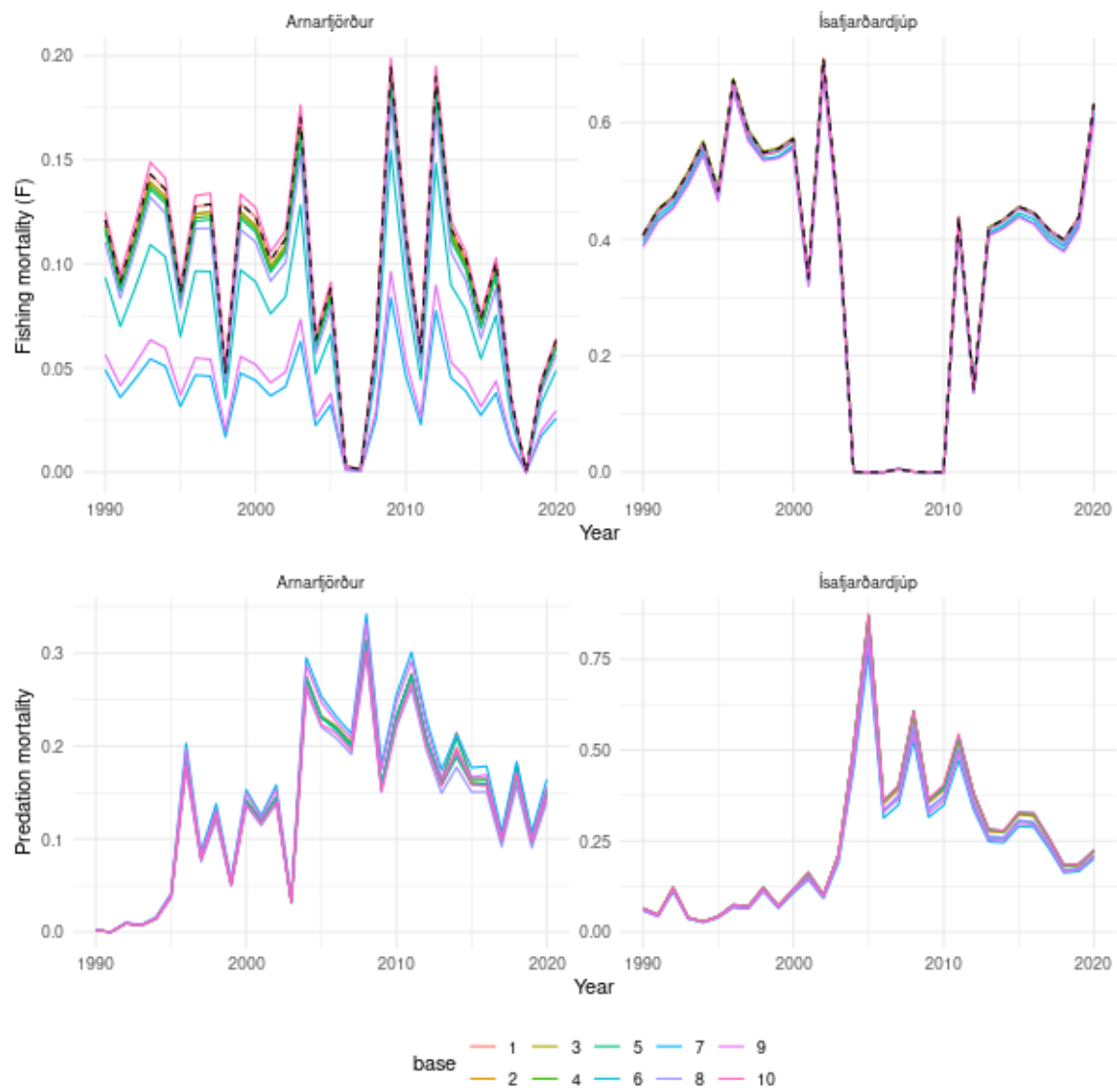


Figure 21: Fishing mortality and predation mortality estimates by fjord across base models represented by colors.

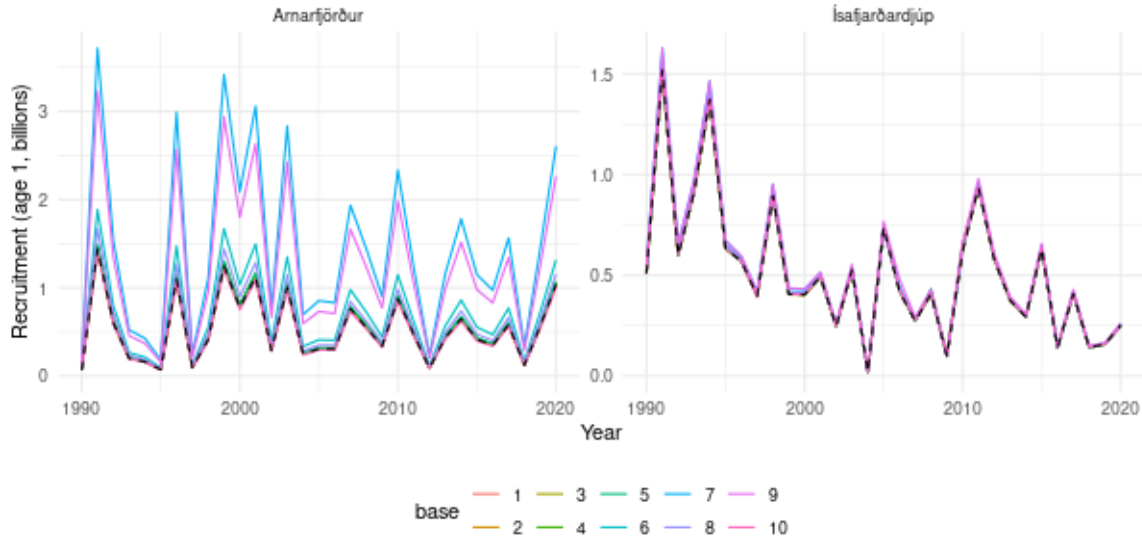


Figure 22: Recruitment estimates by fjord across base models represented by colors.

## 5 Parametric bootstrap results

Survey indices as calculated for input into the Gadget model are shown in Figure 24 from the autumn and winter surveys. Black lines indicate the frequencies of observed indices having a certain value across all years of data. The observed data are the same across all 10 base models, so only a single black line is shown. Indices generated to form the 10 replicates for each base model were designed to closely follow the same distributions as original data (colored lines; frequencies calculated across years and replicates in Figure 24).

Length distribution data generated as parametric bootstrap replicates correspond well with the actual data observed in autumn and winter surveys. Although the median log proportions of actual data is higher than that of replicates, this is consistent across the full length range across all bases, so is not thought to affect model results. Only differences among length proportions generated within the length distribution is expected to bias population dynamics (i.e., consistently greater larger or smaller shrimp in comparison with the rest of the distribution), so a consistent increase or decrease in median proportion is not expected to bias results (Figures 25 and 26).

Replicate patterns observed by fjord and year support this interpretation that no bias is observed in the shape of generated parametric bootstrap replicates, but rather a slight overestimation of the proportions that is consistent across lengths, years, and areas (Figures 27, 28, 29, and 30).

### 5.1 Fits to parametric bootstrap series

#### 5.1.1 Fits to parametric bootstrap index series

Fits to the parametric bootstrap index series appear to adequately represent the base model fits, as medians of the predicted values from parametric bootstrap fits are similar to the base model fits (Figures 31, 32, 33, and 34).

Length distributions generated by the parametric bootstrap were highly variable but, but predictions coming from model fits to the parametric bootstrap replicates followed a similar pattern as predictions generated from the original fit to model data (Figure 35).

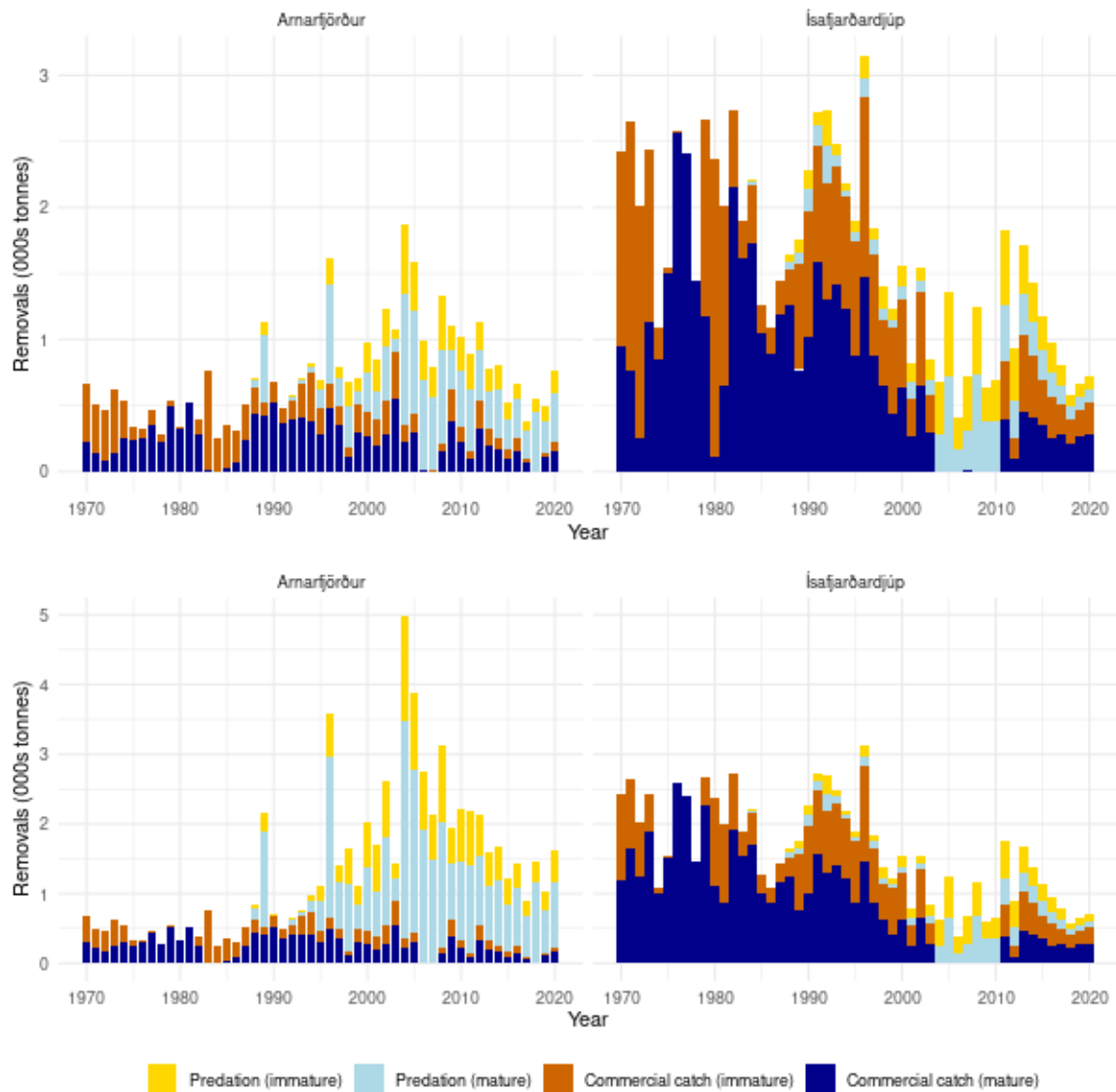


Figure 23: Biomass removals in the form of reported commercial catches by fjord and predation removal estimates, each with proportions estimated between mature and immature stock components, based on the best-fit model (base 1, top), or the model with the highest estimated absolute biomass levels within Arnarfjörður (base 7, bottom).

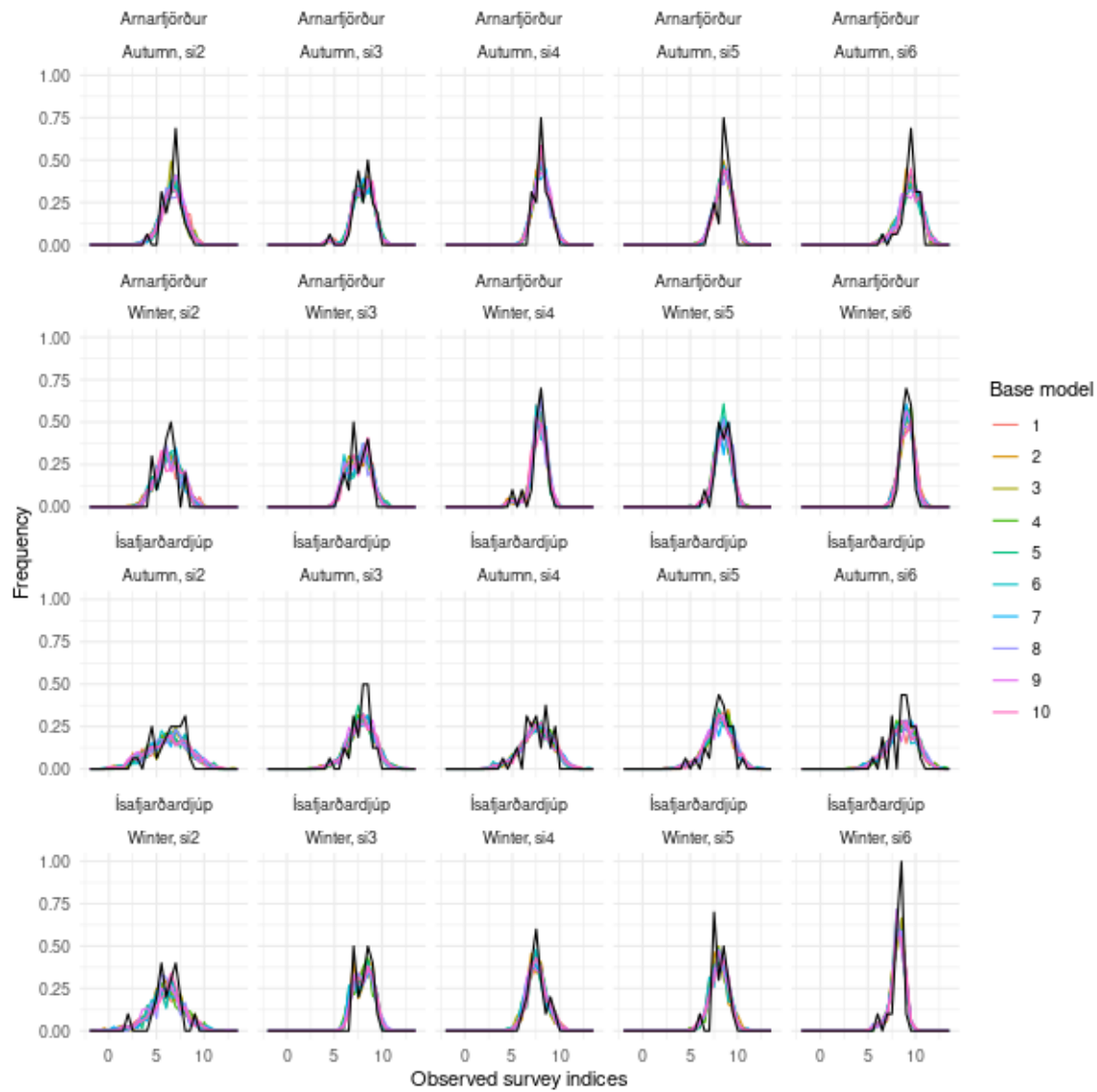


Figure 24: Observed survey index frequencies across years (black lines) are compared with those generated as parametric bootstrap replicates (colored lines) for each of the 10 base models (10 replicates each).

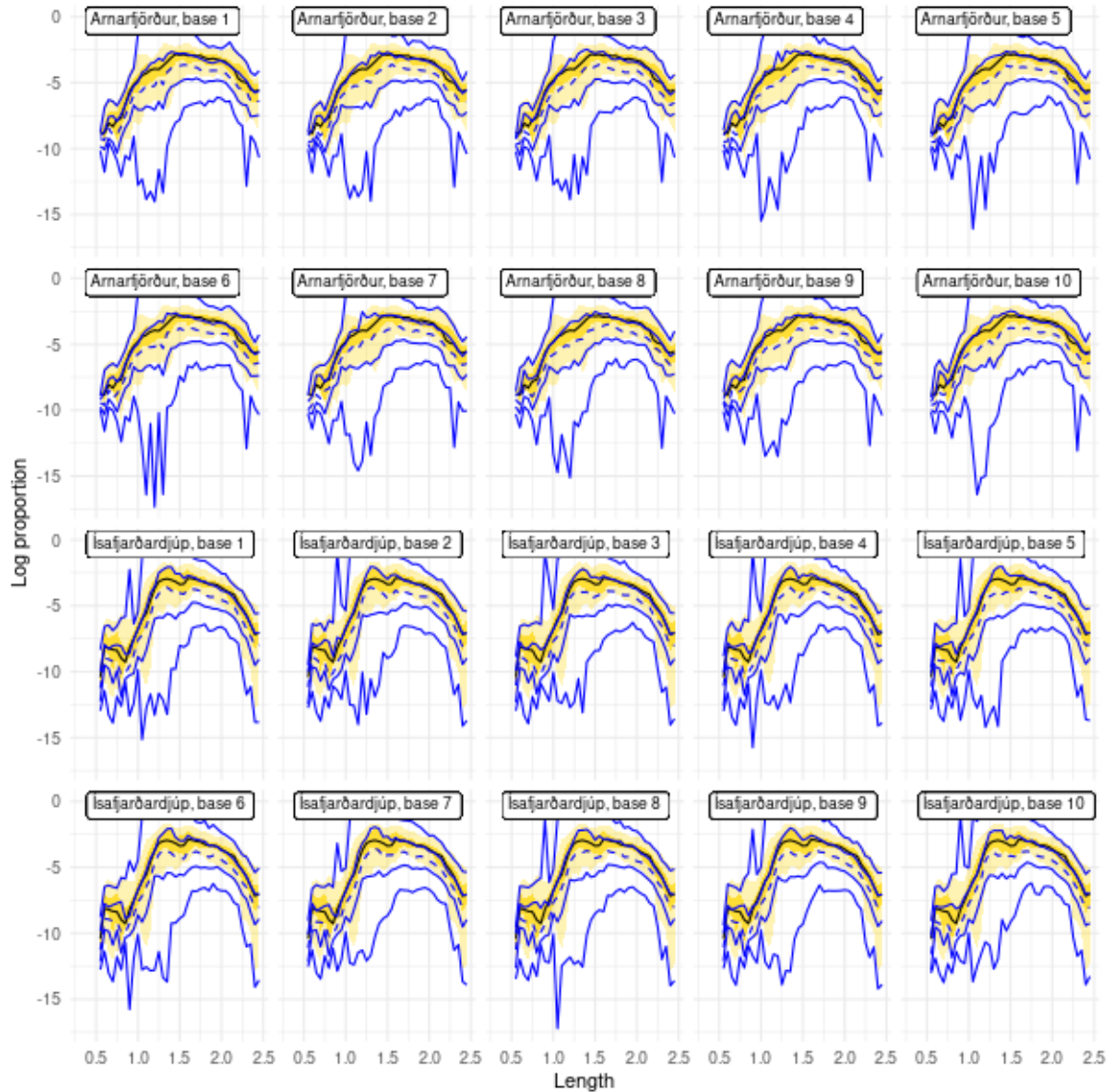


Figure 25: Proportions on the log scale of shrimp carapace lengths observed across years in autumn surveys compared with those generated as parametric bootstrap replicates for each base model. Actual data, which are the same across baselines, are represented by the black line (median) and yellow ribbons. Inner ribbons represent the 50th percentile range and outer edges represent the 95th percentile range. Blue lines represent the median (dashed), 50th percentile range (inner solid lines), and 95th percentile range (outer blue lines), calculated across years and the 10 replicates per base.



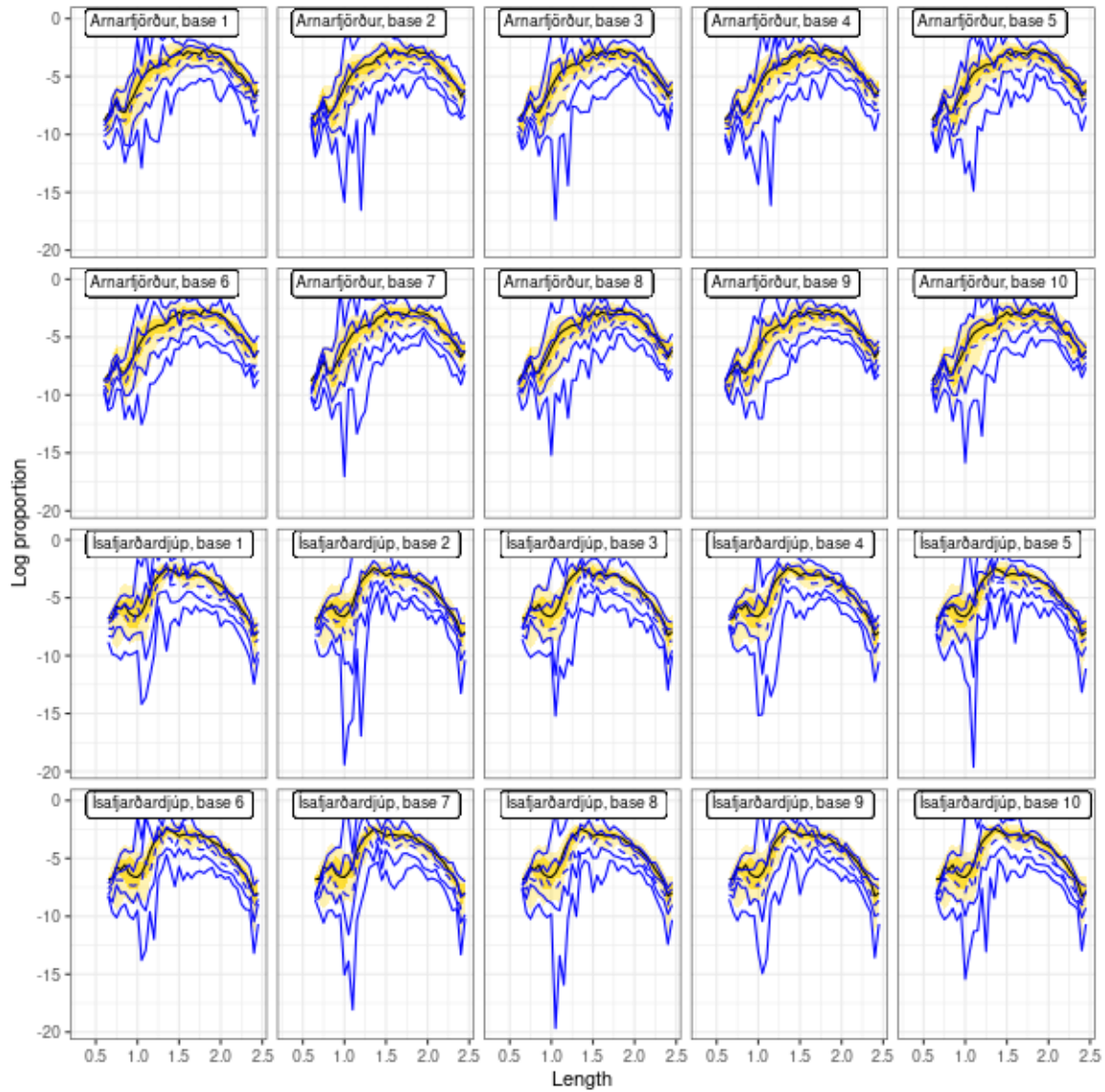


Figure 26: Proportions on the log scale of shrimp carapace lengths observed across years in winter surveys compared with those generated as parametric bootstrap replicates for each base model. Actual data, which are the same across baselines, are represented by the black line (median) and yellow ribbons. Inner ribbons represent the 50th percentile range and outer edges represent the 95th percentile range. Blue lines represent the median (dashed), 50th percentile range (inner solid lines), and 95th percentile range (outer blue lines), calculated across years and the 10 replicates per base.

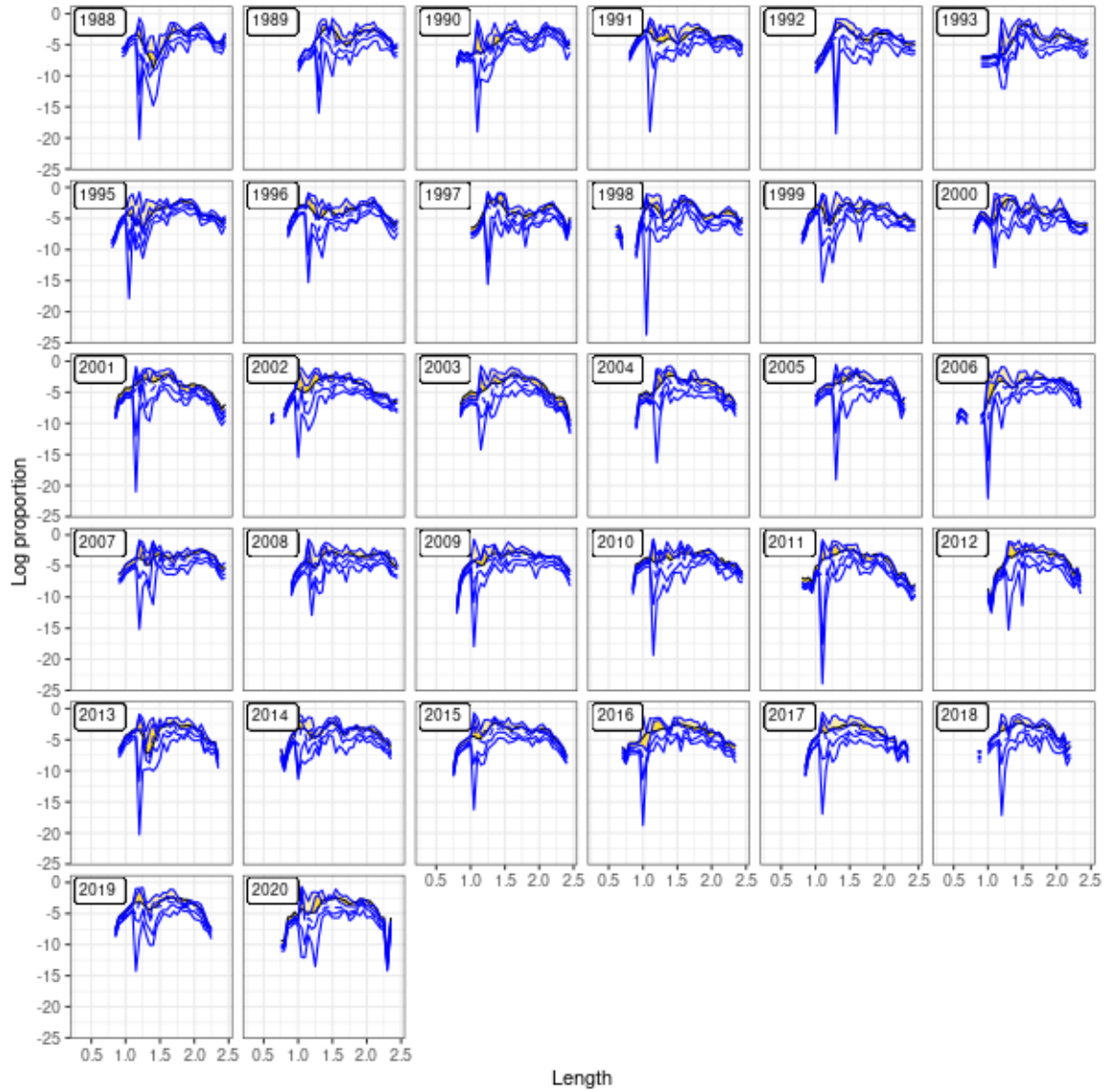


Figure 27: Proportions on the log scale by year of shrimp carapace lengths observed in autumn surveys in Arnarfjörður compared with those generated as parametric bootstrap replicates for base model 1 only. Actual data are represented by the black line (median) and yellow ribbons. Inner ribbons represent the 50th percentile range and outer edges represent the 95th percentile range. Blue lines represent the median of parametric bootstrap replicates (dashed), 50th percentile range (inner solid lines), and 95th percentile range (outer blue lines).

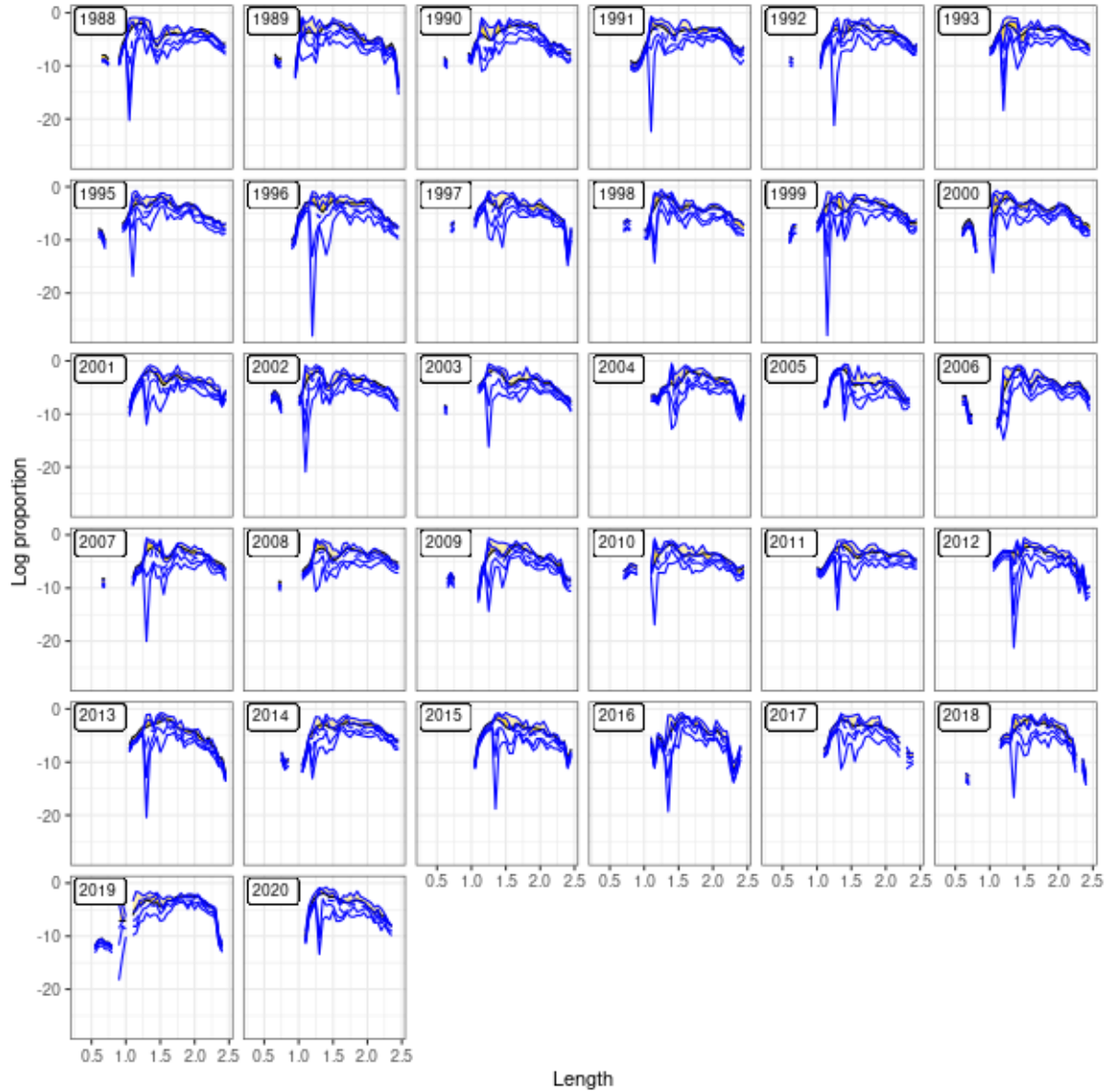


Figure 28: Proportions on the log scale by year of shrimp carapace lengths observed in autumn surveys in Ísafjarðardjúp compared with those generated as parametric bootstrap replicates for base model 1 only. Actual data are represented by the black line and yellow ribbons. Inner ribbons represent the 50th percentile range and outer edges represent the 95th percentile range. Blue lines represent the median of parametric bootstrap replicates, 50th percentile range (inner solid lines), and 95th percentile range (outer blue lines).

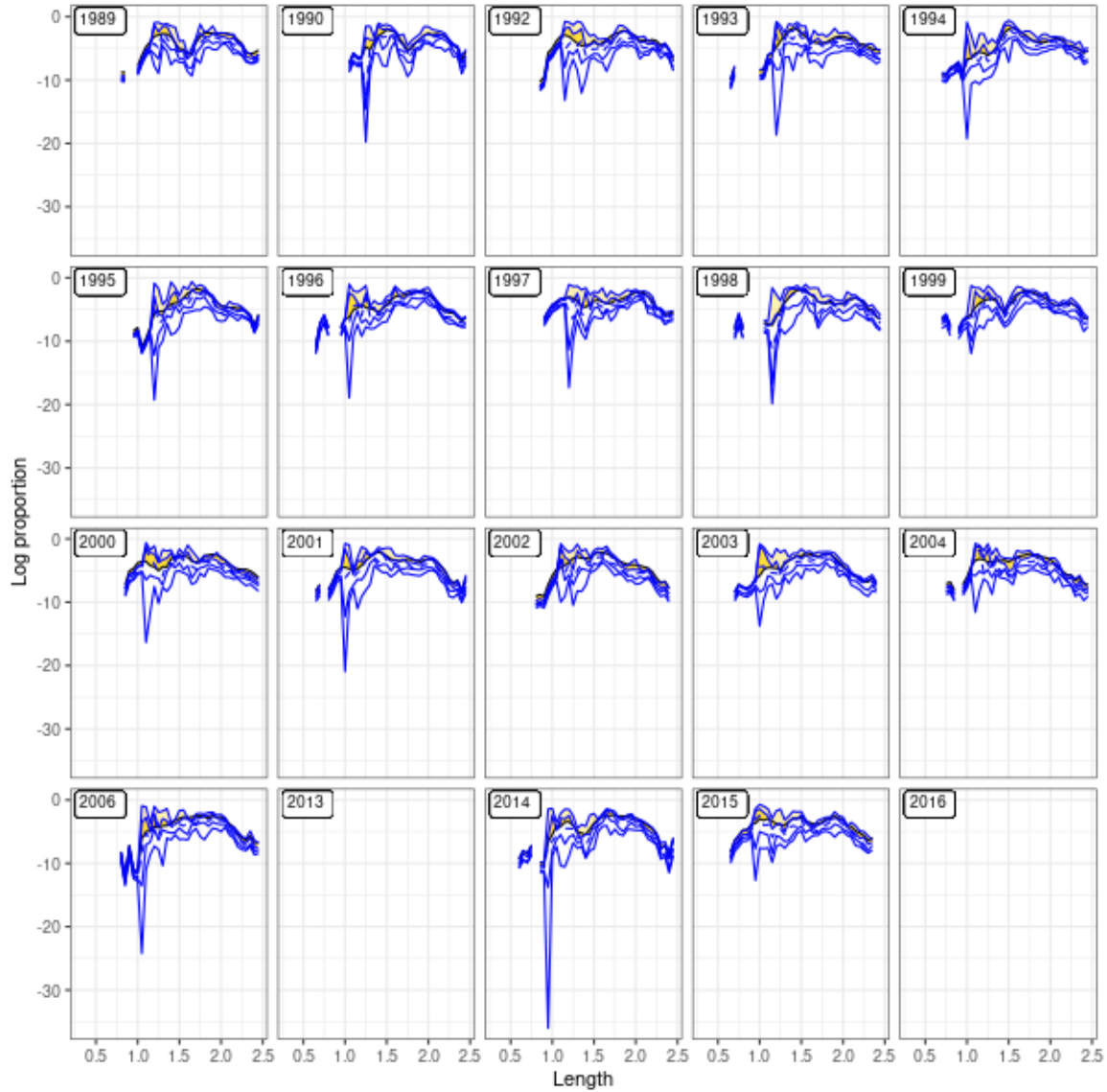


Figure 29: Proportions on the log scale by year of shrimp carapace lengths observed in winter surveys in Arnarfjörður compared with those generated as parametric bootstrap replicates for base model 1 only. Actual data are represented by the black line and yellow ribbons. Inner ribbons represent the 50th percentile range and outer edges represent the 95th percentile range. Blue lines represent the median of parametric bootstrap replicates, 50th percentile range (inner solid lines), and 95th percentile range (outer blue lines).

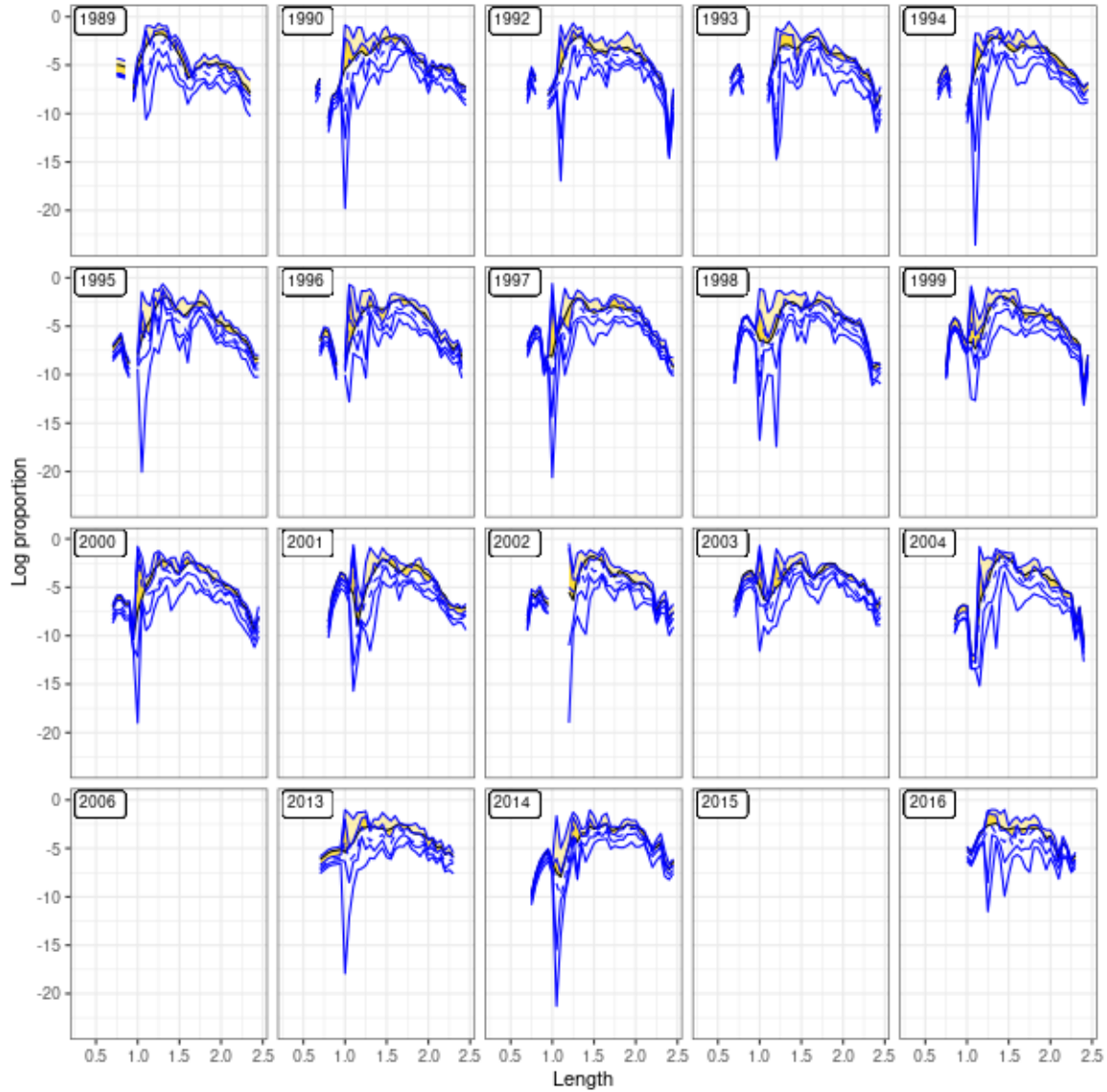


Figure 30: Proportions on the log scale by year of shrimp carapace lengths observed in winter surveys in Ísafjarðardjúp compared with those generated as parametric bootstrap replicates for base model 1 only. Actual data are represented by the black line and yellow ribbons. Inner ribbons represent the 50th percentile range and outer edges represent the 95th percentile range. Blue lines represent the median of parametric bootstrap replicates, 50th percentile range (inner solid lines), and 95th percentile range (outer blue lines).



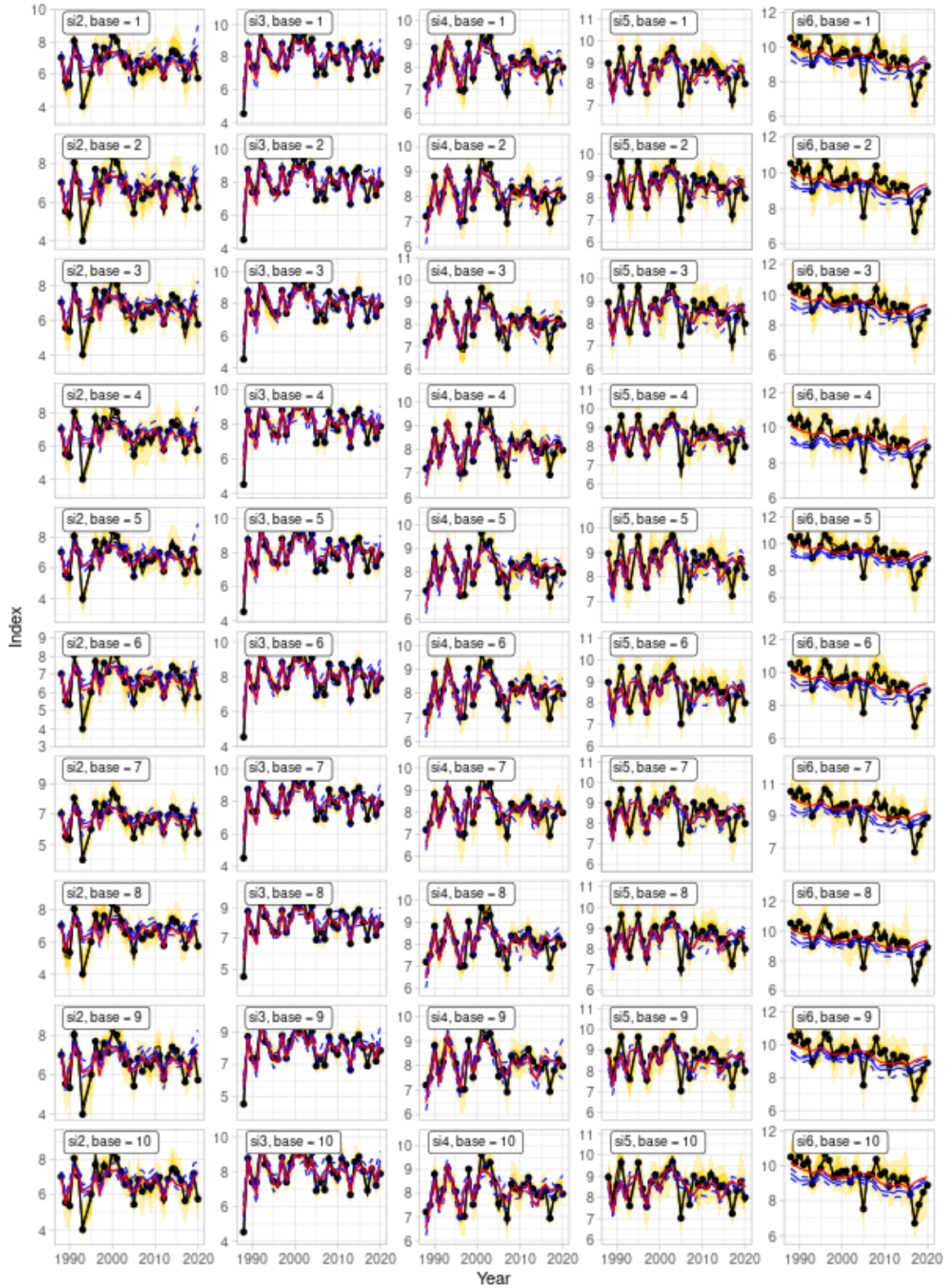


Figure 31: Fits to the parametric bootstrap survey index data replicates from the Autumn survey in Arnarfjörður. Columns correspond with survey indices and the 10 rows correspond with bases. Original data are represented by black lines and points. Original model fits are represented by the red lines. The black line is the bootstrap median and the yellow area is the 5 and 95% percentiles of the parametric bootstrapped indices. The blue solid line is the median of the predicted indices from the bootstrap runs; the blue dotted lines are the 5 and 95% percentiles.

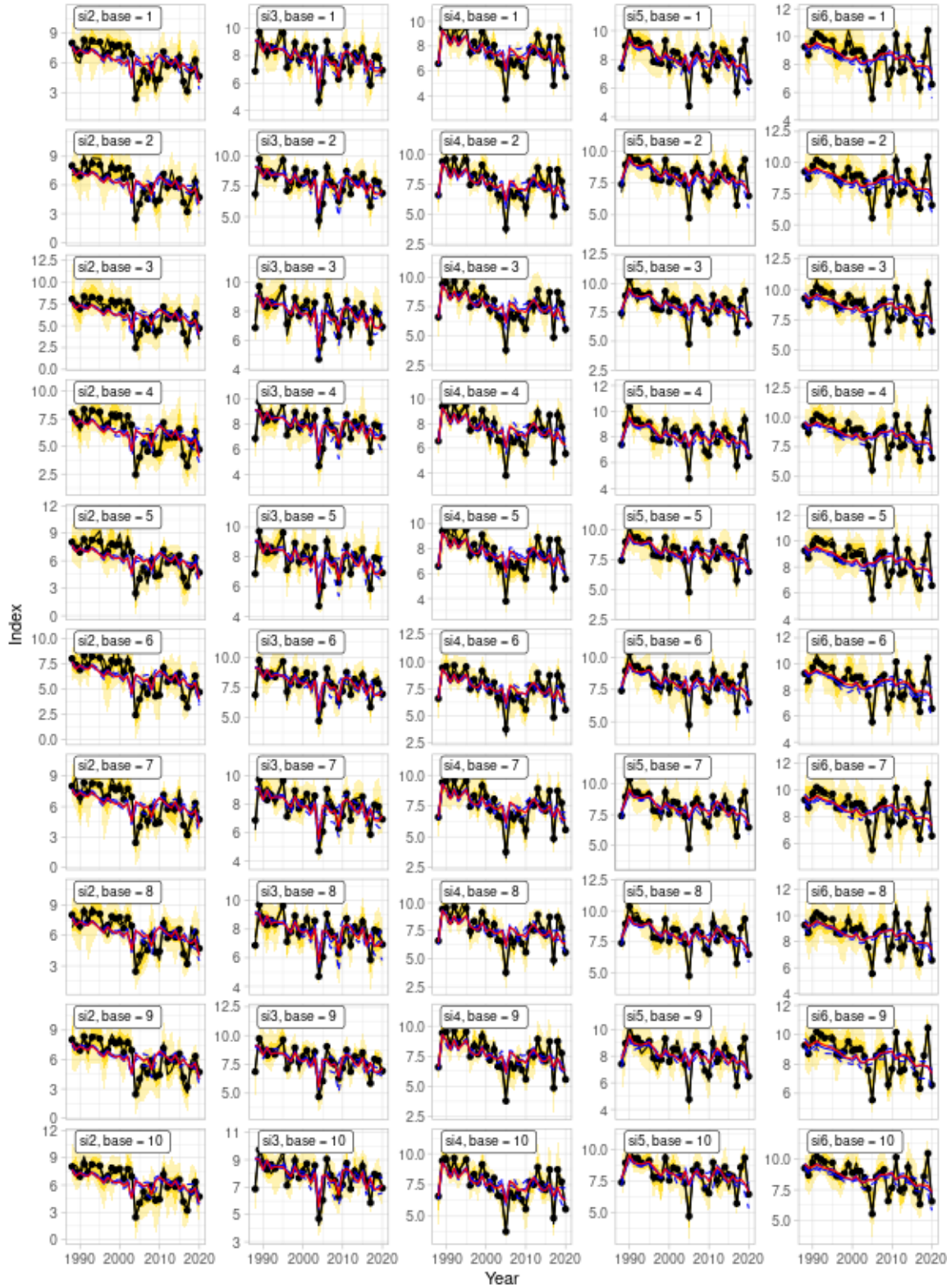


Figure 32: Fits to the parametric bootstrap survey index data replicates from the Autumn survey in Ísaf-jarðardjúp. Columns correspond with survey indices and the 10 rows correspond bases. Original data are represented by the black lines and points. Original model fits are represented by the red lines. The black line is the bootstrap median and the yellow area is the 5 and 95% percentiles of the parametric bootstrapped indices. The blue solid line is the median of the predicted indices from the bootstrap runs; the blue dotted lines are the 5 and 95% percentiles.

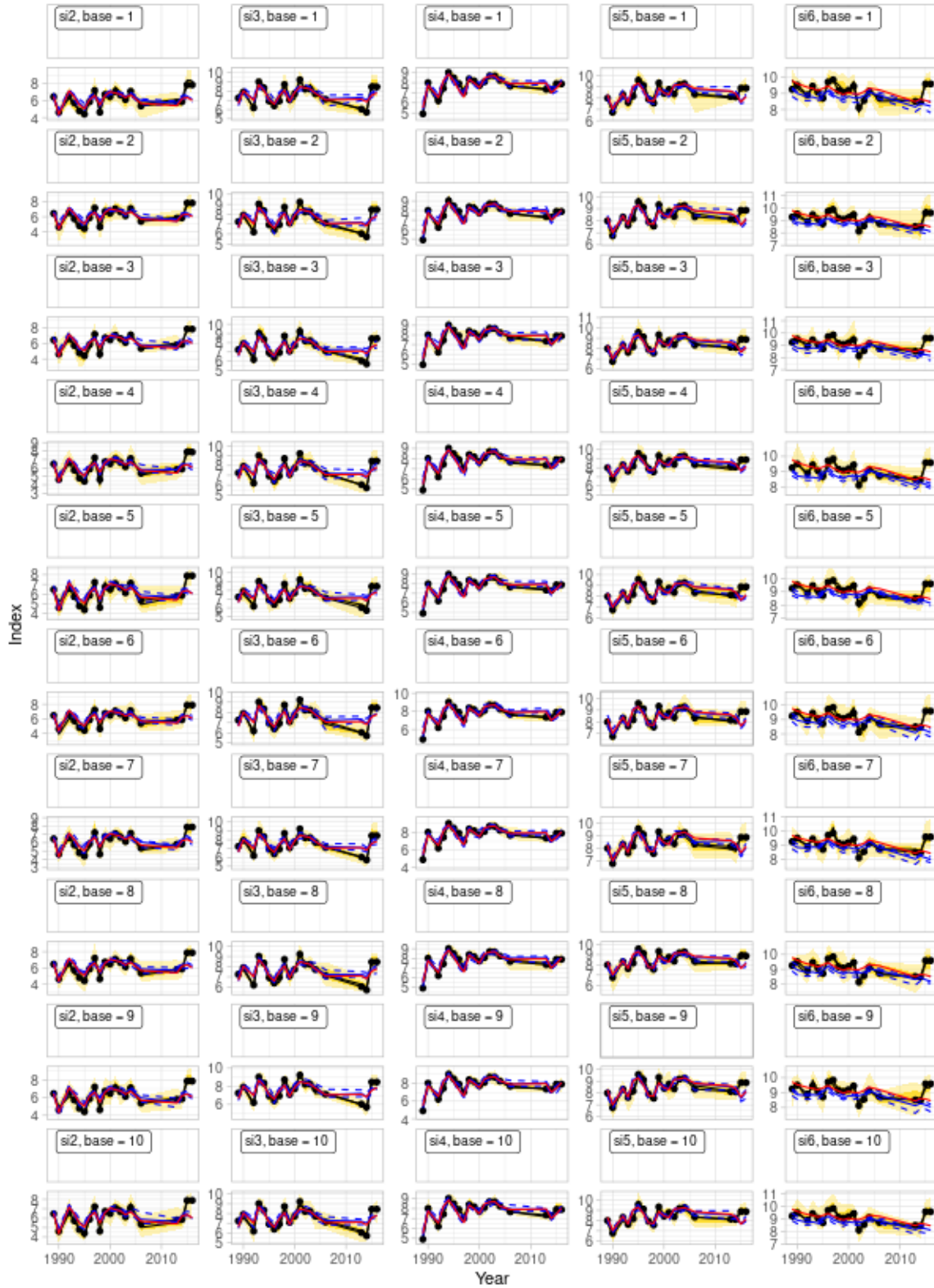


Figure 33: Fits to the parametric bootstrap survey index data replicates from the Winter survey in Arnarfjörður. Columns corresponds with survey indices and the 10 rows correspond with bases. Original survey index data are represented by black lines and points. Original model fits are represented by the red lines. The black line is the bootstrap median and the yellow area is the 5 and 95% percentiles of the parametric bootstrapped indices. The blue solid line is the median of the predicted indices from the bootstrap runs; the blue dotted lines are the 5 and 95% percentiles. 56



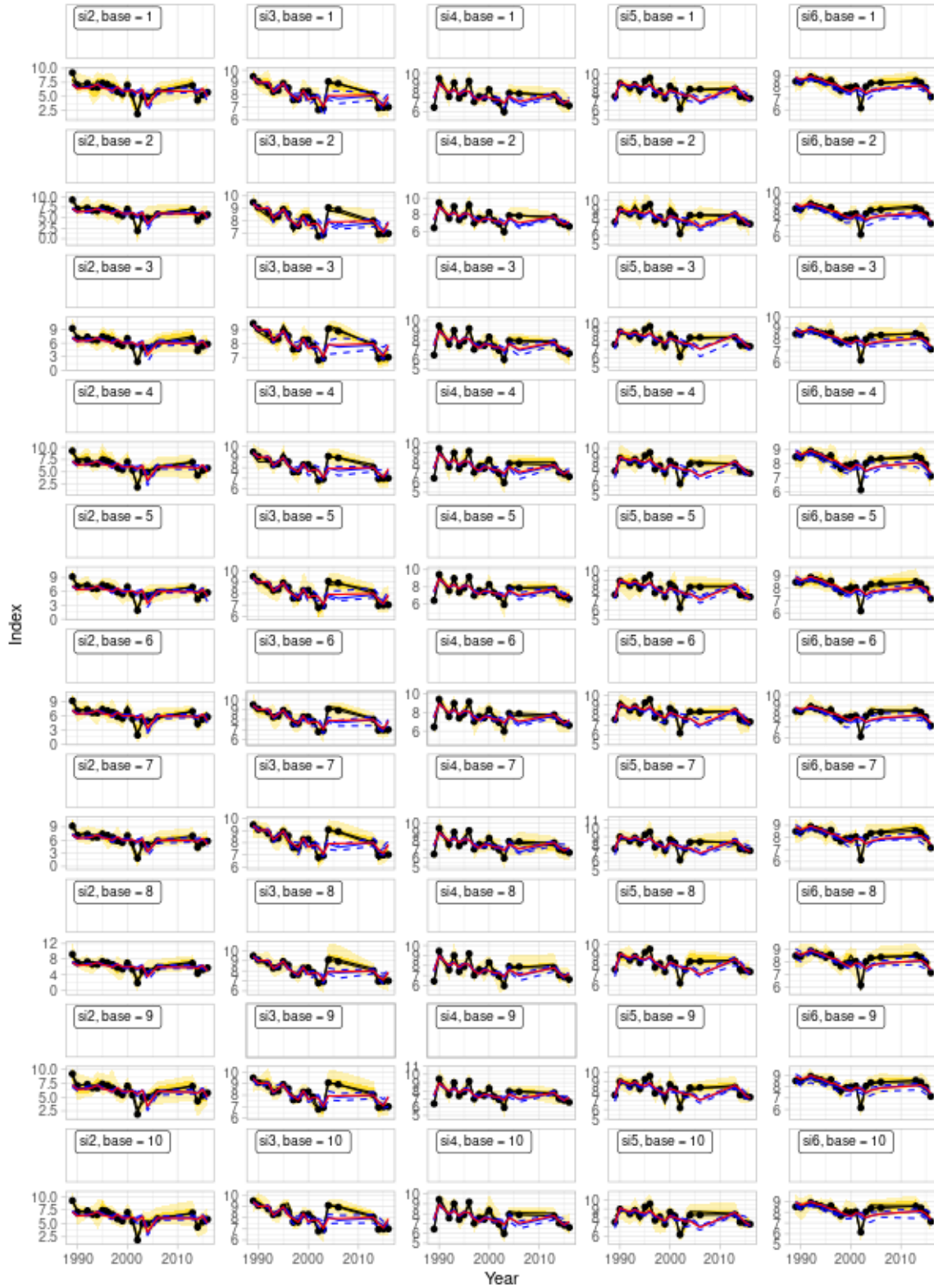


Figure 34: Fits to the parametric bootstrap survey index data replicates from the Winter survey in Ísafjardardjúp. Columns correspond with survey indices and the 10 rows correspond with bases. Original survey index data are represented by the black lines and points. Original model fits to these data are represented by red lines. The black line is the bootstrap median and the yellow area is the 5 and 95% percentiles of the parametric bootstrapped indices. The blue solid line is the median of the predicted indices from the bootstrap runs; the blue dotted lines are the 5 and 95% percentiles.

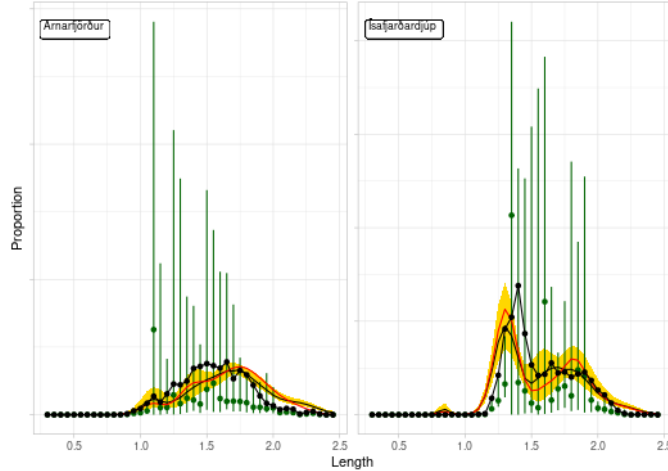


Figure 35: Example of a fit to a parametric bootstrap generated length distribution from the Autumn survey samples compared with model estimates to the parametric bootstrap data (from 2017, step 4, base model 1). Green points and vertical bars denote the median and 95% interval of the parametric bootstrap distribution of observed values, while the solid lines and golden ribbon the median and 95% intervals of the predictions by the model after fitting to the bootstrapped data. The black line with points indicates the original data and the solid red line indicates the fit to these data from the baseline model.

### 5.1.2 Parameter estimates

In some cases, the parameter estimates rarely hit the set parameter boundaries in the base and bootstrap runs, while in other cases they almost exclusively were estimated at the boundary. In these latter cases, hitting the boundary has essentially the same effect as fixing these parameters. In most cases, those hitting boundaries were not expected to affect population dynamics, such as parameters affecting maturity, including  $\lambda_2$  (Figure 36),  $\lambda_2$  was fixed due to difficulties in estimation) and annual  $l_{50}$  maturation estimates (Figure 37). Differences in these parameters may instead slightly affect calculation of absolute levels of spawning stock biomass and  $B_{lim}$  of individual simulations. However, as biomass scales are already variable due to difficulties in calculating catchability (see section **Base model results** above), results are later analysed relative to simulation-specific  $B_{lim}$  values, so this effect likely has minimal impact on model interpretations.

In other cases, parameters likely have an effect on population dynamics and are hitting a boundary because of greater flexibility in the model that leaves some particular parameters poorly determined (Figure 36). For example, the mature-stock growth rate parameter  $k$  and the immature growth coefficients  $\alpha_{k1}$ ,  $\alpha_{k2}$ , and  $\beta_b$ , which control temperature dependence, hit bounds and could not be estimated. The immature growth coefficient  $\beta_s$  was fixed to 0 and beta binomial growth dispersion parameters were fixed to their base-model values because of difficulties in estimation. These in indicates that allowing growth rates to differ among immature and mature stock components and allowing for annual estimation of maturation has enough flexibility to fit growth patterns in the data without additional parameters being well estimated. Similarly,  $c_0$ , suitability estimated for predators below 45 cm length, was poorly determined, but this may be a reflection of  $q_{pred}$  parameters being rather well-determined and accounting for most of the explainable variation in the data. In addition, some of the parameters, including  $q_{pred,1}$ ,  $l_{50,f}$ , and  $l_{50,45}$  were not centered around the base model estimates. Although somewhat concerning, the total variation in these estimates was quite small compared to bounds. For example,  $q_{pred,1}$  bounds ranged 0.0001 – 1,  $l_{50,f}$  bounds ranged 0.4 – 2.4, and  $l_{50,45}$  bounds ranged 2.0 – 2.4, so despite the lack of centering, obtained values were not unreasonably far from original model estimates.

Estimates of recruitment parameters are shown in Figure 38. As explained in the methods, upper bounds were varied in a grid search because of several recruitment upper bounds being reached in individual model optimizations. Therefore, it was not uncommon in model results for recruitment estimates to equal the upper bounds, but most estimates also showed a spread among several values obtained and estimates are

close to the median values (Figure 38). The estimated initial population is illustrated in Fig. (Figure 39). As in the case of the estimated recruitment little discernible bias was observed in the base compared with the bootstrap medians.

Preliminary studies indicated that catchability estimates resulting from base models were substantially lower than those obtained when models were fit to the parametric bootstrap replicates. As a result, catchabilities were fixed to those estimated in the base models when fitting parametric bootstrap replicates. The values used are shown as dome-shaped in Arnarfjörður and roughly logistic in Ísafjarðardjúp in autumn surveys, but dome-shaped in both locations in winter surveys (Figures 40 and 41).

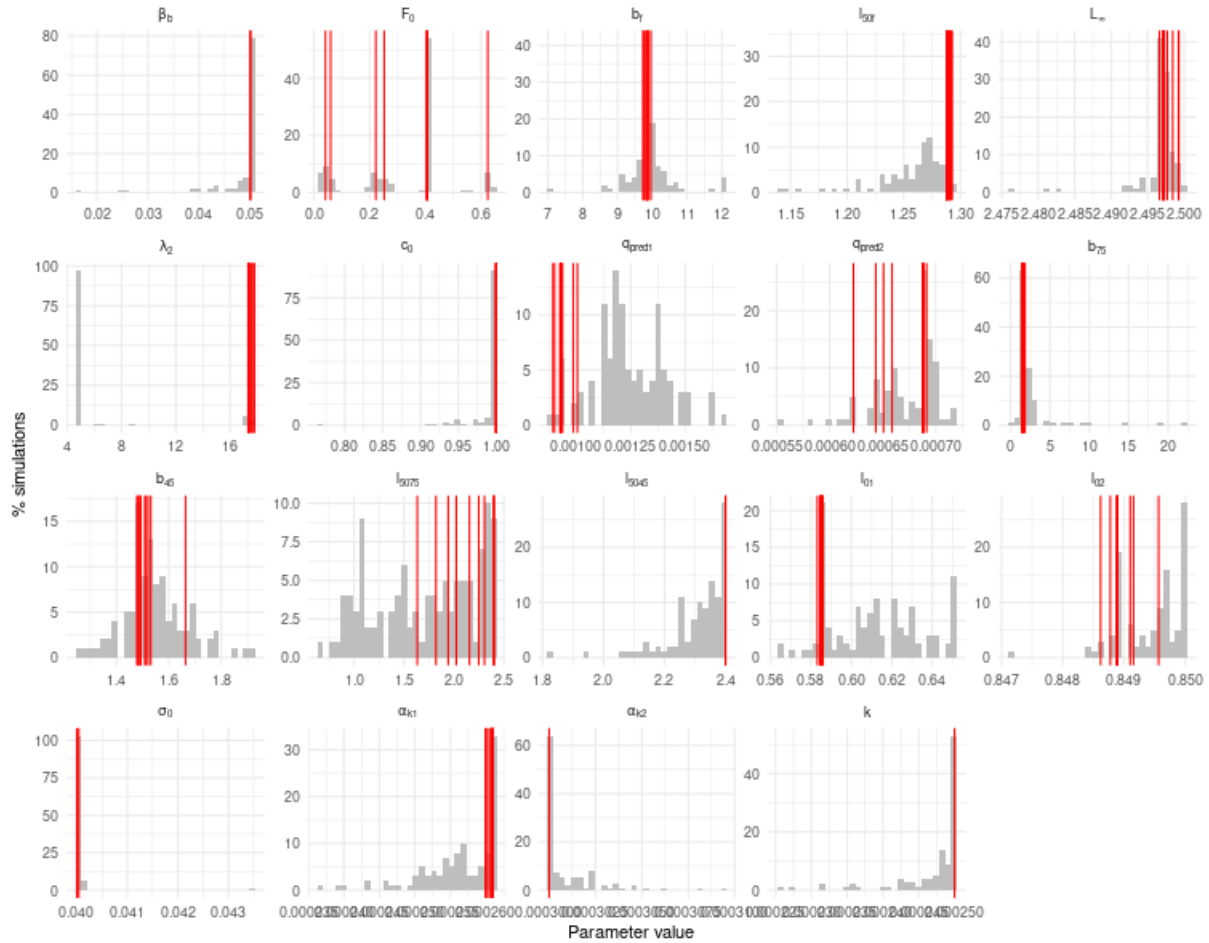


Figure 36: Histogram of parameter estimates from 100 bootstrap samples. The red line indicates the estimates from the base runs. The  $\beta_0$  and  $\beta_1$  originate from the beta-binomial distributions reflecting growth of immature ( $s=0$ ) or mature ( $s=1$ ) shrimp, whereas  $\beta_b$  and  $\beta_s$  indicate coefficients controlling growth rate in immature shrimp related to bottom (b) or surface (s) water temperatures. Subscripts 1 and 2 reflect  $r = \text{Arnarfjörður}$  and  $r = \text{Ísafjarðardjúp}$ , in area  $r$ -specific parameters such as  $\lambda$  (which controls steepness of the logistic maturation function), intercept of immature growth rate ( $\alpha_k$ ), initial length at recruitment  $l_0$ , and catchability of shrimp by predators  $q_{pred}$ . For logistic suitability parameters  $b$  and  $l_{50}$ , where subscripts indicate either selectivity of the survey and commercial fleets ( $f$ ), all predators (cod, haddock, and whiting) above 45 cm ( $h = 45$ ), or all predators above 75 cm ( $h = 75$ ). Constant suitability estimated for predators below 45 cm length was represented by  $c_0$ .

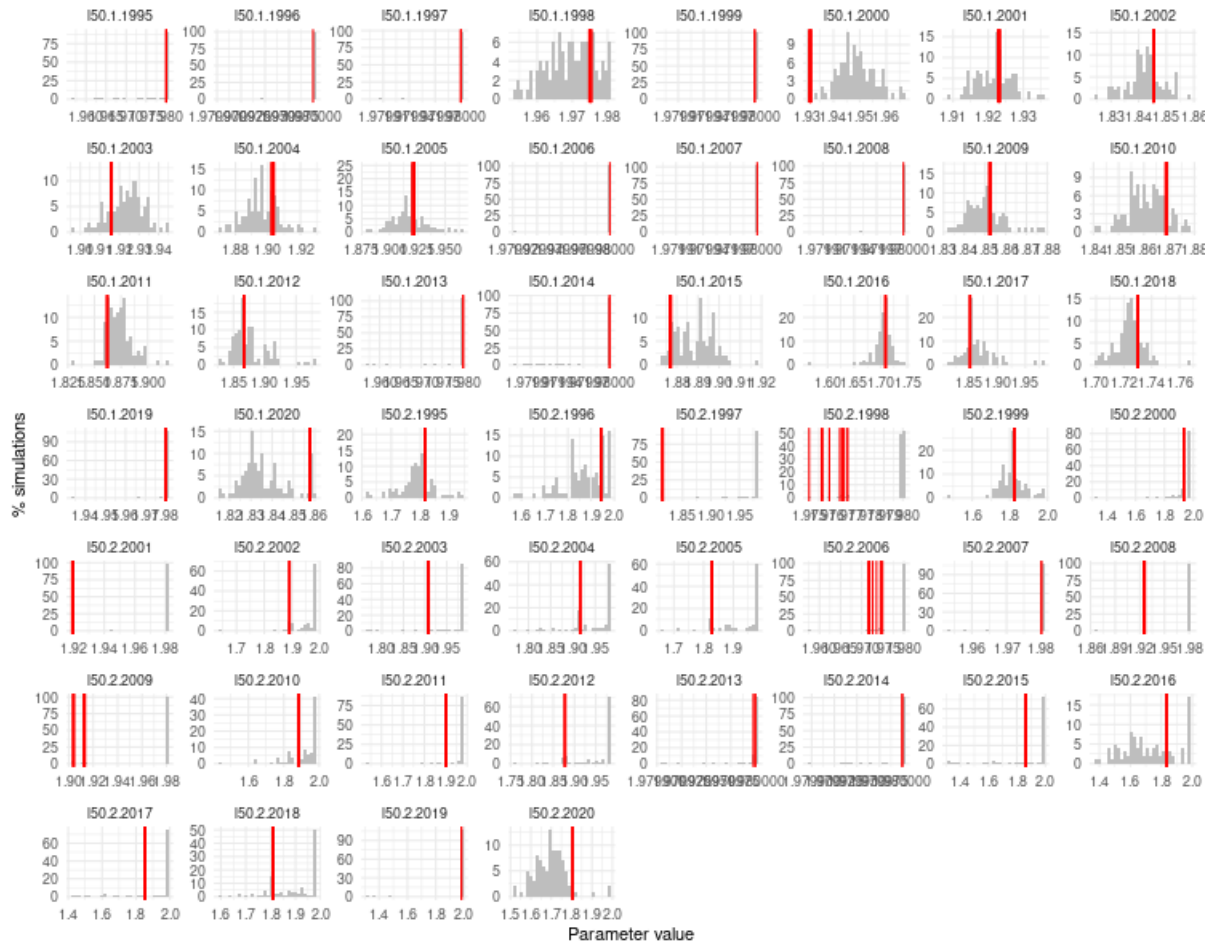


Figure 37: Histogram of  $l_{50}$  annual maturity parameter estimates from 100 bootstrap samples. Parameters are labeled by area and year

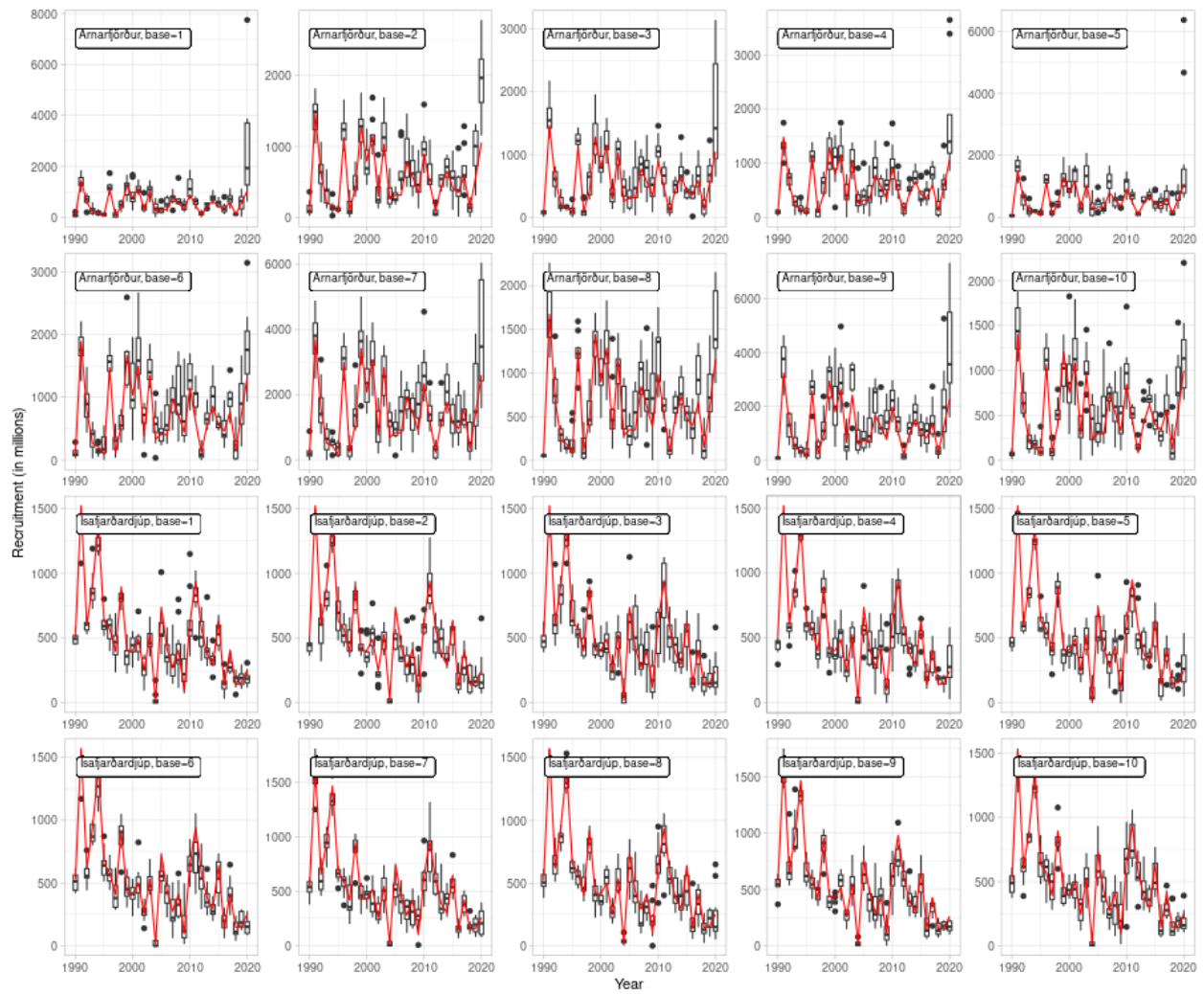


Figure 38: Boxplots of annual recruitment (age 0) bootstrap estimates, the red line indicates the estimate from the base run.

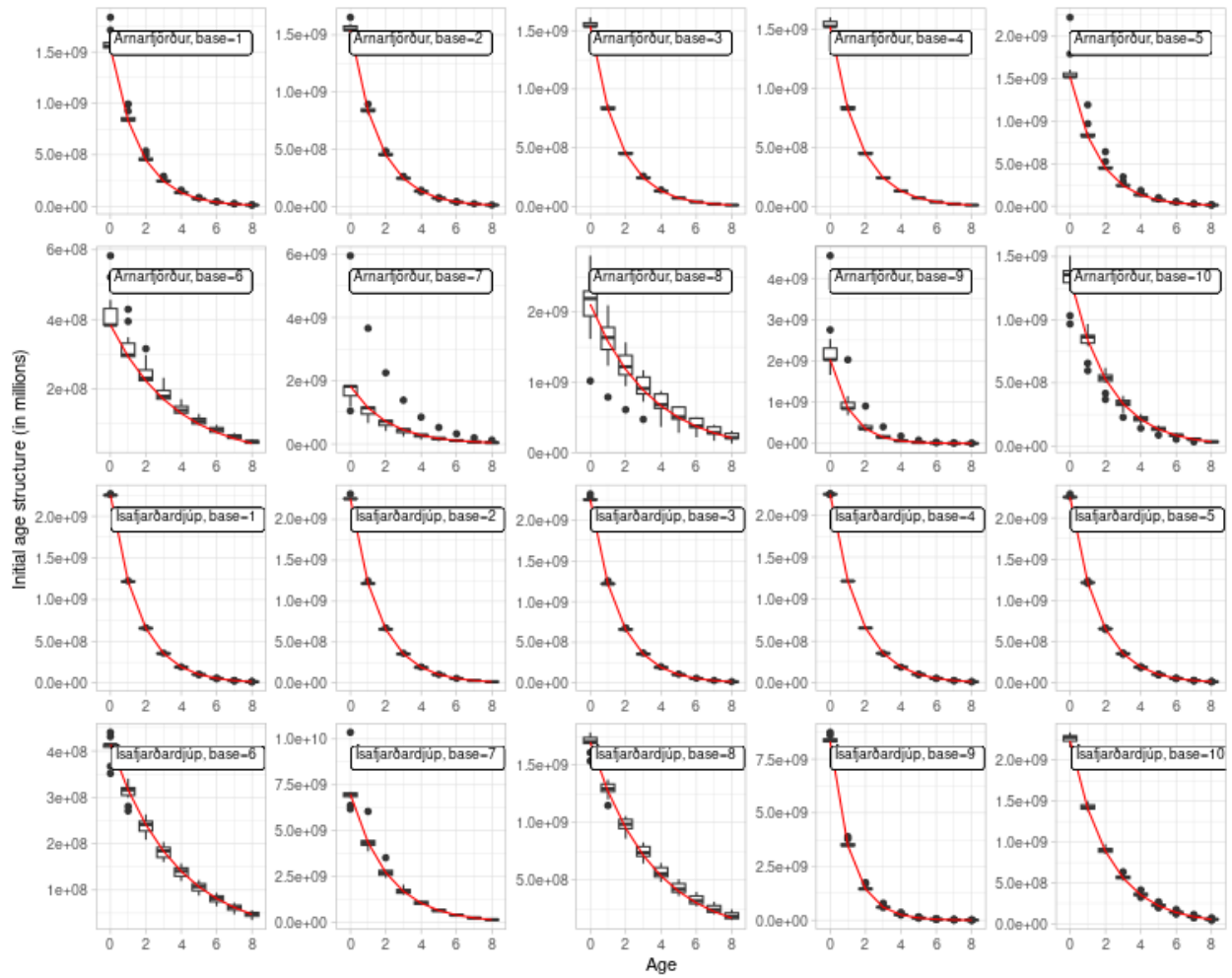


Figure 39: Boxplots of initial age structure bootstrap estimates, the red line indicates the estimate from the base run.

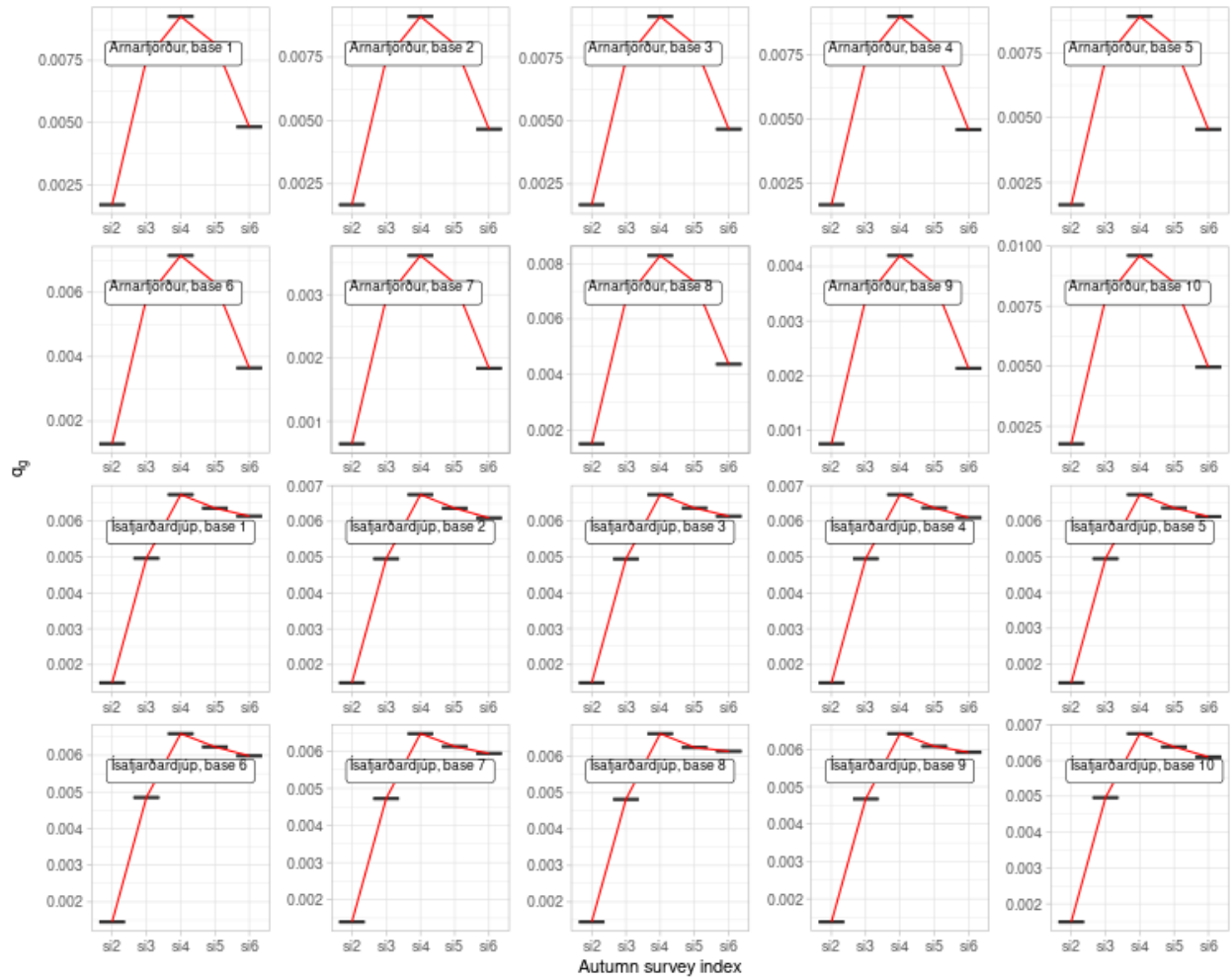


Figure 40: Boxplot of estimated catchability parameters from the autumn survey,  $q_g$ , as a function of the survey index length group.



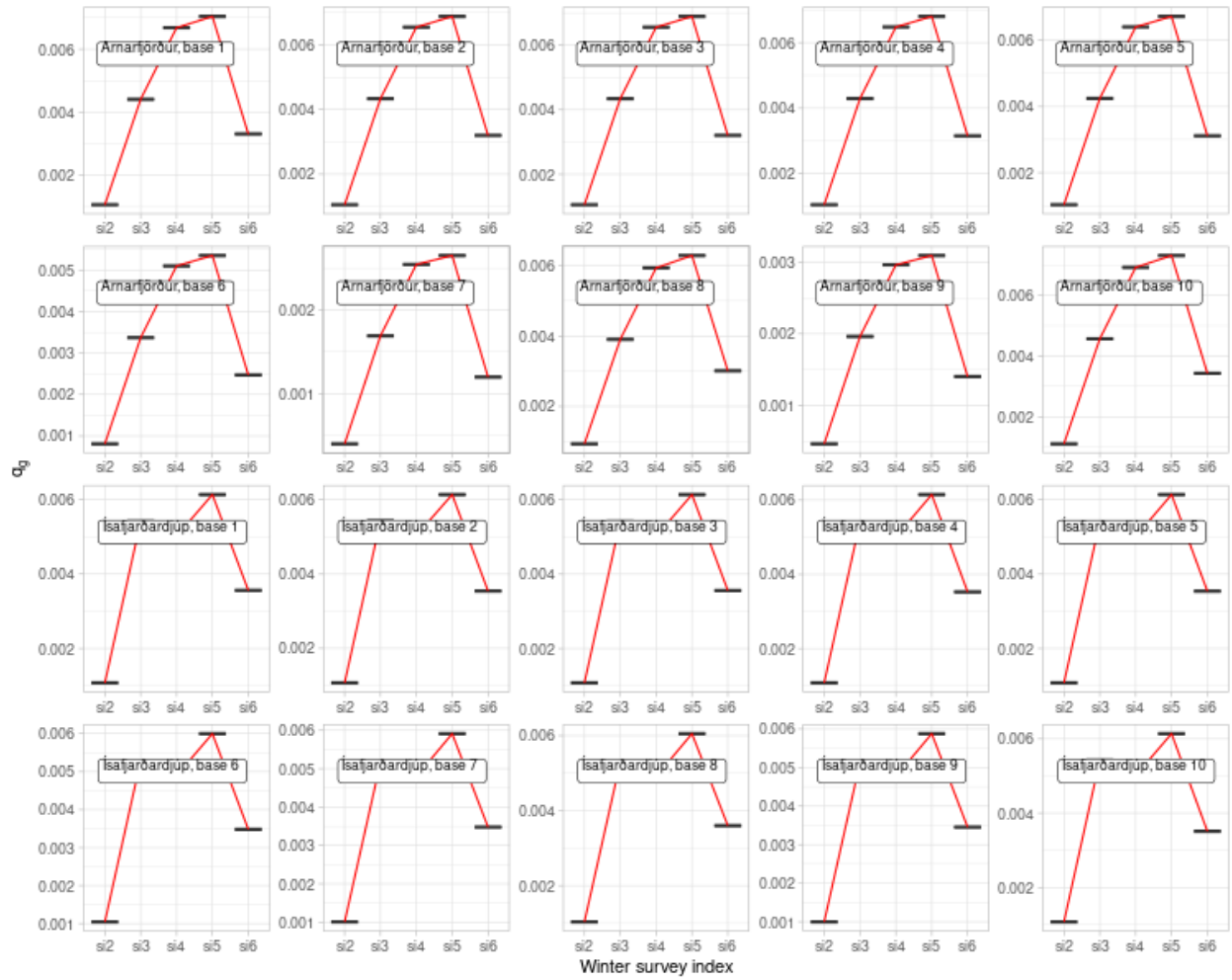


Figure 41: Boxplot of estimated catchability parameters from the winter survey,  $q_g$ , as a function of the survey index length group.



## 5.2 Estimates derived from base models and parametric bootstrap uncertainty

### 5.2.1 Growth

No age data are inputted to the model, so age information is taken from bounds of reasonable values and cohort structure inherent in carapace length distribution data. Growth as depicted here are mean and standard deviations of shrimp predicted to be in the simulated population at a certain age, and therefore already take into account past years of natural, fishing, and predation mortality. The model estimates individuals to be larger at a given age in Ísafjarðardjúp, but sizes begin converge at higher ages. Standard deviation of mean carapace length is especially high at middle age ranges, and remaining high for Ísafjarðardjúp (Figure 42).

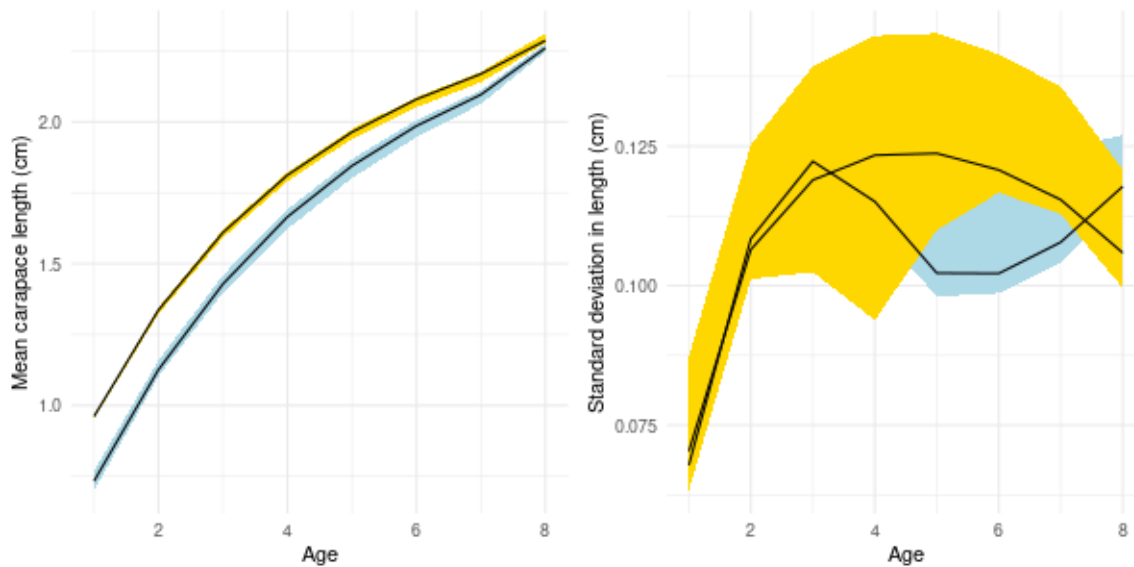


Figure 42: Estimates of growth from parametric bootstrap replicates. Medians are represented by the black lines and 95th percentile ranges are represented by blue (Arnarfjörður) or yellow (Ísafjarðardjúp) ribbons.

### 5.2.2 Selectivity

The estimated selection curves implemented for all commercial and survey fleets, which are not expected to differ greatly due to similarities in gear, are shown in Figure 43 along with the respective bootstrap 95% interquartile range. The length at which 50% of individuals are selected was approximately 1.3 cm.

### 5.2.3 Population estimates

Model results of population estimates from fitting 10 parametric bootstrap replicate to each of the 10 base modes are shown by base model (colors and panels) for each fjord. Both biomass and recruitment have large ranges in biomass or number values, likely as a result of the high uncertainty in catchability values (Figures 44, 45, and 46. Fishing and predation mortality levels are correspondingly higher for lower biomass models and vice versa (Figures 47 and 48). In all base models, results closely align with the medians of the bootstrap estimates in biomass levels and  $\bar{F}_y$ , especially in the last 5 or so years, and recruitment, especially in the middle range of the model. Therefore, interpretations follow those given for *Base model results* (see above). Results in earlier years of the models differ, likely due to differences in highly uncertain recruitment patterns early in the model when little data are available (i.e., sometimes referred to as a ‘burn-in’ period).

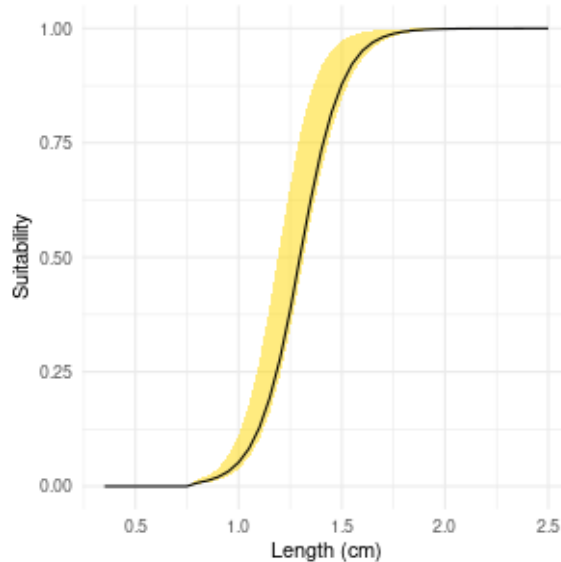


Figure 43: Estimates of selectivity across all fleets from parametric bootstrap replicates. Medians are represented by the black lines and 95th percentile ranges are represented by yellow ribbons.

## 6 Projections

Advice for these stocks is based on an ICES Category 3 stock framework (2022 [2], 2022 [3]), in which short-lived stocks are advised to be managed with a constant harvest rate and an index or biomass trigger value, below which harvest rates should be reduced (ICES [8]). This stock is considered a short-lived stock because of its fast growth rates and highly sporadic recruitment patterns, which are additionally variable due to expected high and variable levels of predation mortality. ICES advises that this constant harvest rate decision rule for short-lived stocks is developed using simulation testing, as done in this study (ICES [8]). ICES technical guidelines for stocks with analytical assessments were used as guidelines for implementing simulations (ICES [7]). These guidelines suggest that target harvest rates should be set as the minimum of either 1) those that produce MSY in the long run, 2) those that cause the population SSB to be maintained at or above  $B_{loss}$  (or a precautionary level above this) in the long term, or 3) those that prevent the population spawning stock biomass from dropping below  $B_{loss}$  with a probability greater than 5%. In this study, we compare harvest rates from the first and third criteria to gain a better understanding of how well current harvest rates are likely to be performing in Arnarfjörður and Ísafjarðardjúp, and only qualitatively analyze long-term SSB levels in relation to  $B_{loss}$ . To do so, the 1000 simulations, derived from 10 model fits to bootstrapped data from 10 base models, each with 10 simulations of recruitment and assessment uncertainty implemented, were projected 50 years into the future to analyze long-term properties of fishing the shrimp populations at a given harvest rate. To perform forward projections, a stock-recruitment relationship and decision rule were implemented as described below. Furthermore, five scenarios of future predation levels were also analyzed to determine the impact of predation on fishing opportunities and management strategies, by projecting predation levels at 25%, 50%, 75%, 100%, and 125% of current levels (i.e., the mean predation level indicated in the last three years of data). Predation levels above these values in preliminary analyses were unsustainable. In addition, several trigger values in addition to the currently implemented triggers were tested, including 50%, 75%, 125%, and 150% of the current trigger. As the current trigger values were chosen based on the 20% of the mean of the 3 highest index values, testing the decision rule with a 75% trigger value implemented also corresponds with NAFO guidelines that indicate setting trigger index values as 15% of the mean of the highest 3 index values would be a sufficient strategy (04/12 [1]).

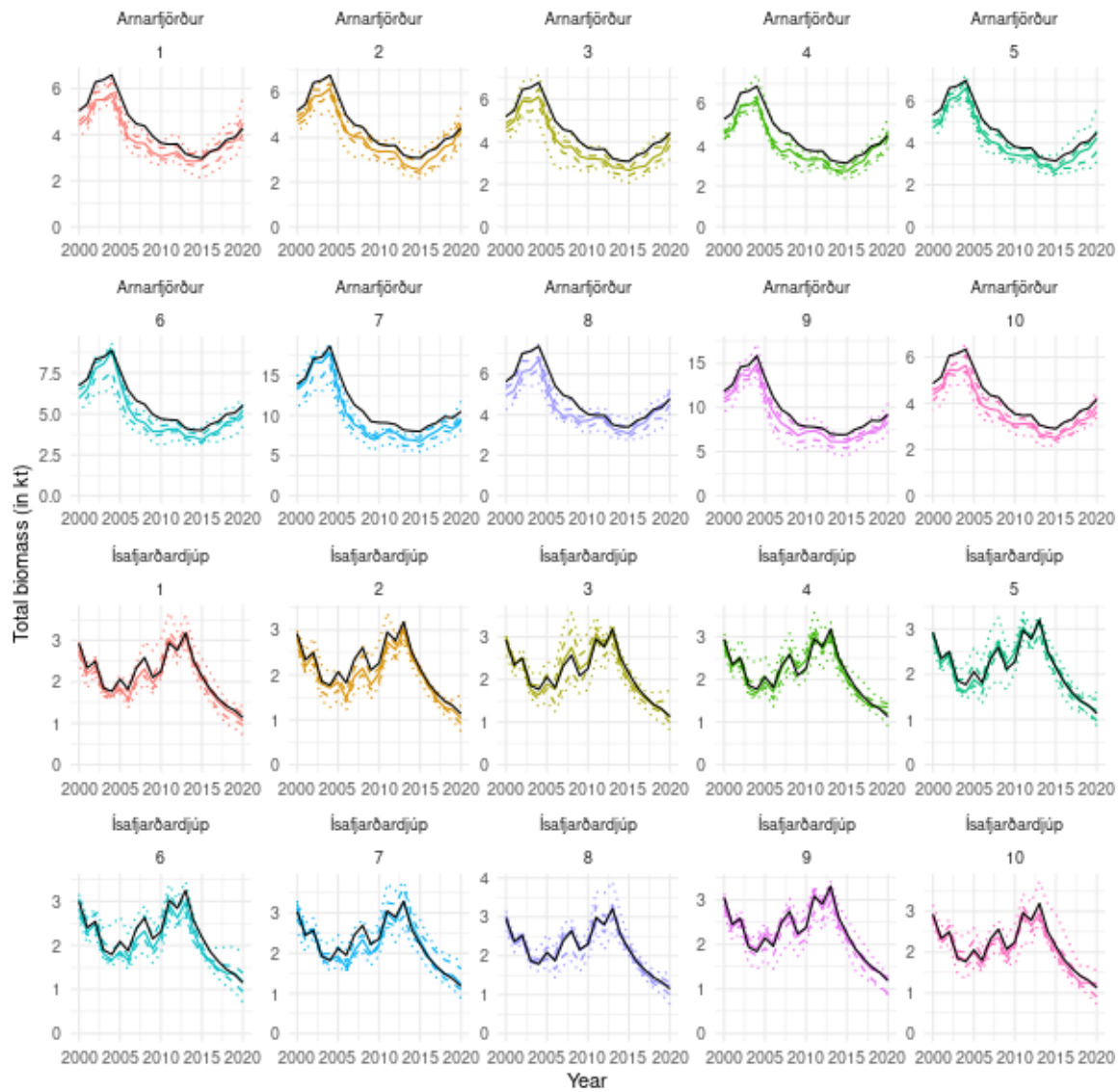


Figure 44: Bootstrap model total biomass results. Colors represent the 10 base models. Each set of solid, dashed, and dotted colored lines represents the median, 50, and 95% intervals of the bootstrapped estimates for a certain base model, as derived from 10 replicates per base model. The solid black lines indicate fits from the 10 base models.

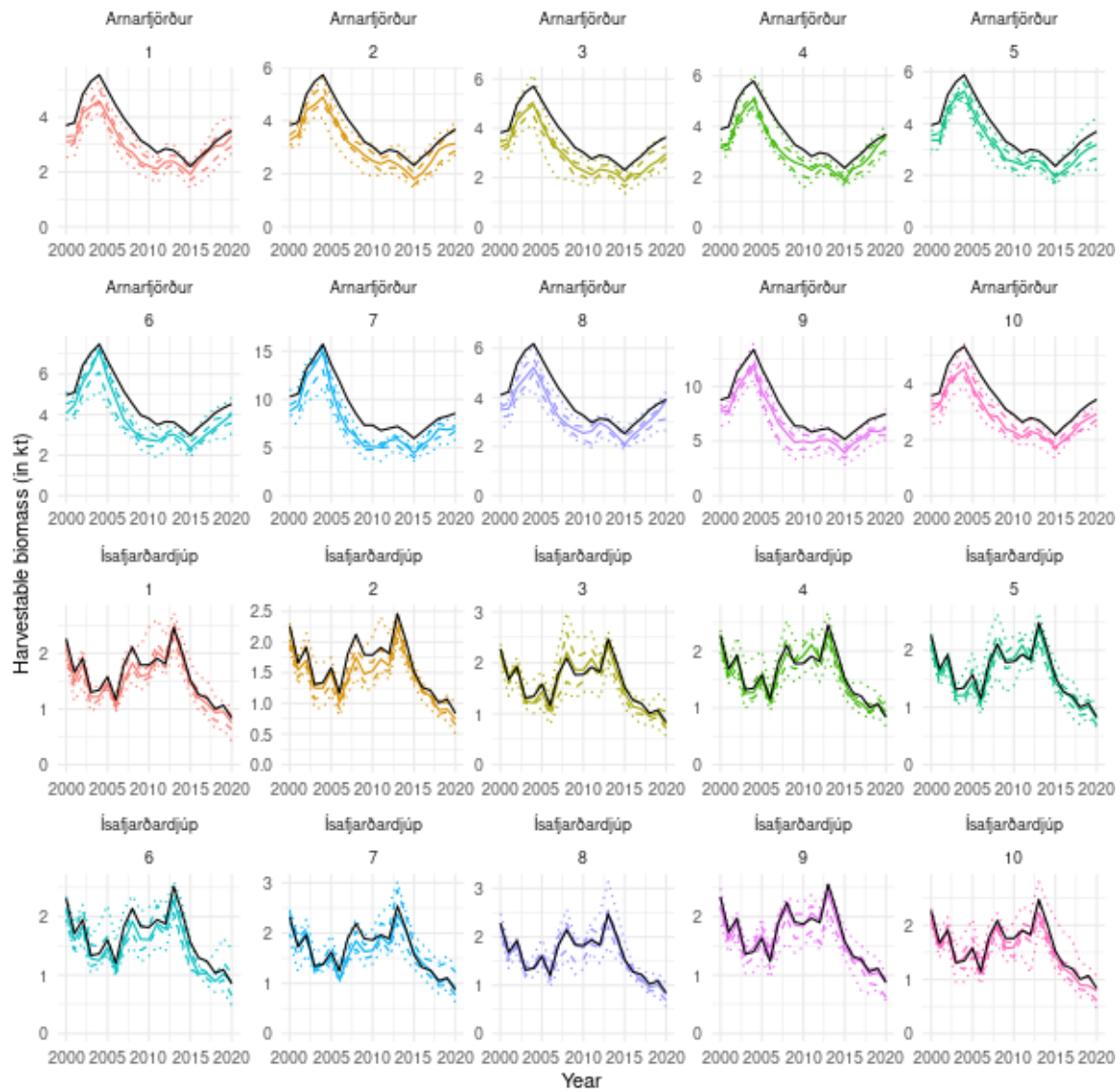


Figure 45: Bootstrap model harvestable biomass results. Colors represent the 10 base models. Each set of solid, dashed, and dotted colored lines represents the median, 50, and 95% intervals of the bootstrapped estimates for a certain base model, as derived from 10 replicates per base model. The solid black lines indicate fits from the 10 base models.

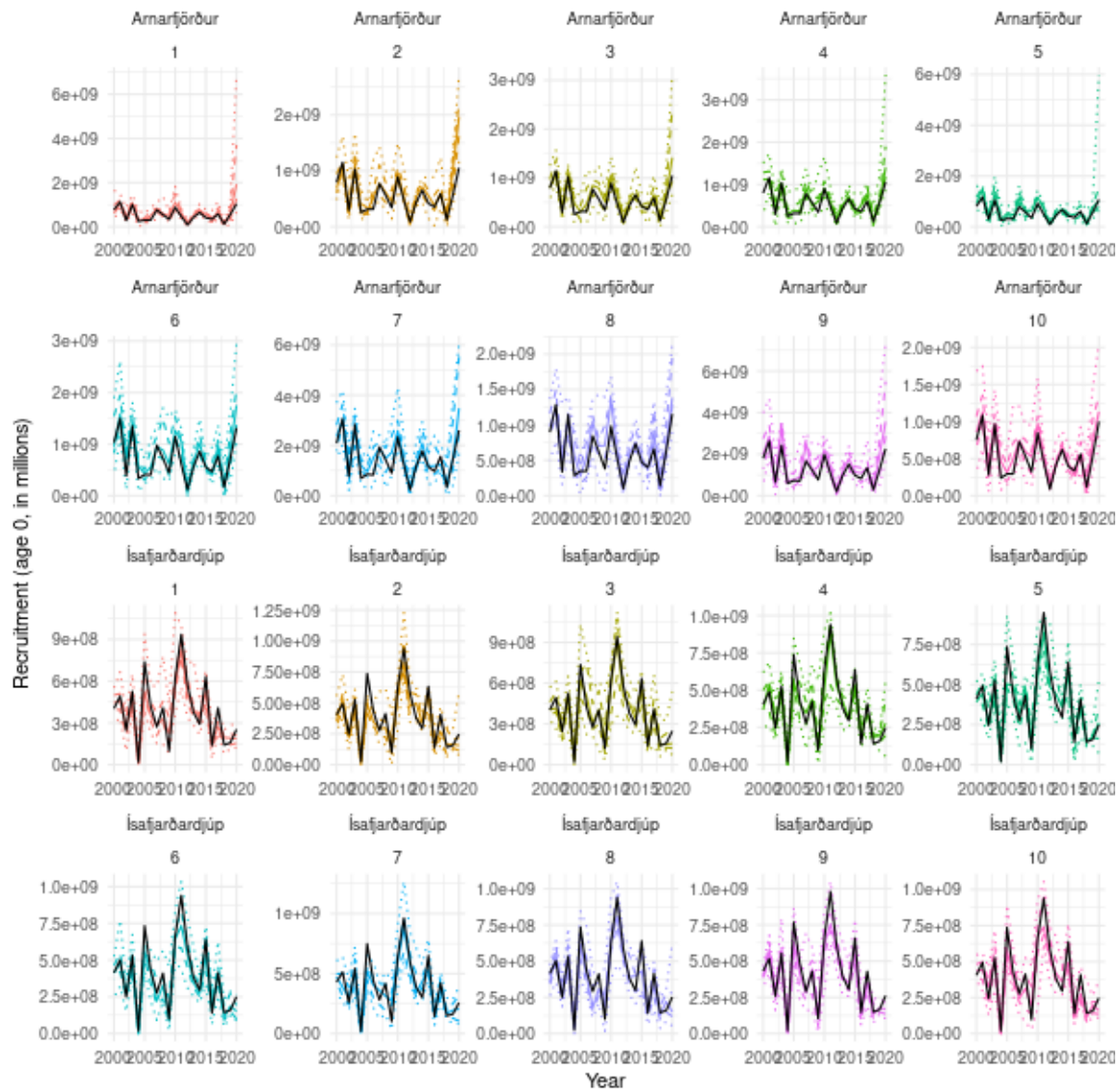


Figure 46: Bootstrap model recruitment results. Colors represent the 10 base models. Each set of solid, dashed, and dotted colored lines represents the median, 50, and 95% intervals of the bootstrapped estimates for a certain base model, as derived from 10 replicates per base model. The solid black lines indicate fits from the 10 base models.

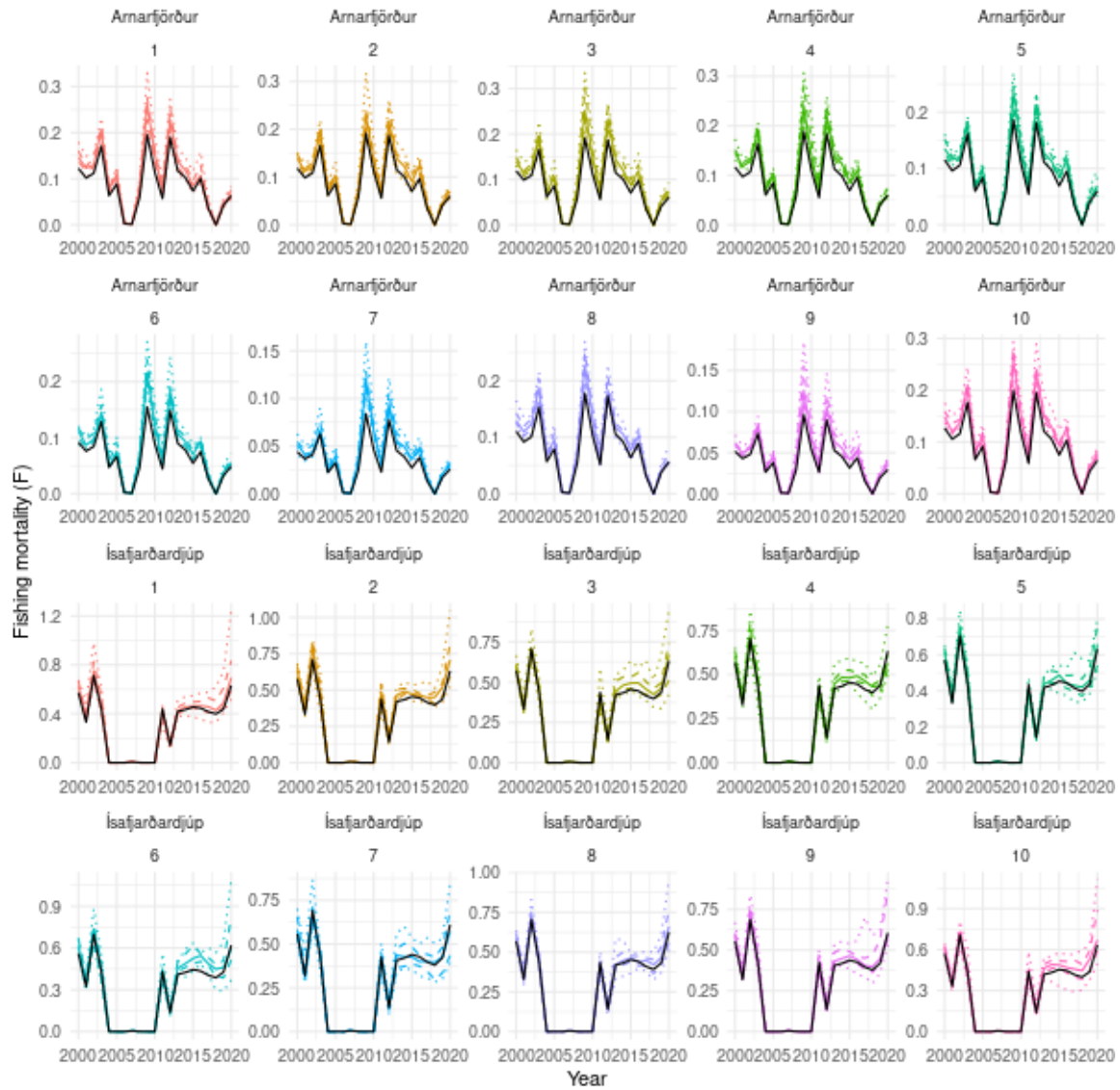


Figure 47: Bootstrap model fishing mortality (F) results. Colors represent the 10 base models. Each set of solid, dashed, and dotted colored lines represents the median, 50, and 95% intervals of the bootstrapped estimates for a certain base model, as derived from 10 replicates per base model. The solid black lines indicate fits from the 10 base models.



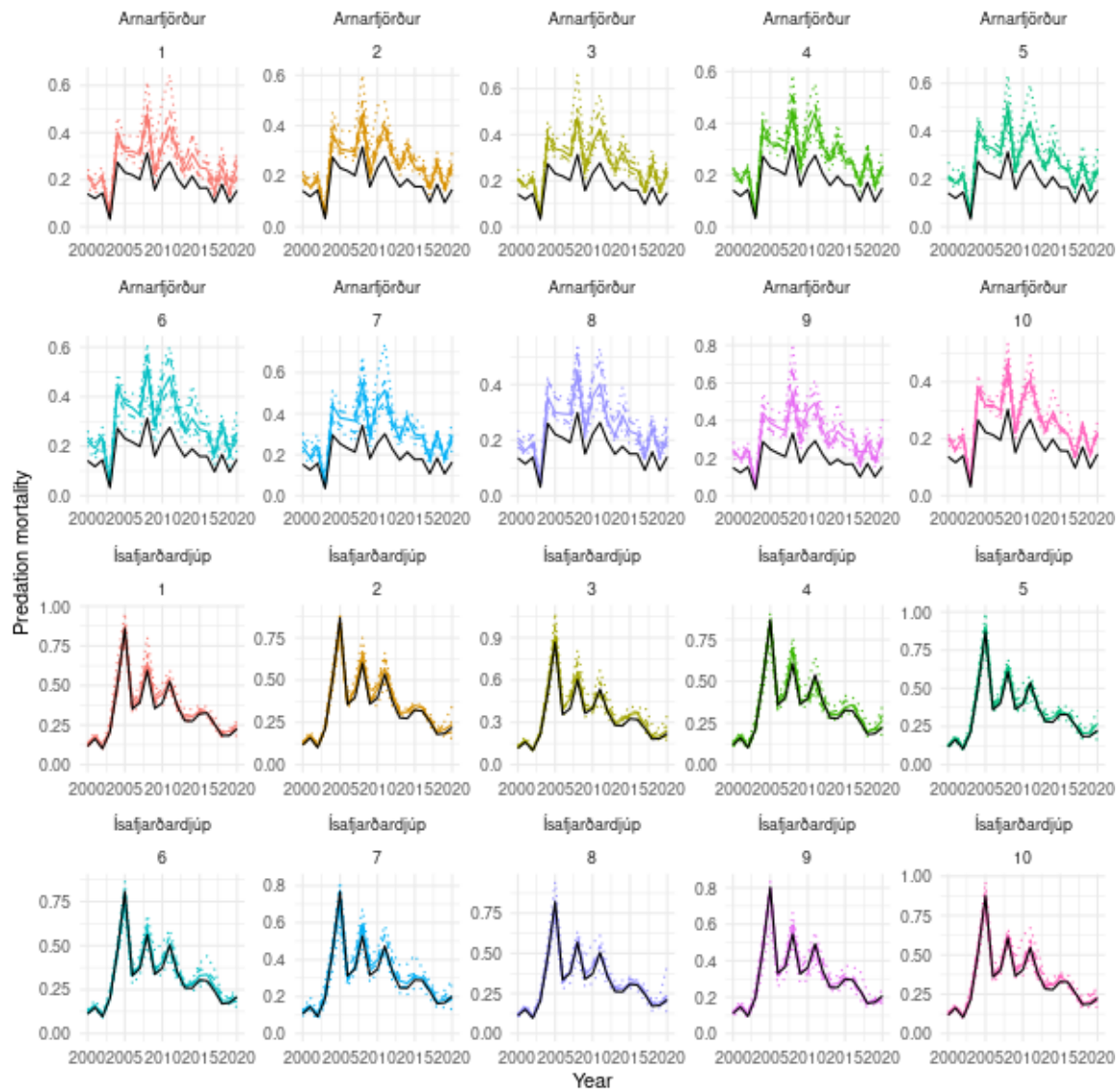


Figure 48: Bootstrap model predation mortality results. Colors represent the 10 base models. Each set of solid, dashed, and dotted colored lines represents the median, 50, and 95% intervals of the bootstrapped estimates for a certain base model, as derived from 10 replicates per base model. The solid black lines indicate fits from the 10 base models.

## 6.1 Estimating a stock-recruitment relationship

A variety of approaches are common when estimating a stock recruitment relationship. In the absence of a stock-recruitment signal from the available historical data, the ICES guidelines for evaluating Category 1 stocks (those with analytical stock assessment models, ICES [7]) suggest that the ‘‘hockey-stick’’ recruitment function is used, i.e.

$$R_y = \bar{R}_y \min(1, S_y/B_{loss}) \quad (20)$$

where  $R_y$  is annual recruitment,  $S_y$  the spawning stock biomass,  $B_{loss}$  the break point in hockey stick function and  $\bar{R}_y$  is the recruitment when not impaired due to low levels of spawning stock biomass (SSB). In the case of both Arnarfjörður and Ísafjarðardjúp populations, although SSB levels have declined in both fjords, substantially decreased recruitment are not detected, but rather naturally lower recruitment levels in Ísafjarðardjúp over most of the time series are indicated (Figure 9). The most recent years in Ísafjarðardjúp do appear to have lower recruitment than in the past, but as there is a large spread in the amount of recruitment generated from similar spawning stock biomasses, then it is difficult to diagnose this reduced recruitment as recruitment impairment as opposed to natural variation. Because  $B_{loss}$  cannot be estimated from these patterns, it is taken as the lowest observed SSB level over the period observed, after 1989 where the model has more reliable estimates for each of the 100 model replicates. For Ísafjarðardjúp, these values are on par with the most recent years’ spawning stock biomass level estimates being chosen as  $B_{loss}$ ; therefore possible recent recruitment impairment is accounted for by this procedure. In model projections, recruitment is then projected as  $\bar{R}_y$  and is drawn from the historical distribution using block-bootstrap resampling. Only recruitment values after 1999 are sampled to account for relatively reduced recruitment values observed in Ísafjarðardjúp that are more likely to reflect future recruitment. Each of the 10 simulations run for each of the 100 model replicates has implemented a series of 7 consecutive years in the blocks with random starting years. This is done to account for intra-correlation in the recruitment time-series. The hockey-stock form ensures that when SSB drops below  $B_{loss}$ , these recruitment values are scaled downward according to the proportion  $SSB/B_{loss}$ , so that 0 recruitment is generated at  $SSB = 0$ .

## 6.2 Management procedure in forward projections

The decision rule tested took the same form as that currently implemented, where a harvest rate is multiplied against a survey index obtained from the fall survey, to obtain the quota set for the following fishing year. Observation error and to some degree process error (in the use of the 10 base models) are addressed by the bootstrap approach employed in here. The rule evaluation framework can be classified as simulation without an assessment feedback (ICES 2006), i.e. it is thus assumed that the simulation within the operating model represents the true stock dynamics. Errors in the assessment procedure that relate to harvest advice model are emulated as:

$$\hat{B}_y^{harv} = e^{E_y} B_y^{harv} \quad (21)$$

where  $B_y^{harv}$  is the harvestable biomass,  $E_y = \sigma(\rho\epsilon_{y-1} + \sqrt{1-\rho^2}\epsilon_y)$  is the assessment error and  $\sigma$  is CV of the reference biomass,  $\rho$  the autocorrelation between assessment years and  $\epsilon_y \sim N(0, 1)$ . In the management procedure, survey index is intended to represent an estimated harvestable biomass quantity  $\hat{B}_y^{harv}$ , so this procedure essentially assumes that the actual harvest rate being applied to that harvestable biomass estimate is the implemented harvest rate  $H$  multiplied by catchability ( $H * q$ ). This harvest rate drops to 0 below a certain limit harvestable biomass level, which is indicated by a limit survey index  $\hat{I}_y^{lim}$ . The error applied to estimated biomass levels can therefore also be thought to include error in translating the biomass trigger to the implemented index trigger, as these can not be distinguished. The

$$TAC_{y+1} = \begin{cases} H\hat{B}_y^{harv} = Hq\hat{I}_y^{harv} & \text{where } \hat{I}_y^{harv} > \hat{I}_y^{lim} \\ 0 & \text{where } \hat{I}_y^{harv} \leq \hat{I}_y^{lim} \end{cases} \quad (22)$$



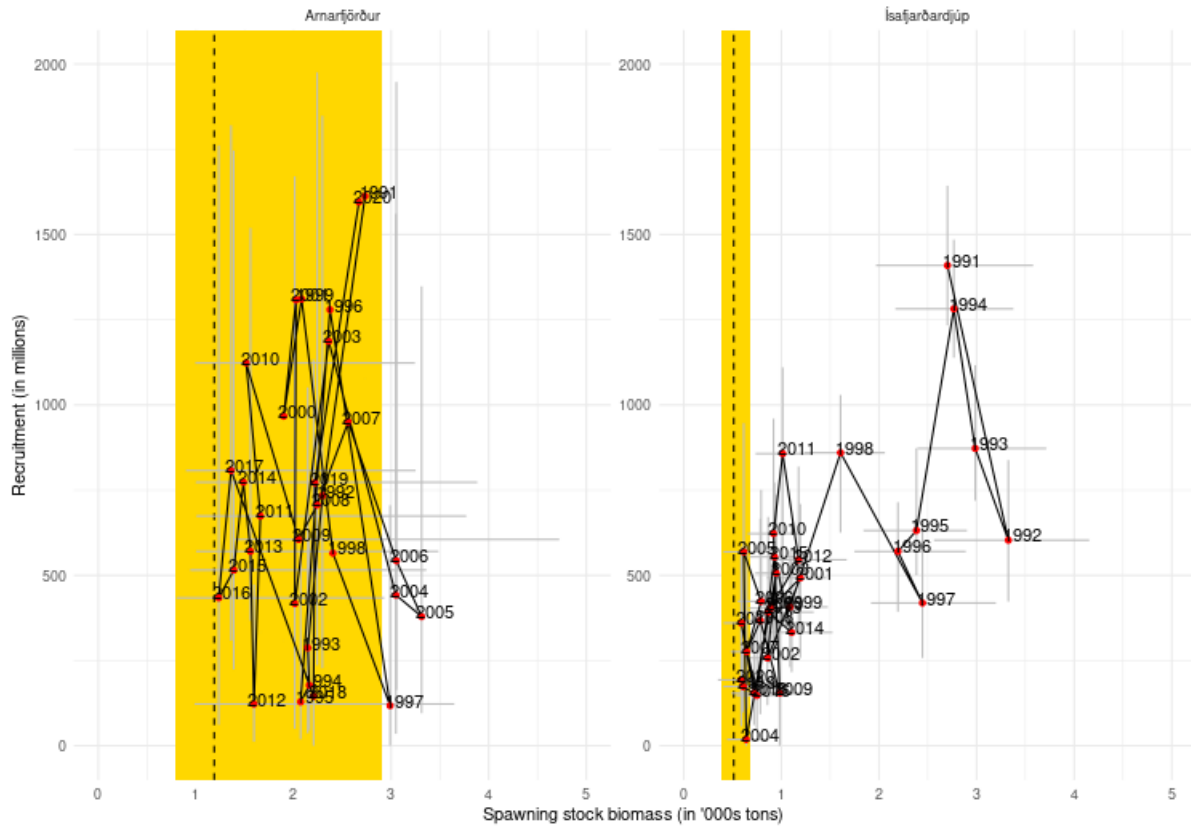


Figure 49: Spawning stock biomass (SSB) and recruitment relationship. Uncertainty in recruitment and SSB is indicated with 95% quantile intervals. Error bars missing from points range beyond the limits of the figure. The yellow vertical bar represents the 95% inter-quantile range of  $B_{loss}$ . All quantiles are calculated across all 10 replicates x 10 base model run.  $B_{loss}$  values do not match annual estimates exactly as the medians of minimum SSB levels over several years are used to calculate  $B_{loss}$ , whereas medians are calculated within years to indicate SSB levels.

where the evaluation assumes that 1 quarter elapsed between the time at which the harvestable biomass is estimated and the beginning of the fishing year to which the TAC applies. This is to approximate the situation that will normally be encountered when providing advice in practice, where the stock assessment will cover until the end of quarter 4. In practice, however, fishing may occur in reality immediately after the assessment and advice are published during the same quarter, while in the model, fishing under the new quota begins with the new year.

As the indices used to tune the gadget model are not calculated using the same stratification schemes or length slicing as those calculated in management, they cannot be used directly to calculate next year's catch in projections. Instead, harvestable biomass was used directly, but to do so, an assumption regarding catchability is needed. As catchability could vary by each of the 100 model base and replicate combinations, the entire time series of survey indices used for management was divided by the harvestable biomasses observed in a model replicate at the same time step to obtain catchability estimates per year. The median catchability of the time series was then used for that model replicate to both implement the decision rule as above and convert the trigger survey index. The trigger survey index was the limit below which fishery was closed (604 for Ísafjarðardjúp and 390 for Arnarfjörður), and was translated into a limit harvestable biomass level against which harvestable biomass levels were compared in projected iterations of the decision rule. When harvestable biomass dropped below this limit in simulations, the quota for the following year was set to 0.

## 7 Management strategy evaluation results

Each of the 1000 simulations was run with for 60 possible harvest rates  $H$  implemented, under 5 scenarios of future predation or 5 scenarios of different trigger values. The status quo were set with constant predation at the mean estimated predation effort levels experienced over the previous three years, while three scenarios of less predation were analyzed at at 75%, 50% and 25% of that mean predation effort level and one scenario of greater predation was analyzed at 125%. Preliminary analyses indicated that predation levels of 150% or greater were unsustainable. The scenarios of status quo (100%), low predation (25%), and high predation (125%) are presented here in more detail before looking at overall relationships among predation levels and harvest rates. Status quo represents currently implemented fishing strategies. The low predation scenario represents a best-case scenario (in terms of shrimp fishing opportunities), considering what happens if predation levels substantially decrease in the future. The high predation scenario was chosen to illustrate whether management strategy changes should be considered for only a relatively small increase in predation.

In the case of Ísafjarðardjúp, biomass levels were relatively stable among base models, so ranges are likely relatively accurate. For Arnarfjörður, biomass levels ranged widely among base models, indicating that not enough contrast were available in the data to estimate biomass. Instead, absolute recruitment levels (which controlled biomass levels) scaled with the recruitment upper bounds given (see *Optimization* section). In the section *Base model results*, it is explained that the base models that provide the highest absolute biomass levels are unlikely to show accurate biomass levels within Arnarfjörður (i.e., base models 7 and 9). Therefore, ranges in harvest rate results are explored across base models medians, but final results are based on taking a median across all results regardless of base. As a result, sustainable harvest rates were sometimes illustrated in figures by base under absolute biomass levels, and sometimes illustrated as a single value calculated across bases after removing the absolute scale of biomass by dividing by that model's  $B_{lim}$  value.

### 7.1 Status quo

Results for the status quo show Ísafjarðardjúp to have naturally higher long-term productivity than Arnarfjörður when considered relative to  $B_{lim}$  levels (Figure 51), likely because minimum biomass levels recorded in Ísafjarðardjúp were lower than those recorded in Arnarfjörður. However, in absolute terms, less can be expected to be harvested from Ísafjarðardjúp annually (Figure 51), where lower biomass (Figure 20) and recruitment levels (Figure 22) were estimated in base models. The model also indicates that past commercial removals exceeded predation in Ísafjarðardjúp, but that stocks in both locations have experienced substantial predation (Figure 54), yielding lower estimated biomass levels for Ísafjarðardjúp (Figure 53). Expected yield ranged 360 to 415 tonnes within individual base model runs for Ísafjarðardjúp, and 400 to 780 tonnes for Arnarfjörður. In Ísafjarðardjúp, harvest rates that generated maximum sustainable (MSY), defined as the greatest median yield across replicates under a given base model, ranged 0.78 to 0.9 with the survey index limit implemented. In Arnarfjörður, harvest rates that generated maximum sustainable (MSY) ranged 0.63 to 1.8 with the survey index limit implemented (Figure 51). However, these harvest rates also had high probabilities that population would fall to low levels at which productivity could be impaired. For Ísafjarðardjúp these probabilities ranged 0.13 to 0.26 and for Arnarfjörður these values ranged 0.52 to 0.89. According to ICES guidelines, in this case,  $H_{msy}$  should be based on the maximum harvest rate that allows for the annual probability of spawning stock biomass dropping below  $B_{loss}$  to remain below 0.05. In Ísafjarðardjúp, these harvest rates ranged 0.3 to 0.72, and in Arnarfjörður, these ranged 0.33 to 0.54.  $H_{msy}$  can be defined by taking all base models into account after scaling biomass levels by  $B_{lim}$ , resulting in 0.6 for Ísafjarðardjúp and 0.42 for Arnarfjörður (Figure 52).

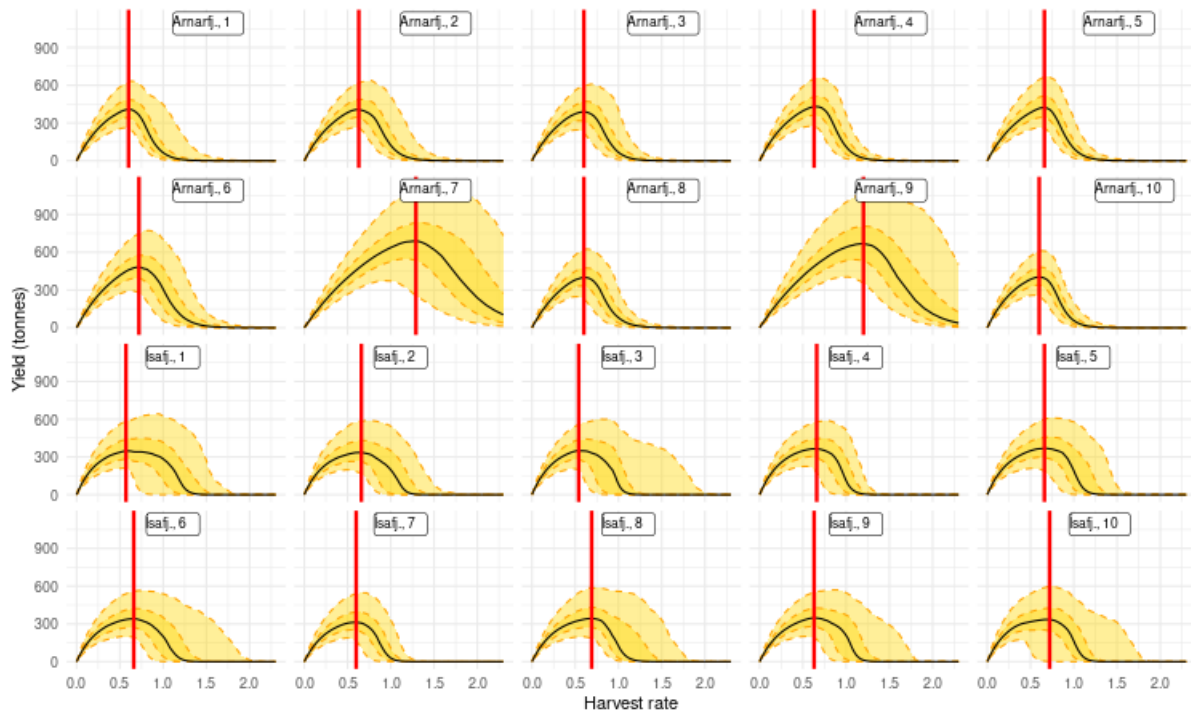


Figure 50: Equilibrium catch curves of Northern shrimp in Arnarfjörður and Ísafjarðardjúp according to 10 base models, shown as a function of  $H$ , under status quo predation and without the survey index limit implemented. The black solid curves indicate the median projected catch and the shaded yellow regions the 25% – 75% and 5% – 95% ranges. Vertical lines indicate the harvest rate generating the greatest yield in the long term. In this case, these harvest rates caused the annual probability of SSB dropping below  $B_{lim}$  to exceed 5%, and cannot be used to reflect  $H_{msy}$  according to ICES guidelines.

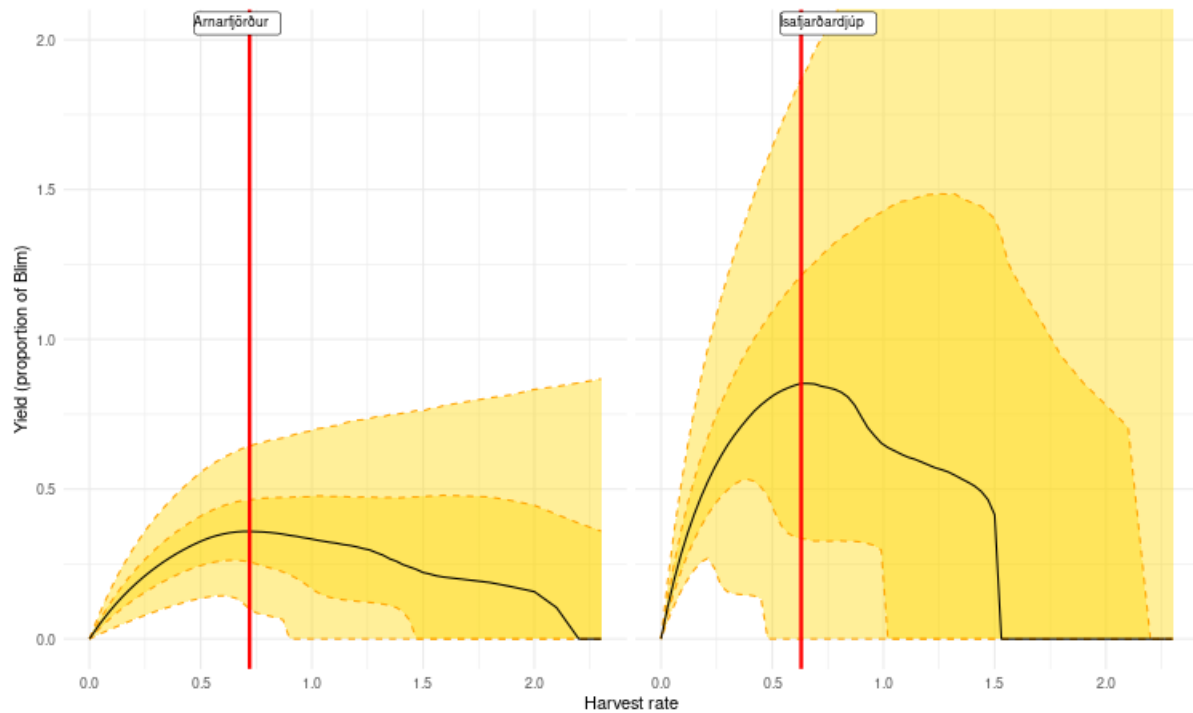


Figure 51: Equilibrium catch curves of Northern shrimp in Arnarfjörður and Ísafjarðardjúp across the 10 base models, shown as a function of  $H$ , under status quo predation and with the fishery closing below the implemented survey index limit. The black solid curves indicate the median projected catch and the shaded yellow regions the 25% – 75% and 5% – 95% ranges. Vertical lines indicate the harvest rate generating the greatest yield in the long term. In this case, these harvest rates caused the annual probability of SSB dropping below  $B_{lim}$  to exceed 5%, and cannot be used to reflect  $H_{msy}$  according to ICES guidelines.

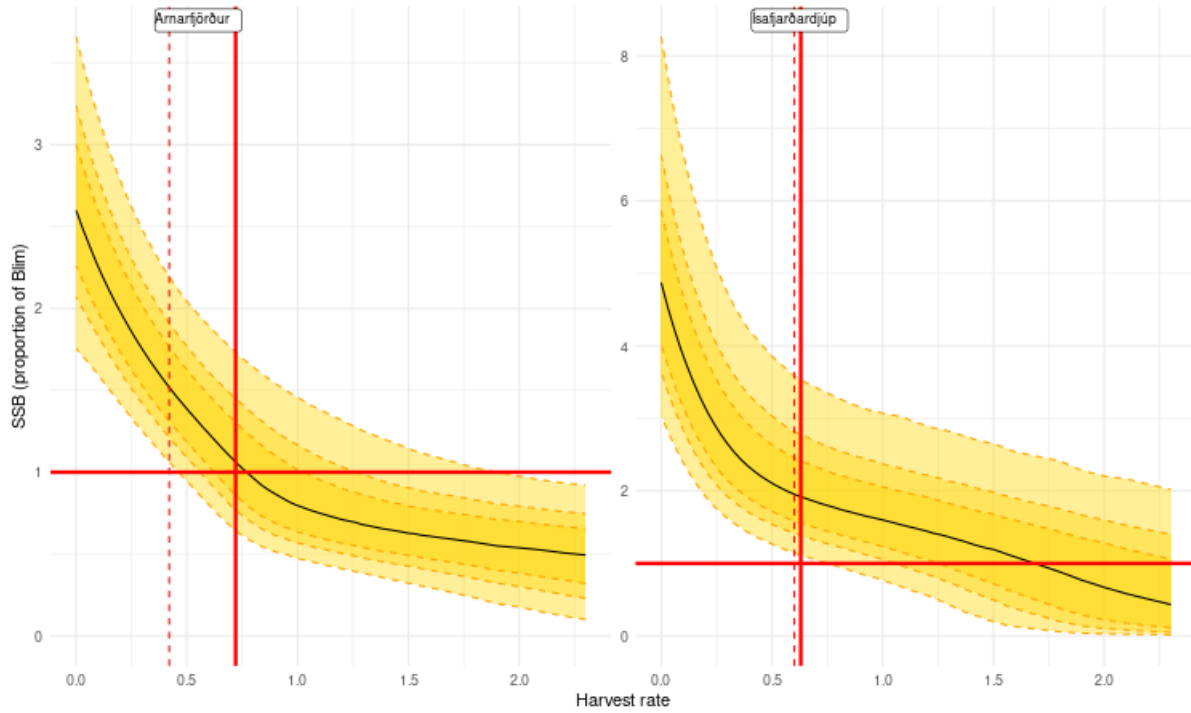


Figure 52: Equilibrium spawning stock biomass curves of Northern shrimp in Arnarfjörður and Ísafjarðardjúp according to 10 base models, shown as a function of  $H$ , under status quo predation and with the fishery closing below the implemented survey index limit. The black solid curves indicate the median projected harvestable biomass and the shaded yellow regions the 25% – 75%, 15% – 85%, and 5% – 95% ranges.  $B_{lim}$  is shown by the red solid horizontal line, set as minimum spawning stock biomass level observed since 1989, and set to as  $B_{loss}$  in the hockey stick recruitment function. The solid red vertical lines indicate harvest rates producing maximum yield in the long term. The dashed red vertical lines indicate the harvest rates below which the population dropped below  $B_{lim}$  over 5% of the time annually, and are used to define  $H_{msy}$  according to ICES guidelines.



Figure 53: Results of harvestable biomass levels from a single simulation used as an example from each of the 10 base models (indicated by color) under status quo predation. Harvest rate is indicated by  $H$ . All colors overlap during the base model years ( $< 2020$ ), but uncertainty implemented in recruitment and management procedures causes variability in future years. All simulations show slight population growth under no fishing ( $H = 0$ ) versus a rapid decrease under high fishing rates.

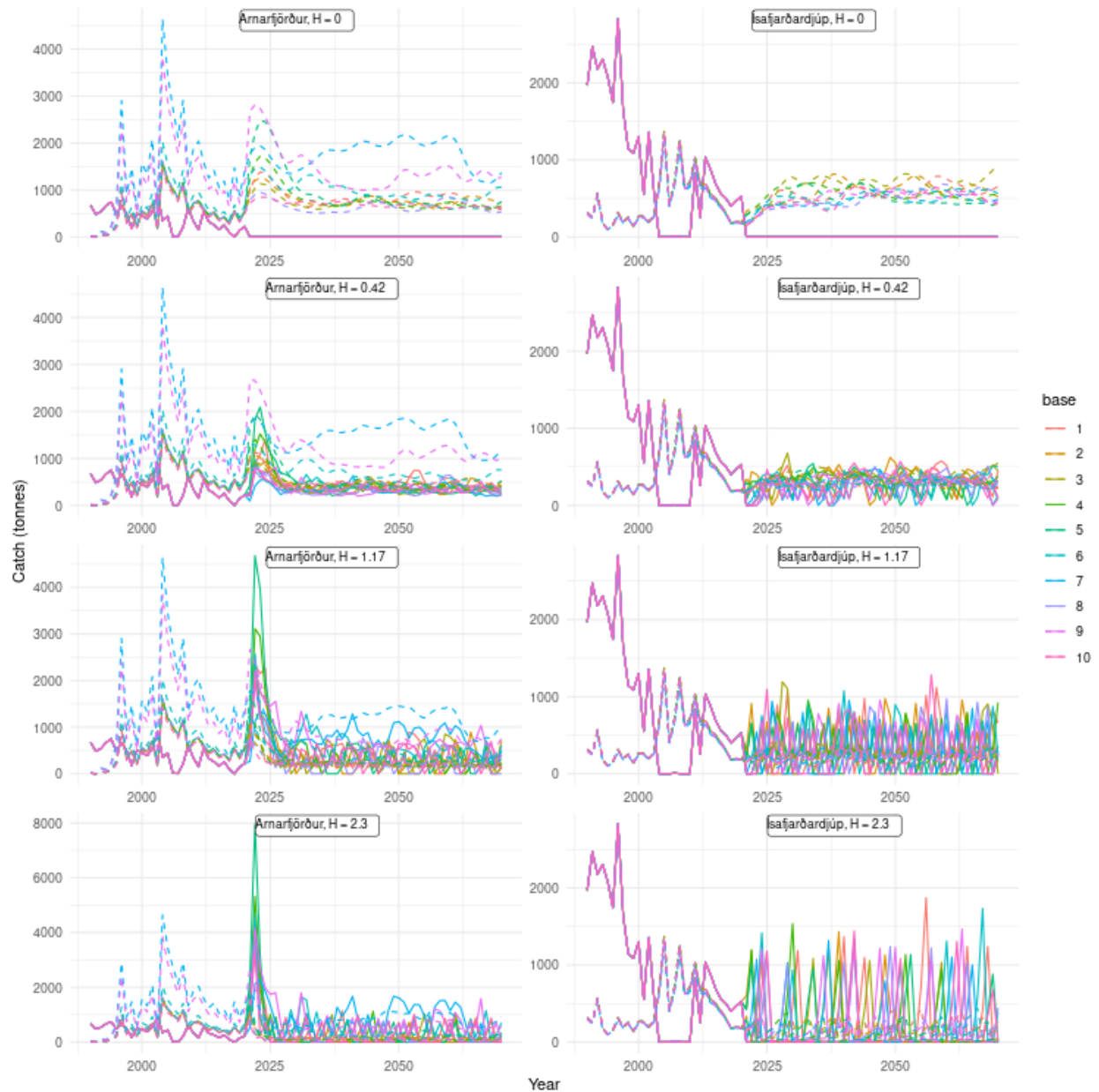


Figure 54: Results of catch (solid) and predation (dashed) levels from a single simulation used as an example from each of the 10 base models (indicated by color) under status quo predation. Note that predation levels scale with biomass levels across base models in Arnarfjörður. Harvest rate is indicated by  $H$ . All colors overlap during the base model years ( $< 2020$ ), but uncertainty implemented in recruitment and management procedures causes variability in future years. All simulations show high catch at intermediate harvest rates versus a rapid decrease under high fishing rates.



## 7.2 Predation scenarios

### 7.2.1 Low predation

The lowest predation rates exemplified here are given by the scenario in which future predation was set to 25% of current levels. Under low levels higher yield could be expected and a substantially higher harvest rate could be implemented (Figure 55). In Ísafjarðardjúp, these harvest rates ranged 0.68 to 1.04, and in Arnarfjörður, these ranged 0.72 to 1.88.  $H_{msy}$  can be defined by taking all base models into account after scaling biomass levels by  $B_{lim}$ , resulting in 0.96 for Ísafjarðardjúp and 0.88 for Arnarfjörður (Figure 56). In this case, Ísafjarðardjúp  $H_{msy}$  would be based on the value that generates the greatest yield in the long term, as the risk of SSB falling below  $B_{lim}$  did not exceed 5% at this harvest rate when taking into account all base models together. Population trajectories (Figure 57) and catches (Figure 58) of a single simulation taken from each base model at a range of harvest rates exemplify possible outcomes under 25% predation.

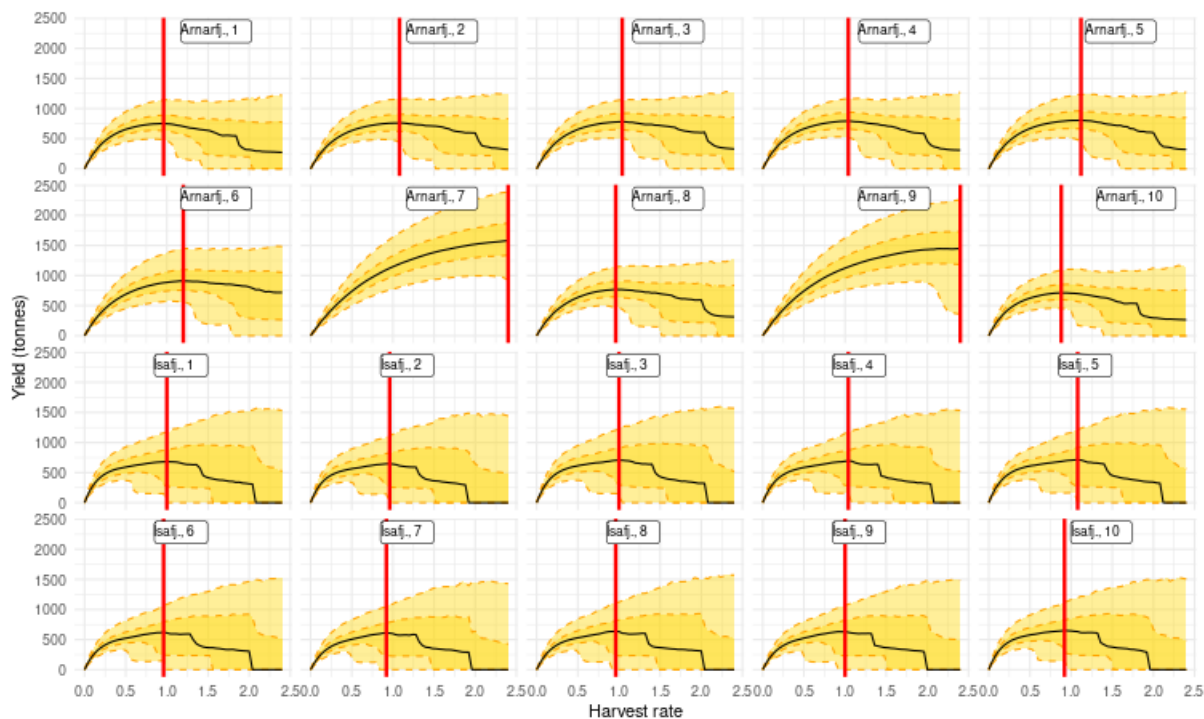


Figure 55: Equilibrium catch curves of Northern shrimp in Arnarfjörður and Ísafjarðardjúp according to 10 base models, shown as a function of  $H$ , under 25% current predation levels and with the fishery closing below the implemented survey index limit. The black solid curves indicate the median projected catch and the shaded yellow regions the 25% – 75% and 5% – 95% ranges. Vertical lines indicate the harvest rate generating the greatest yield in the long term. In Arnarfjörður, these harvest rates caused the annual probability of SSB dropping below  $B_{lim}$  to exceed 5%, and cannot be used to reflect  $H_{msy}$  according to ICES guidelines.

### 7.2.2 High predation

High predation rates are exemplified here by the scenario in which future predation was set to 125% of current levels. Results show that in general, and especially for Ísafjarðardjúp, yield would be reduced and harvest rates should be reduced under higher predation levels to avoid the risk of population levels falling to levels that reduce productivity of the population (Figure 59). In Ísafjarðardjúp, these harvest rates ranged 0.2 to 0.58, and in Arnarfjörður, these ranged 0.02 to 0.28.  $H_{msy}$  can be defined by taking all base models into account after scaling biomass levels by  $B_{lim}$ , resulting in 0.5 for Ísafjarðardjúp and 0.24 for Arnarfjörður

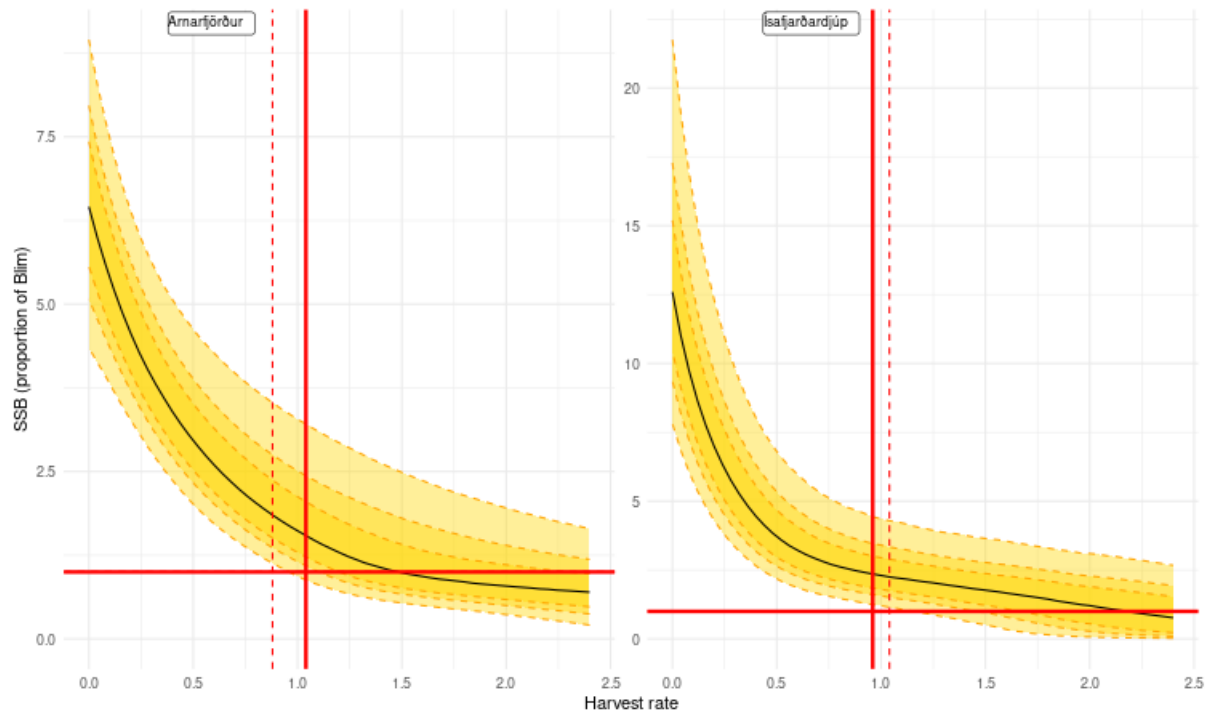


Figure 56: Equilibrium spawning stock biomass curves of Northern shrimp in Arnarfjörður and Ísafjarðardjúp across 10 base models, shown as a function of  $H$ , under 25% current predation levels and with the fishery closing below the implemented survey index limit. The black solid curves indicate the median projected harvestable biomass and the shaded yellow regions the 25% – 75%, 15% – 85%, and 5% – 95% ranges.  $B_{lim}$  is shown by the red solid horizontal line, set as minimum spawning stock biomass level observed since 1989, and set to as  $B_{loss}$  in the hockey stick recruitment function. The dashed red vertical lines indicate the harvest rates below which the population dropped below  $B_{lim}$  over 5% of the time, and the solid red vertical lines indicate the harvest rates that generate maximum yield. Therefore,  $H_{msy}$  is represented by the red dashed line for Arnarfjörður and the red solid line for Ísafjarðardjúp.

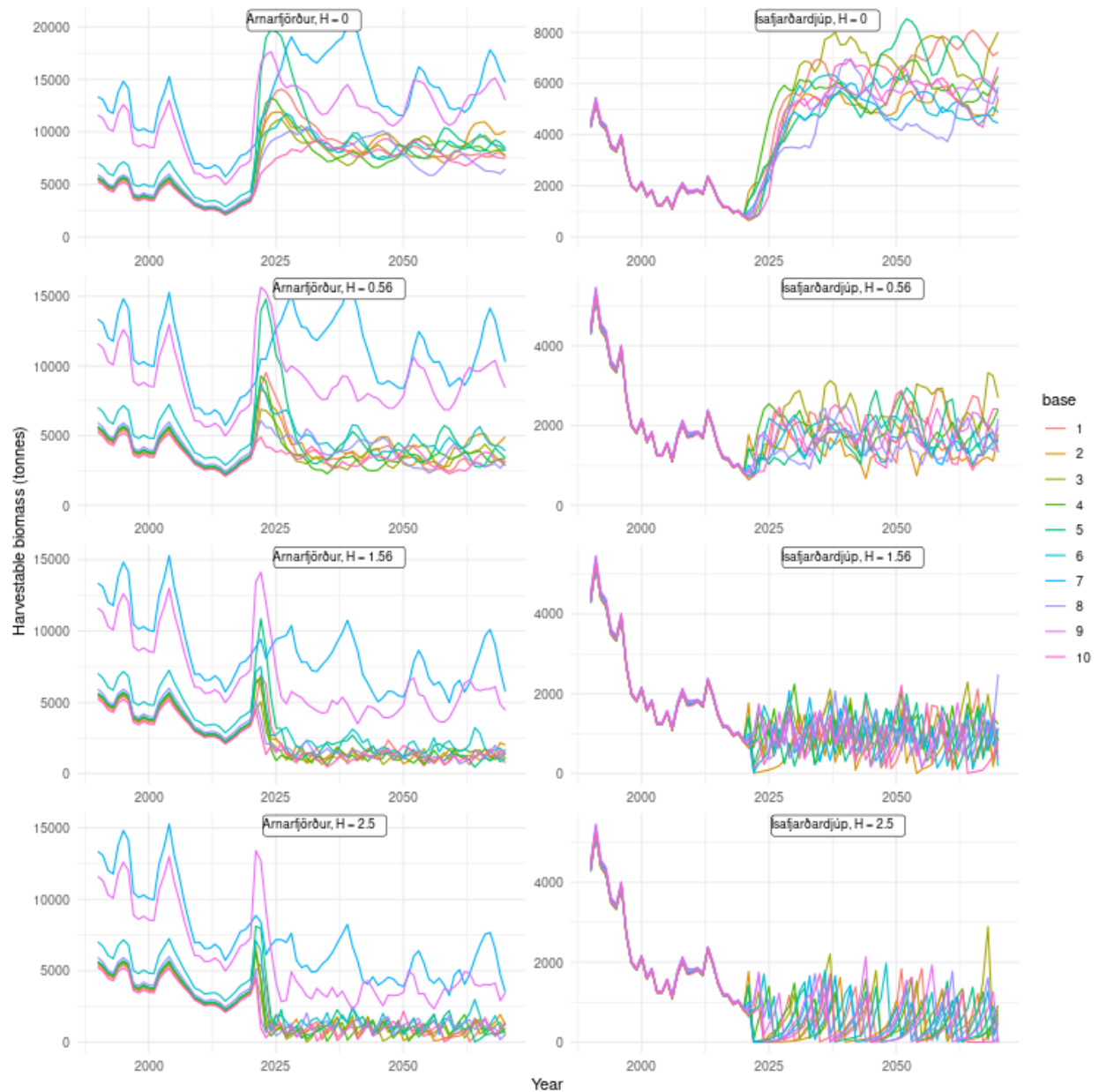


Figure 57: Results of harvestable biomass levels from a single simulation used as an example from each of the 10 base models (indicated by color) under 25% current predation levels and with the fishery closing below the implemented survey index limit. Harvest rate is indicated by  $H$ . All colors overlap during the base model years ( $< 2020$ ), but uncertainty implemented in recruitment and management procedures causes variability in future years. All simulations show slight population growth under no fishing ( $H = 0$ ) versus a rapid decrease under high fishing rates.

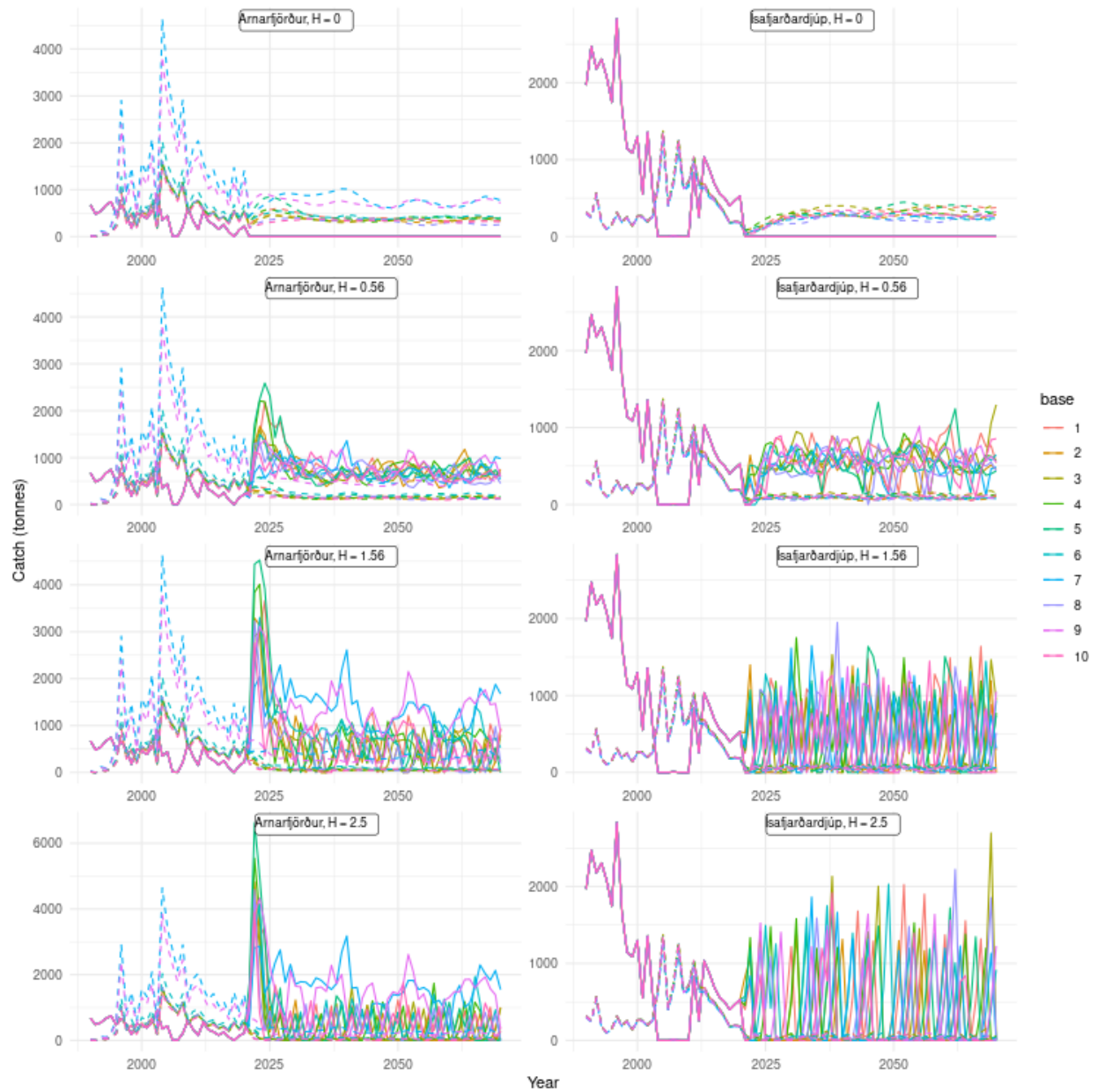


Figure 58: Results of catch (solid) and predation (dashed) levels from a single simulation used as an example from each of the 10 base models (indicated by color) under 25% current predation levels and with the fishery closing below the implemented survey index limit. Harvest rate is indicated by  $H$ . Note that predation levels scale with biomass levels across base models. All colors overlap during the base model years, but uncertainty implemented in recruitment and management procedures causes variability in future years. All simulations show high catch at intermediate harvest rates versus a rapid decrease under high fishing rates.

(Figure 60). Population trajectories (Figure 61) and catches (Figure 62) of a single simulation taken from each base model at a range of harvest rates exemplify possible outcomes under 125% predation.

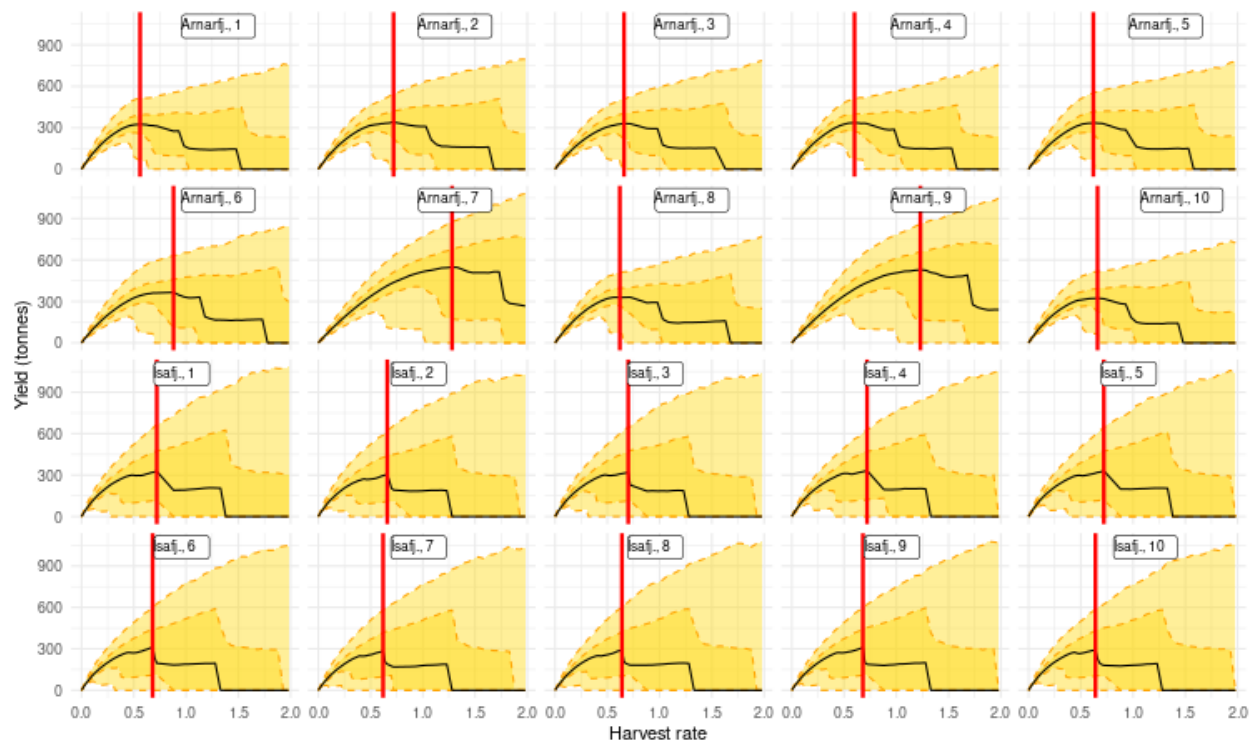


Figure 59: Equilibrium catch curves of Northern shrimp in Arnarfjörður and Ísafjardardjúp across 10 base models, shown as a function of  $H$ , under 125% current predation levels and with the fishery closing below the implemented survey index limit. The black solid curves indicate the median projected catch and the shaded yellow regions the 25% – 75% and 5% – 95% ranges. Vertical lines indicate the harvest rate generating the greatest yield in the long term. In this case, these harvest rates caused the annual probability of SSB dropping below  $B_{lim}$  to exceed 5%, and cannot be used to reflect  $H_{msy}$  according to ICES guidelines.

### 7.2.3 Relationships between predation levels, $H_{msy}$ , and the risk of productivity impairment

Predation levels clearly affected MSY, the probability of recruitment impairment due to spawning stock biomass levels dropping below  $B_{loss}$ , and therefore target  $H_{MSY}$  values as generated using ICES guidelines. Increased predation levels roughly linearly decreased both harvest rates that maximized yield and those that maintained SSB over  $B_{loss}$  with a 5% probability (Figure 63). In Ísafjardardjúp, the median harvest rate that maximized over the long term, taken across the 10 base lines, was 0.6, just above the currently implemented harvest rate of 0.5. This current harvest rate corresponds closely instead with the scenario in which predation rate increased by 25% in the long term. In Arnarfjörður, this median rate was 0.42, slightly higher than the currently implemented 0.346. However, an increase in predation by 25% would lead to a substantial decrease in harvest rate to 25% in order to maintain the 5% probability that SSB does not drop below  $B_{lim}$ .

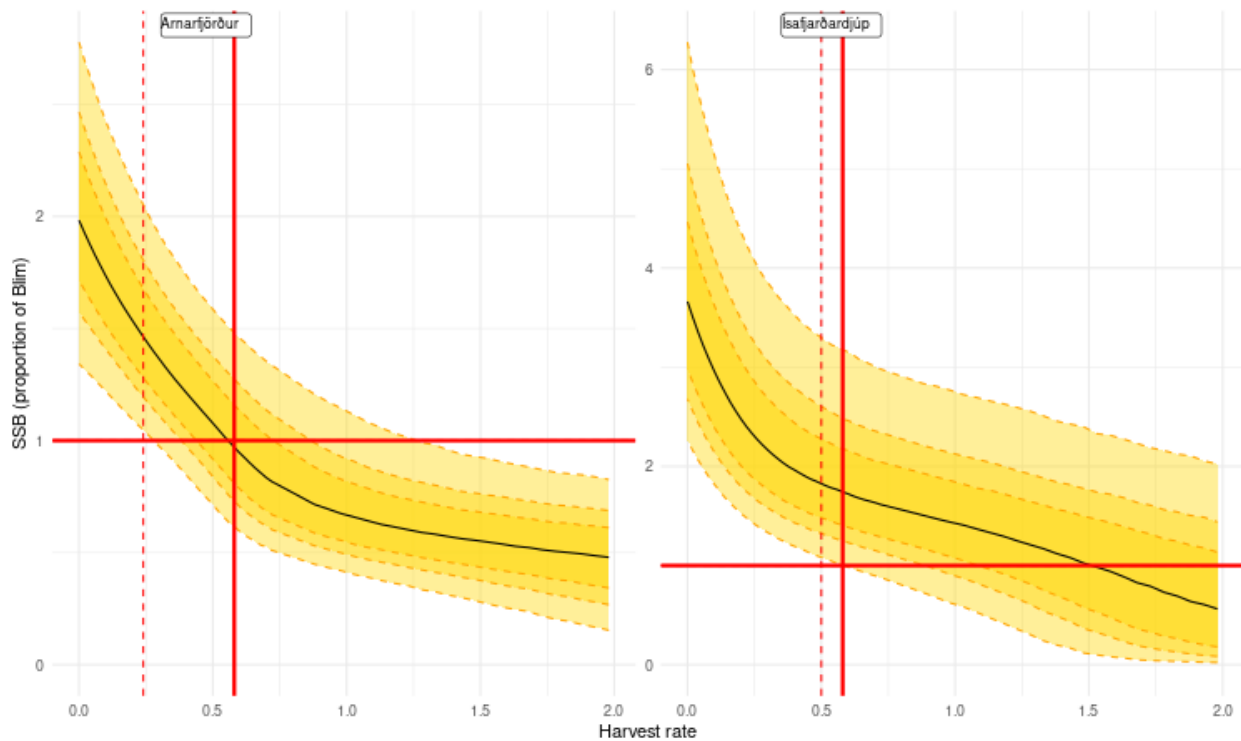


Figure 60: Equilibrium spawning stock biomass curves of Northern shrimp in Arnarfjörður and Ísafjarðardjúp across 10 base models, shown as a function of  $H$ , under 125% current predation levels and with the fishery closing below the implemented survey index limit. The black solid curves indicate the median projected harvestable biomass and the shaded yellow regions the 25% – 75%, 15% – 85%, and 5% – 95% ranges.  $B_{lim}$  is shown by the red solid horizontal line, set as minimum spawning stock biomass level observed since 1989, and set to as  $B_{loss}$  in the hockey stick recruitment function. The solid red vertical lines indicate harvest rates producing maximum yield in the long term. The dashed red vertical lines indicate the harvest rates below which the population dropped below  $B_{lim}$  over 5% of the time annually, and are used to define  $H_{msy}$  according to ICES guidelines.



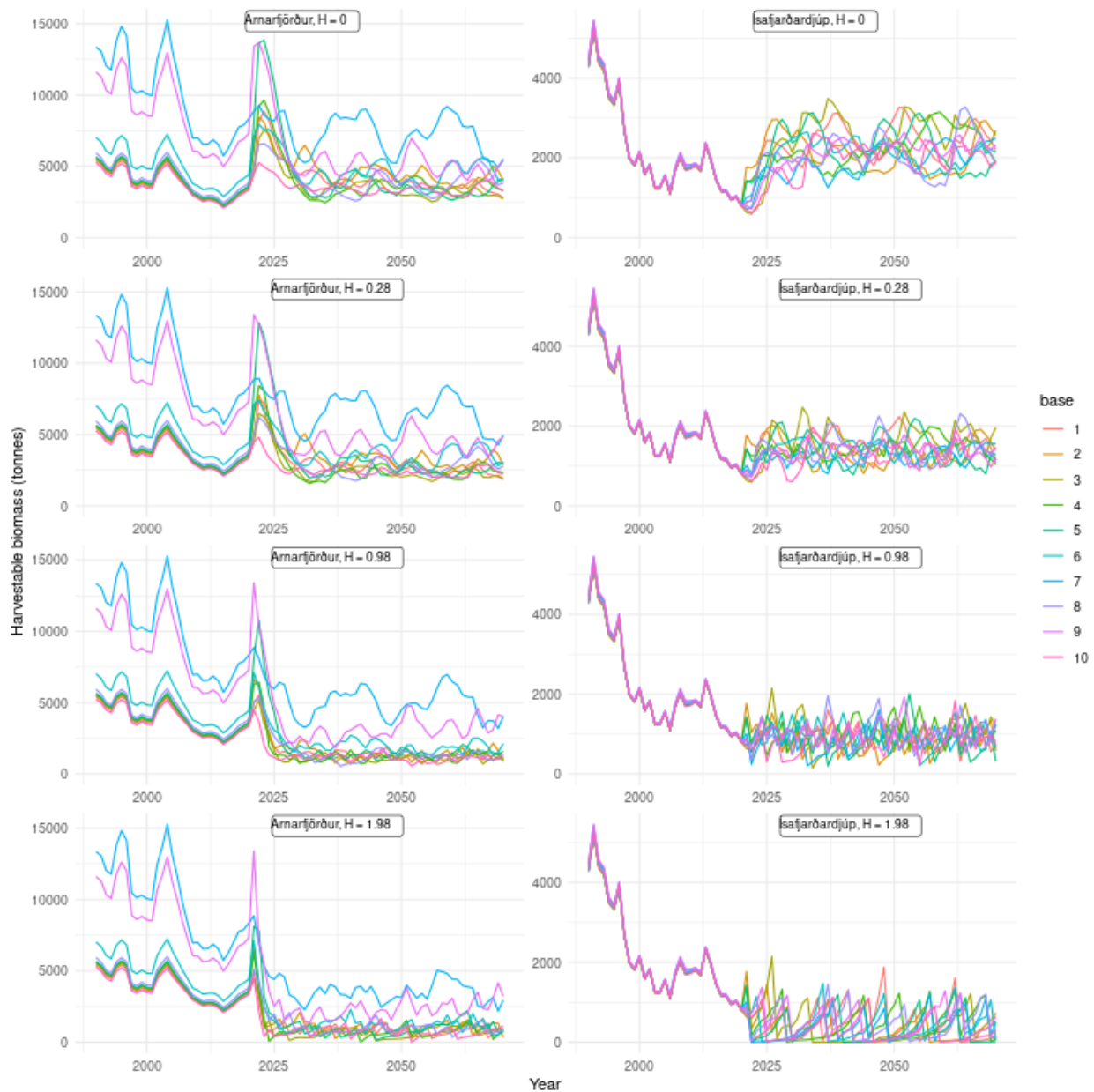


Figure 61: Results of harvestable biomass levels from a single simulation used as an example from each of the 10 base models (indicated by color) under 125% current predation levels. Harvest rate is indicated by  $H$ . All colors overlap during the base model years, but uncertainty implemented in recruitment and management procedures causes variability in future years. All simulations show slight population growth under no fishing ( $H = 0$ ) versus a rapid decrease under high fishing rates.

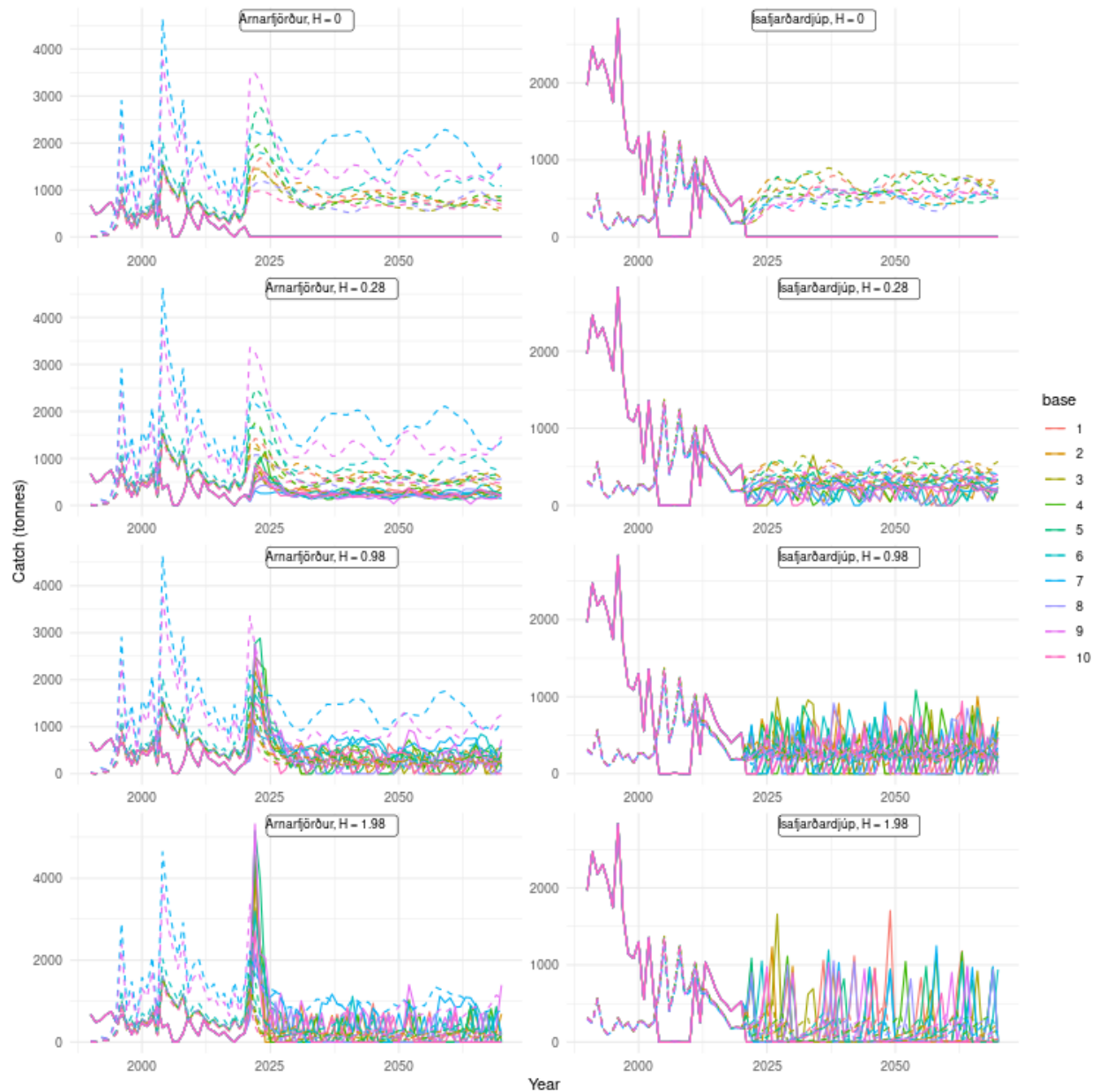


Figure 62: Results of catch (solid) and predation (dashed) levels from a single simulation used as an example from each of the 10 base models (indicated by color) under 125% current predation levels. Note that predation levels scale with biomass levels across base models. Harvest rate is indicated by  $H$ . All colors overlap during the base model years, but uncertainty implemented in recruitment and management procedures causes variability in future years. All simulations show high catch at intermediate harvest rates versus a rapid decrease under high fishing rates.



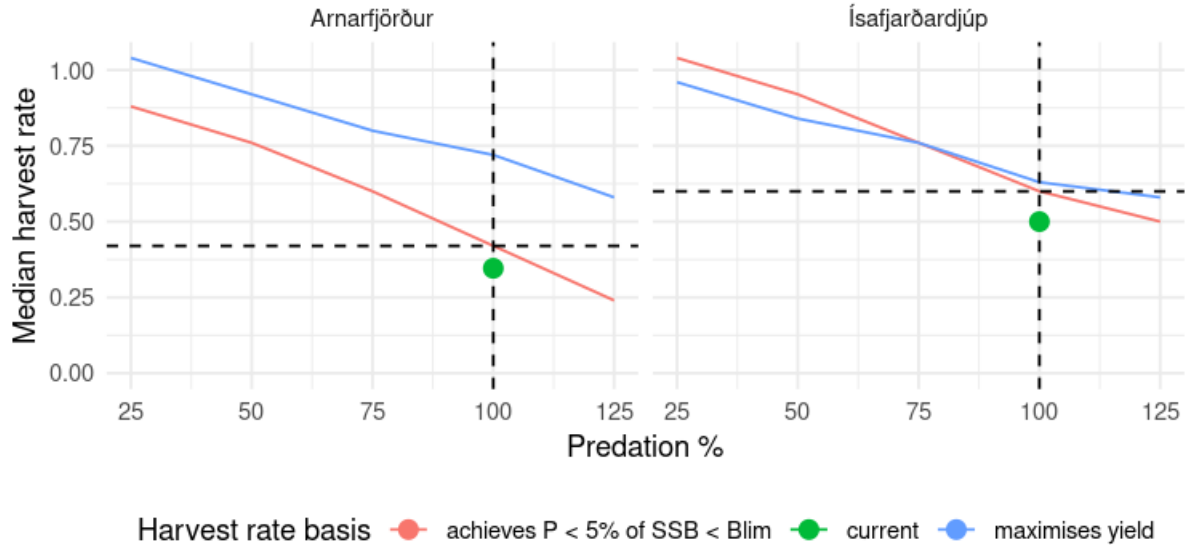


Figure 63: Relationship between predation level and median of the maximum harvest rate that can also achieve a spawning stock biomass that does not drop below a level with increased risk of recruitment impairment ( $B_{lim}$ ). Relationships are depicted across base models, across 5 future predation scenarios: 25%, 50%, 75%, 100%, and 125% of the mean level experienced during the last three years of data. Vertical dashed lines show the status quo scenario values (100% predation level), and horizontal dashed lines indicate the median harvest rate at the 100% trigger value that achieves  $P < 5\%$  of  $SSB < B_{lim}$ . Green dots represent currently implemented values.

### 7.3 Trigger value scenarios

#### 7.3.1 Index trigger set at 75% of current

Assuming that predation levels remain at status quo levels, changing the trigger value can also have an impact on choosing target harvest rates based on ICES guidelines. In particular, 75% of the index limit was chosen as an alternative to the current index limit as this value corresponds with NAFO guidelines that indicate setting trigger index values as 15% of the mean of the highest 3 index values would be a sufficient strategy (04/12 [1]). Results show that in general, maximum yield changes very little with 75% of the current trigger level implemented, although the harvest rates that maximized yield generally increased for Ísafjarðardjúp but decreased for Arnarfjörður (Figure 64). However, all harvest rates would need to be reduced in order to avoid the risk of population levels falling to levels that reduce productivity of the population. In Ísafjarðardjúp, these harvest rates ranged 0.3 to 0.57, and in Arnarfjörður, these ranged 0.3 to 0.51.  $H_{msy}$  can be defined by taking all base models into account after scaling biomass levels by  $B_{lim}$ , resulting in 0.51 for Ísafjarðardjúp and 0.42 for Arnarfjörður (Figure 65). Population trajectories (Figure 66) and catches (Figure 67) of a single simulation taken from each base model at a range of harvest rates exemplify possible outcomes under 75% trigger value implementation.

#### 7.3.2 Index trigger set at 125% of current

When the trigger value is instead set to 125% the currently implemented level, results show that in general, maximum yield changed very little for Arnarfjörður but decreased for Ísafjarðardjúp. In addition, the harvest rates that maximized yield generally decreased for Ísafjarðardjúp but increased for Arnarfjörður (Figure 68). However, the Arnarfjörður harvest rates would need to be reduced in order to avoid the risk of population levels falling to levels that reduce productivity of the population. In Ísafjarðardjúp, harvest rates maximizing

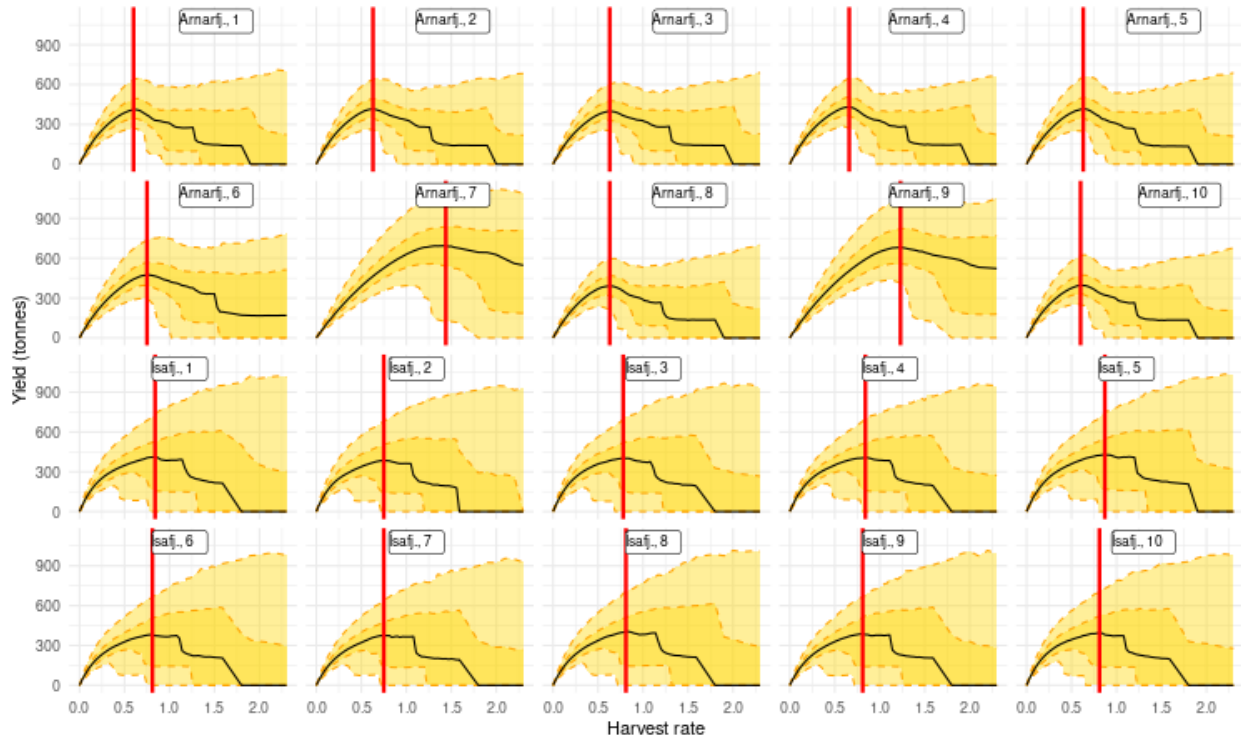


Figure 64: Equilibrium catch curves of Northern shrimp in Arnarfjörður and Ísafjarðardjúp across 10 base models, shown as a function of  $H$ , under status quo predation and with the fishery closing below the implemented survey index limit. The index trigger is set at 75% of the current level. The black solid curve indicates the median projected catch and the shaded yellow regions the 25% – 75% and 5% – 95% ranges. Vertical lines indicate the harvest rate generating the greatest yield in the long term. In this case, these harvest rates caused the annual probability of SSB dropping below  $B_{lim}$  to exceed 5%, and cannot be used to reflect  $H_{msy}$  according to ICES guidelines.

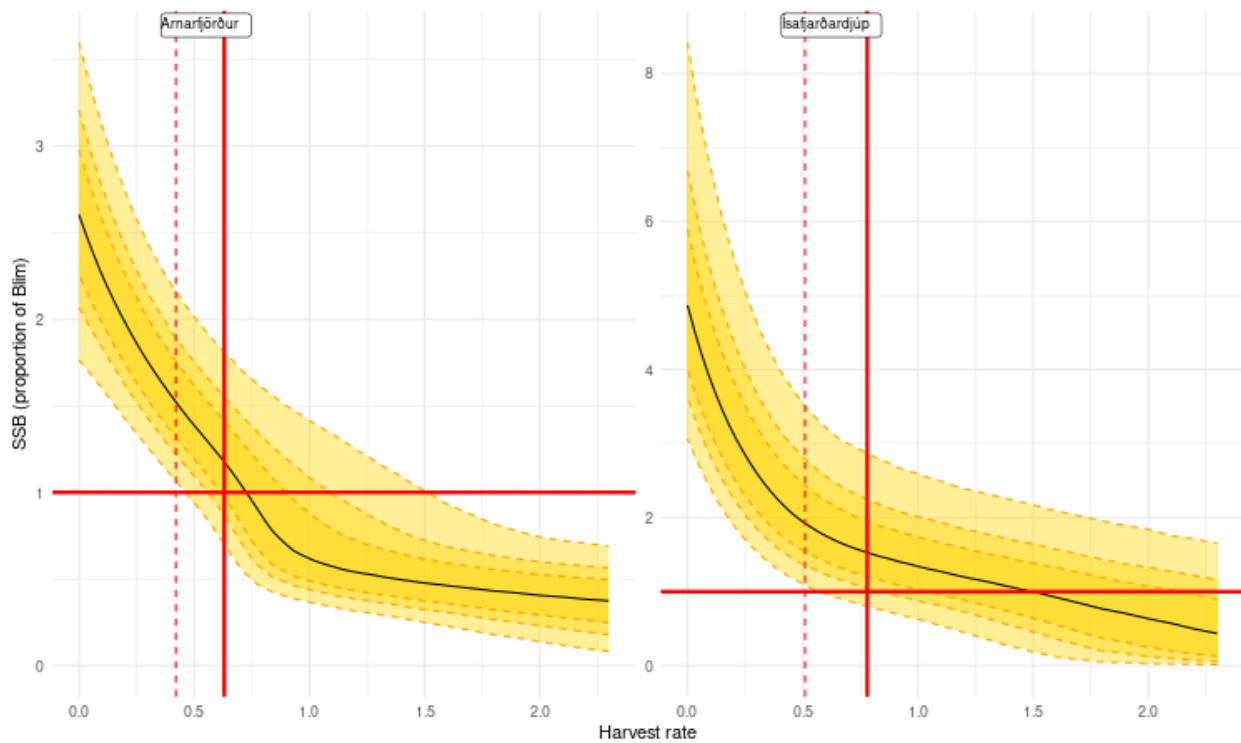


Figure 65: Equilibrium spawning stock biomass curves of Northern shrimp in Arnarfjörður and Ísafjarðardjúp according to 10 base models, shown as a function of  $H$ , under status quo predation and with the fishery closing below the implemented survey index limit. The index trigger is set at 75% of the current level. The black solid curves indicate the median projected harvestable biomass and the shaded yellow regions the 25% – 75%, 15% – 85%, and 5% – 95% ranges.  $B_{lim}$  is shown by the red solid horizontal line, set as minimum spawning stock biomass level observed since 1989, and set to as  $B_{loss}$  in the hockey stick recruitment function. The solid red vertical lines indicate harvest rates producing maximum yield in the long term. The dashed red vertical lines indicate the harvest rates below which the population dropped below  $B_{lim}$  over 5% of the time annually. In this case, these harvest rates caused the annual probability of SSB dropping below  $B_{lim}$  to exceed 5%, and cannot be used to reflect  $H_{msy}$  according to ICES guidelines.

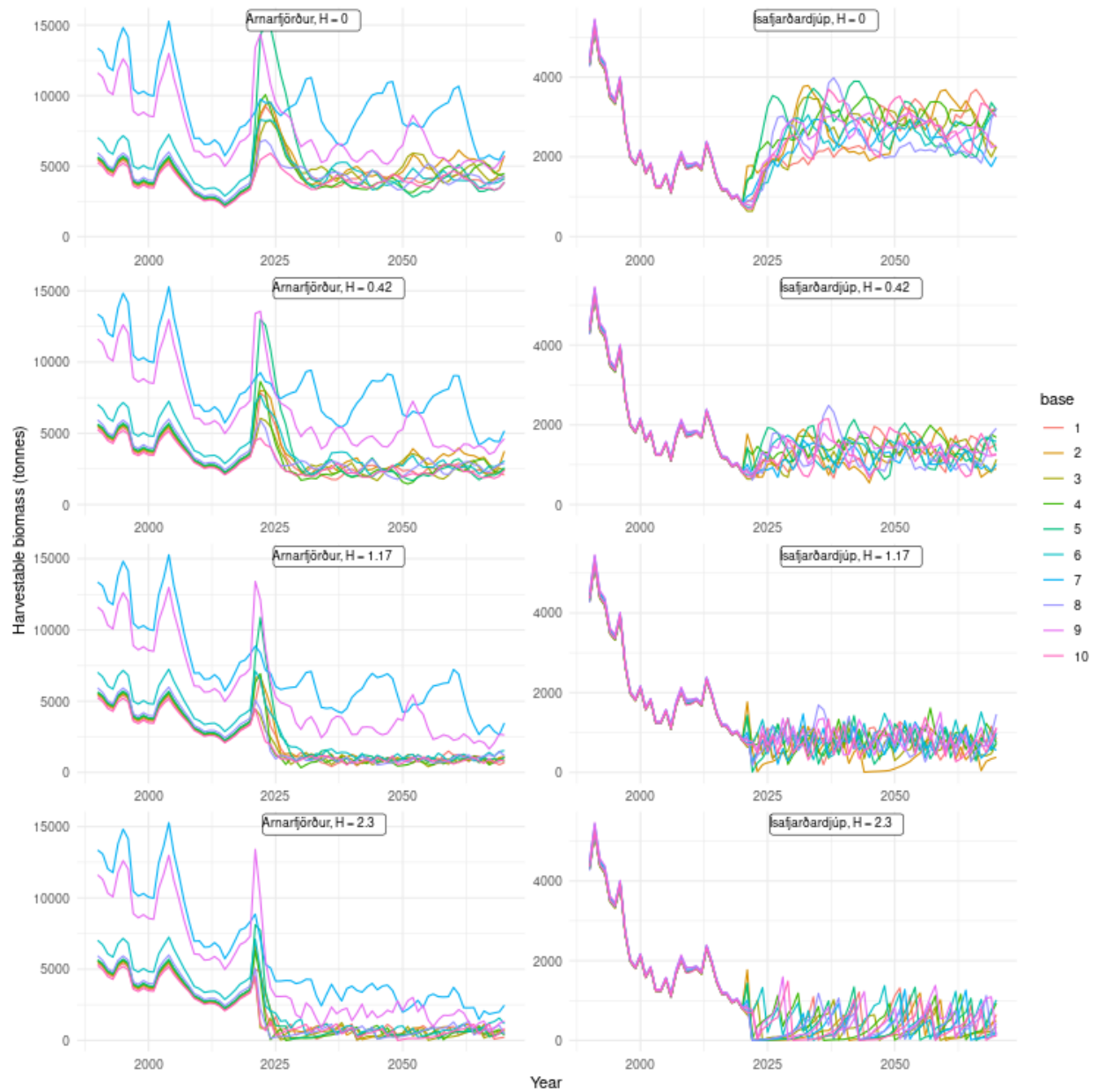


Figure 66: Results of harvestable biomass levels from a single simulation used as an example from each of the 10 base models (indicated by color) under status quo predation. Harvest rate is indicated by  $H$ . All colors overlap during the base model years, but uncertainty implemented in recruitment and management procedures causes variability in future years. The index trigger is set at 75% of the current level. All simulations show slight population growth under no fishing ( $H = 0$ ) versus a rapid decrease under high fishing rates.

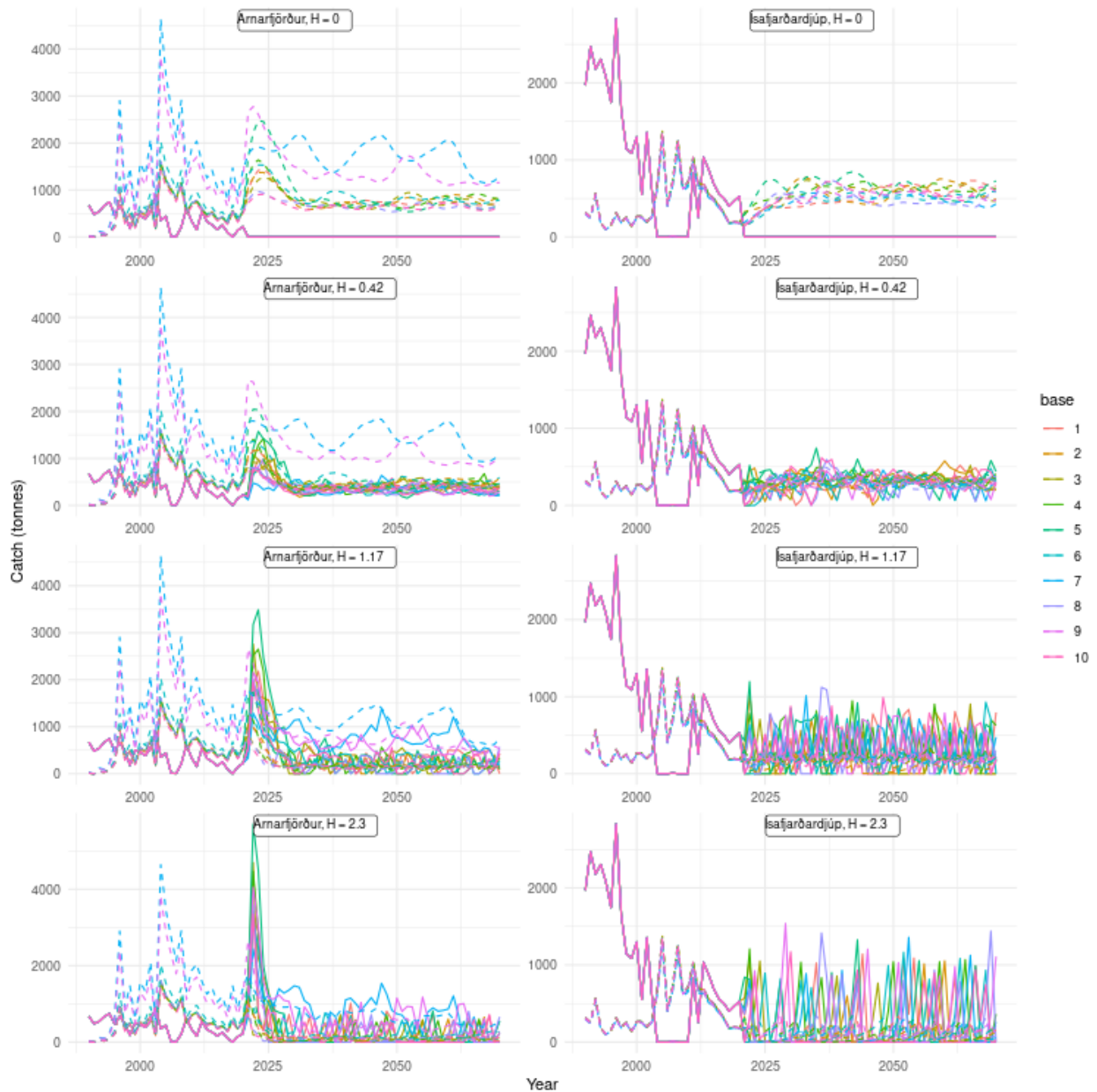


Figure 67: Results of catch (solid) and predation (dashed) levels from a single simulation used as an example from each of the 10 base models (indicated by color) under status quo predation. Harvest rate is indicated by  $H$ . Note that predation levels scale with biomass levels across base models. The index trigger is set at 75% of the current level. All colors overlap during the base model years, but uncertainty implemented in recruitment and management procedures causes variability in future years. All simulations show high catch at intermediate harvest rates versus a rapid decrease under high fishing rates.

yield while maintaining SSB over  $B_{lim}$  with a 5% probability ranged 0.54 to 0.69. In Arnarfjörður, harvest rates maintaining SSB over  $B_{lim}$  with a 5% probability ranged 0.33 to 0.6.  $H_{msy}$  can be defined by taking all base models into account after scaling biomass levels by  $B_{lim}$ , resulting in 0.51 for Ísafjarðardjúp and 0.42 for Arnarfjörður (Figure 69). Population trajectories (Figure 70) and catches (Figure 71) of a single simulation taken from each base model at a range of harvest rates exemplify possible outcomes under 125% trigger value implementation.

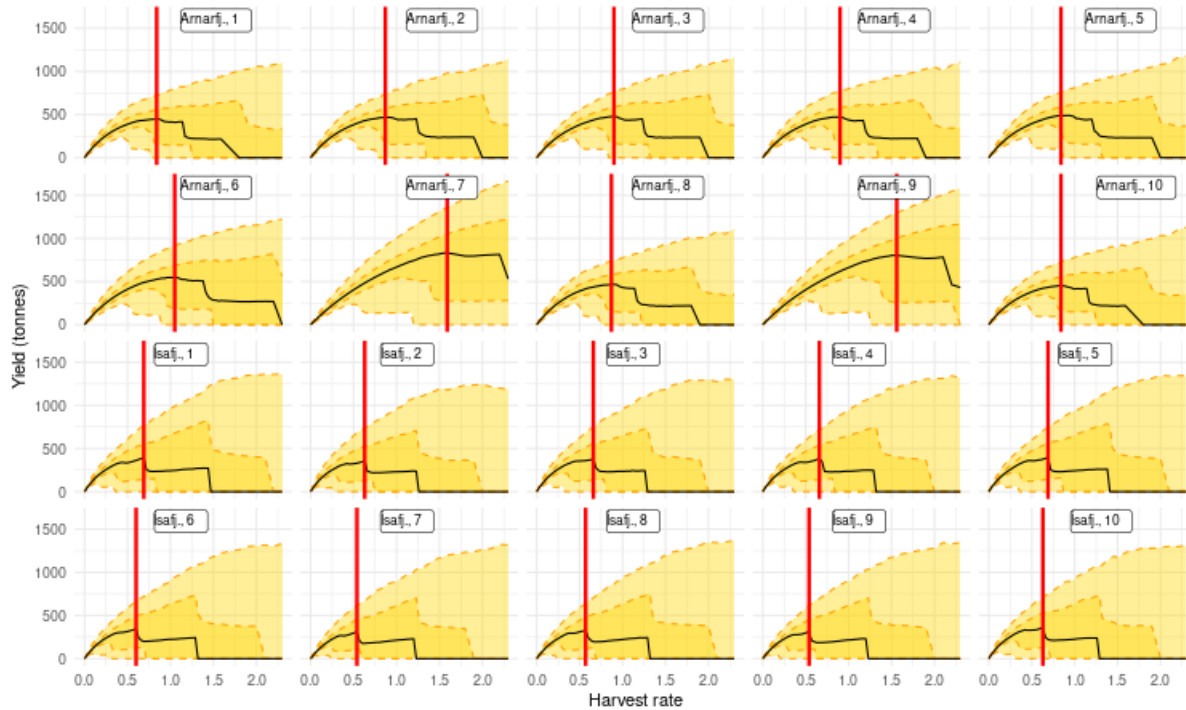


Figure 68: Equilibrium catch curves of Northern shrimp in Arnarfjörður and Ísafjarðardjúp according to 10 base models, shown as a function of  $H$ , under status quo predation and with the fishery closing below the implemented survey index limit. The index trigger is set at 125% of the current level. The black solid curves indicate the median projected catch and the shaded yellow regions the 25% – 75% and 5% – 95% ranges. Vertical lines indicate the harvest rate generating the greatest yield in the long term. For Arnarfjörður, these harvest rates caused the annual probability of SSB dropping below  $B_{lim}$  to exceed 5%, and cannot be used to reflect  $H_{msy}$  according to ICES guidelines.

### 7.3.3 Relationships between trigger levels, harvest rates leading to maximized yield, and the risk of productivity impairment

Implemented trigger levels clearly affect yield outcomes, harvest rates that generate maximal yield in the long term, and the probability of recruitment impairment due to spawning stock biomass levels dropping below  $B_{lim}$ . Higher index triggers allowed for slightly higher harvest rates maximizing yield in Arnarfjörður, but lower rates in Ísafjarðardjúp (blue lines, Figure 72). The harvest rates that ensured the annual probability SSB dropping below  $B_{lim}$  did not exceed 5% probability increased with trigger values in both locations, but more dramatically for Ísafjarðardjúp (red lines, Figure 72). In Ísafjarðardjúp, the median harvest rate maximizing yield over the long term, considering all base lines, was 0.6, slightly above the currently implemented 0.5. However, because harvest rates that maximized yield decreased with trigger values while those that maintained SSB above  $B_{lim}$  with a 5% probability increased with trigger values (Figure 72), both an increase and decrease in the trigger value by 25% would lead to a reduction in the  $H_{msy}$  to roughly 0.5, very close to the currently implemented value. Trigger values in Arnarfjörður had less of an effect on the

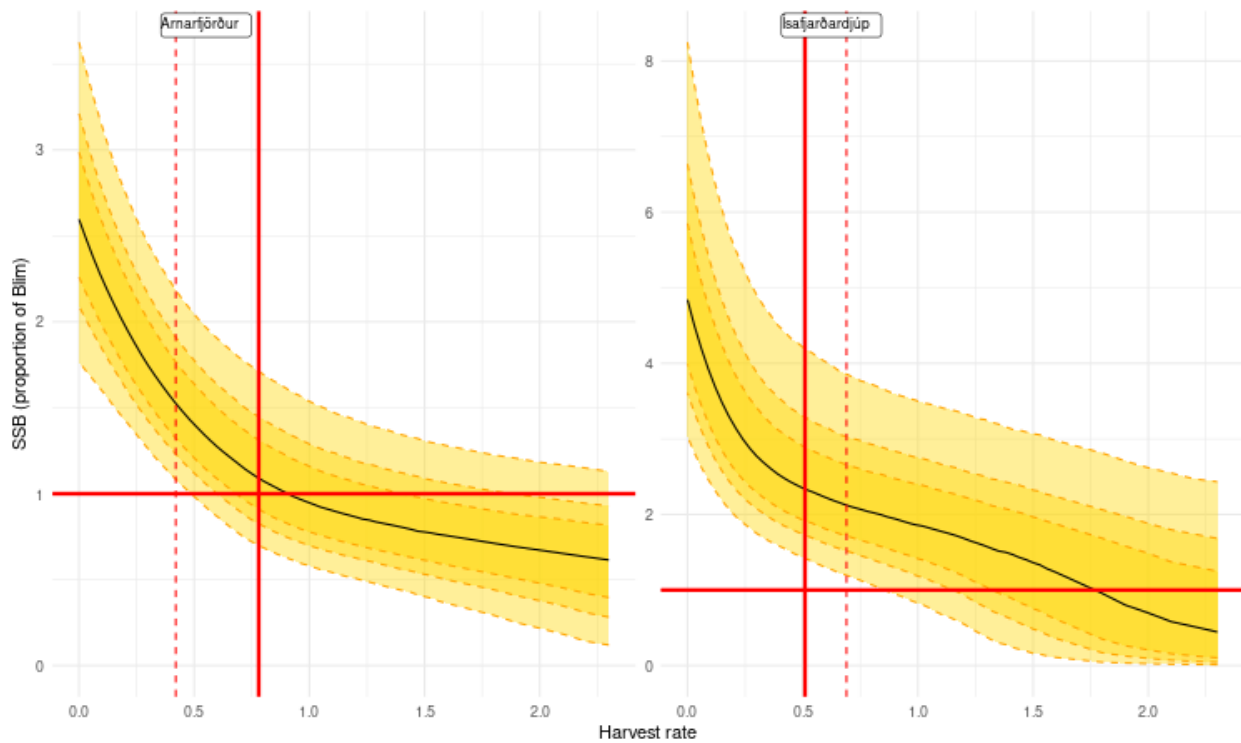


Figure 69: Equilibrium spawning stock biomass curves of Northern shrimp in Arnarfjörður and Ísafjarðardjúp according to 10 base models, shown as a function of  $H$ , under status quo predation and with the fishery closing below the implemented survey index limit. The index trigger is set at 125% of the current level. The black solid curves indicate the median projected harvestable biomass and the shaded yellow regions the 25% – 75%, 15% – 85%, and 5% – 95% ranges.  $B_{lim}$  is shown by the red solid horizontal line, set as minimum spawning stock biomass level observed since 1989, and set to as  $B_{loss}$  in the hockey stick recruitment function. The solid red vertical lines indicate harvest rates producing maximum yield in the long term. The dashed red vertical lines indicate the harvest rates below which the population dropped below  $B_{lim}$  over 5% of the time, and the solid red vertical lines indicate the harvest rates that generate maximum yield. Therefore,  $H_{msy}$  is represented by the red dashed line for Arnarfjörður and the red solid line for Ísafjarðardjúp.



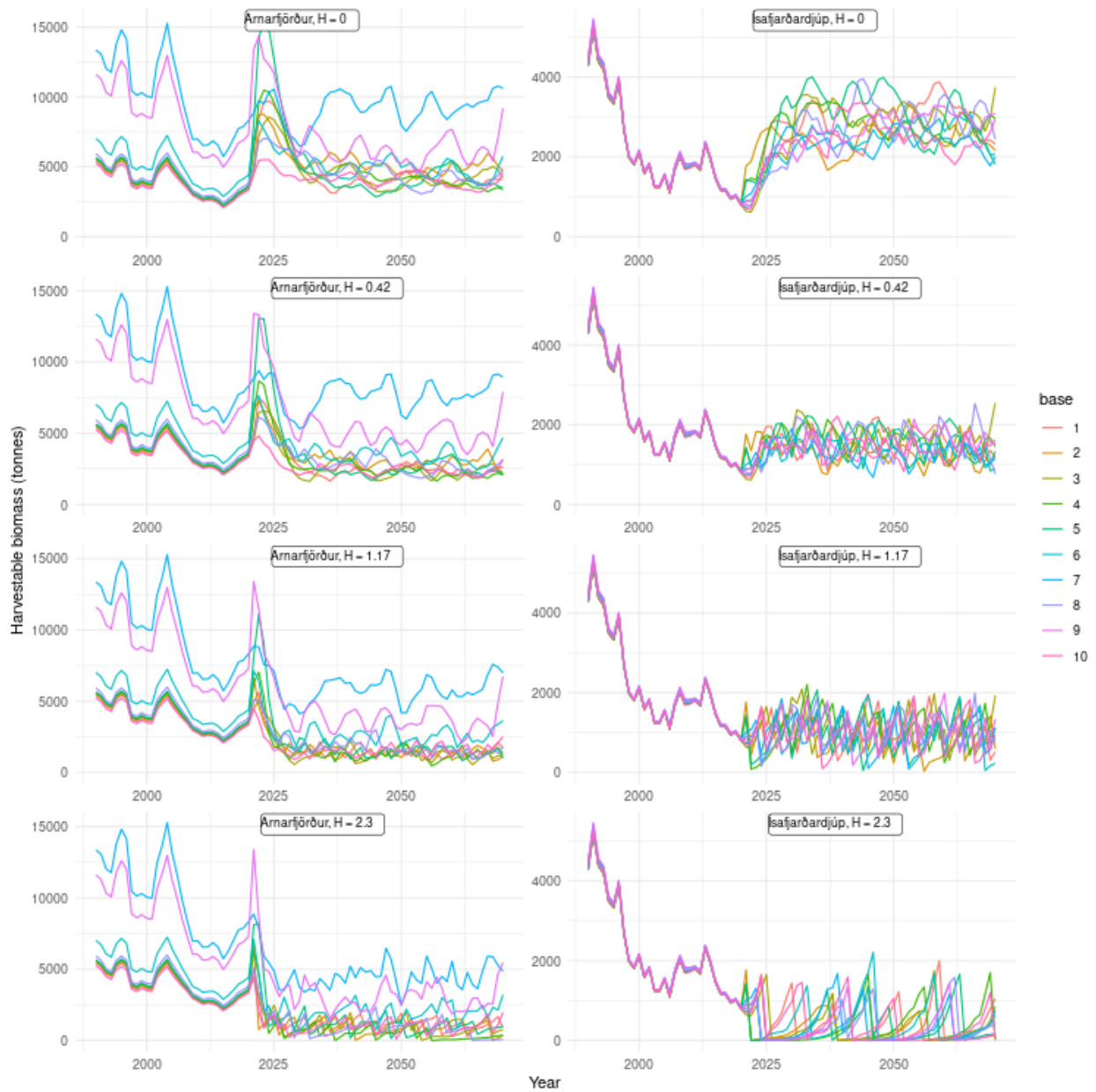


Figure 70: Results of harvestable biomass levels from a single simulation used as an example from each of the 10 base models (indicated by color) under status quo predation. Harvest rate is indicated by  $H$ . All colors overlap during the base model years, but uncertainty implemented in recruitment and management procedures causes variability in future years. The index trigger is set at 125% of the current level. All simulations show slight population growth under no fishing ( $H = 0$ ) versus a rapid decrease under high fishing rates.



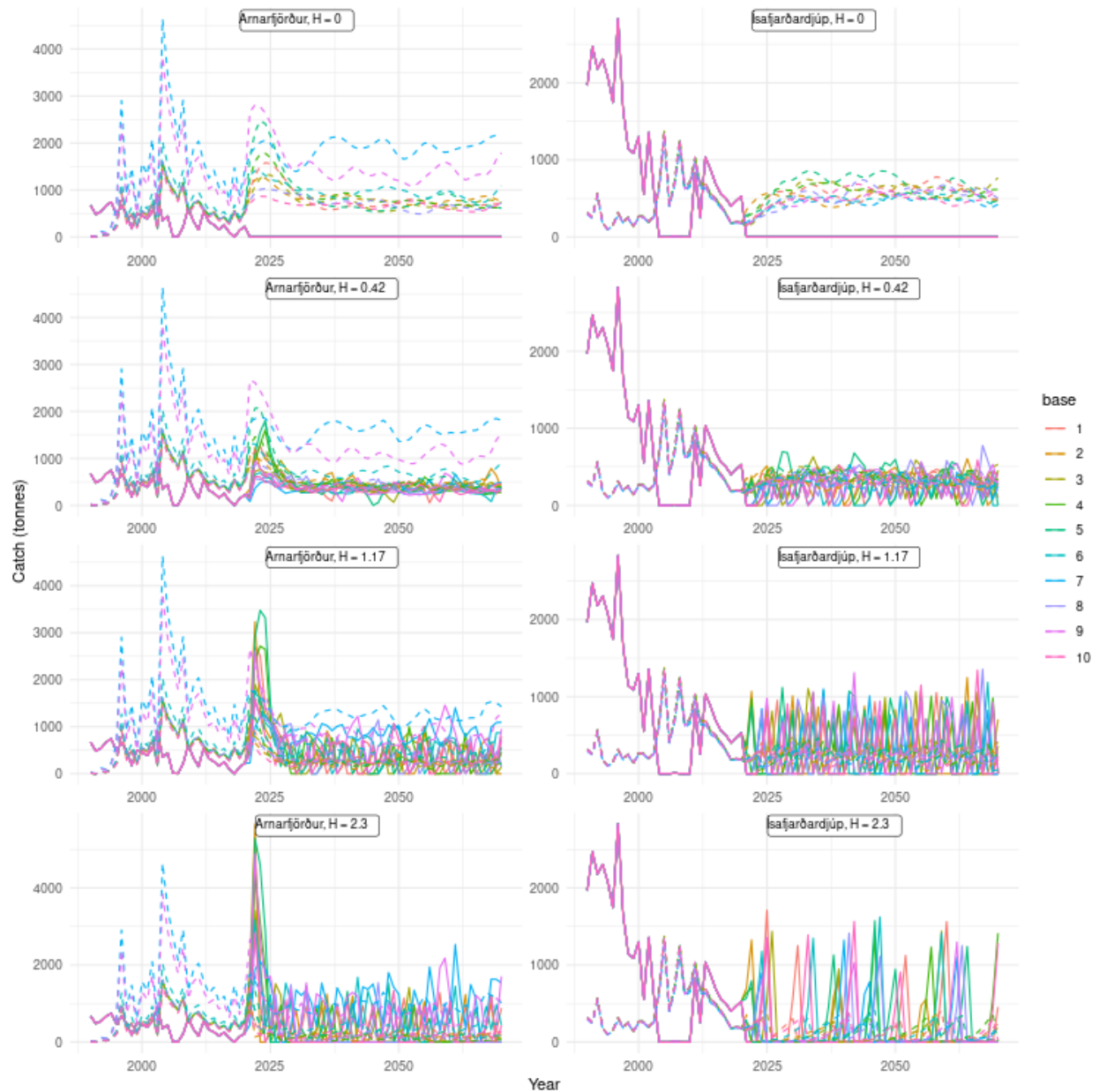


Figure 71: Results of catch (solid) and predation (dashed) levels from a single simulation used as an example from each of the 10 base models (indicated by color) under status quo predation. Harvest rate is indicated by  $H$ . Note that predation levels scale with biomass levels across base models. The index trigger is set at 125% of the current level. All colors overlap during the base model years, but uncertainty implemented in recruitment and management procedures causes variability in future years. All simulations show high catch at intermediate harvest rates versus a rapid decrease under high fishing rates.

resulting  $H_{msy}$  value, which were all limited by the requirement to maintain SSB above  $B_{lim}$  with a 5% probability and had a smaller range across all trigger scenarios, from 0.76 to 0.24.

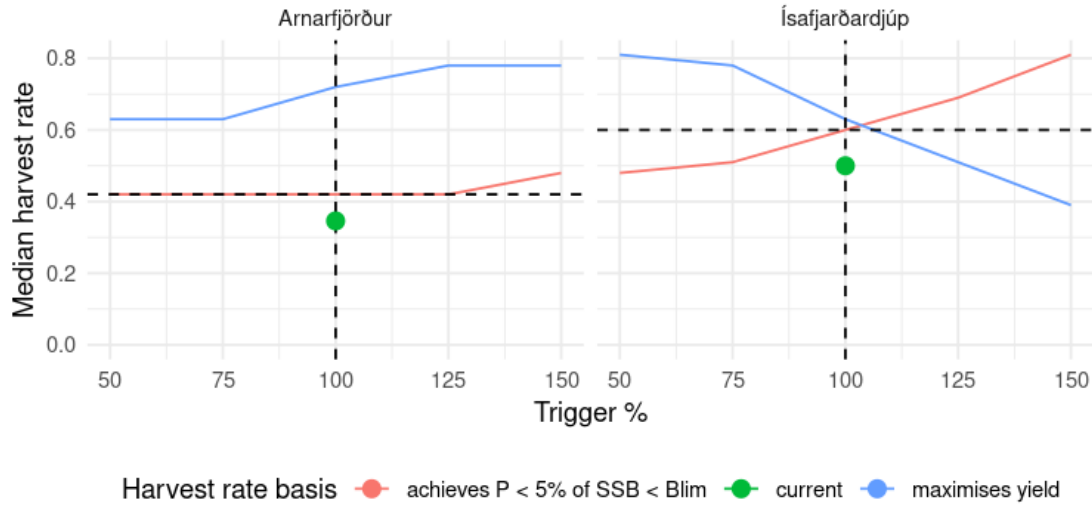


Figure 72: Relationship between index trigger level and median harvest rates that either reflect the maximum harvest rate that can also achieve a spawning stock biomass that does not drop below a level with increased risk of recruitment impairment ( $P < 5\%$  of  $SSB < B_{lim}$ ) or harvest rates that maximise yield. Five scenarios were explored where the index trigger values were set to 50%, 75%, 100%, 125%, and 150% of the current level. Vertical dashed lines show current trigger values (100%) and horizontal dashed lines indicate the median harvest rate at the 100% trigger value that achieves  $P < 5\%$  of  $SSB < B_{lim}$ . Green dots represent currently implemented values.

### 7.3.4 Relationships between trigger levels, yield and annual probability of fishery closures

The criteria discussed in the previous section facilitate adherence to ICES guidelines (ICES [7], ICES [8]); however, they are not necessarily all criteria that may be interesting to consider when deciding which harvest rate to implement. Here we present median yield and probabilities of fishery closures (i.e., the quota being set to 0) due to the index falling below the index trigger.

The evaluation of harvest rates under different trigger values indicate rather different outcomes for each location. In the case of Arnarfjörður, harvest rates considered acceptable for defining  $H_{msy}$  according to ICES guidelines were always defined as those providing an annual probability  $< 5\%$  of SSB exceeding  $B_{lim}$  across all trigger values implemented (red line in Figure 72). Changing the trigger value had little impact on the optimal harvest rate (red line in Figure 72), and this result was echoed when considering yield and the probability of the total allowable catch being set to 0: in both cases, implementing different trigger values had little effect (red lines in Figures 73 and 74). This lack of sensitivity to trigger value is likely to be an effect of highly variable recruitment estimates, as well as the lower absolute trigger value implemented in that location.

In the case of Ísafjarðardjúp, implementing  $H_{msy}$  can only be considered as target harvest rates when the trigger is set as a value  $> 100\%$  according to ICES guidelines (blue line right of 100% in Figure 72), as these are the only harvest rates both maximizing yield and providing an annual probability  $< 5\%$  of SSB exceeding  $B_{lim}$ . If the trigger value were instead decreased, harvest rates that achieved a 5% or less probability of SSB dropping below  $B_{lim}$  would limit the harvest rates to a slightly lower level (red line left of 100% in Figure 72). Yield corresponding to these options are substantially lower when the trigger value was increased (blue line right of 100% in Figure 73), but barely lower or at a similar level when the trigger was decreased (red line left of 100% in Figure 73). When trigger values either remained unchanged or decreased (red line at or left

of 100% in Figure 73), yield values were also very similar to those expected from today's decision rule with a harvest rate of 0.5 implemented (green dots). Therefore, the options of 1) maintaining today's implemented decision rule, 2) maintaining the same trigger value but increasing harvest rate to 0.6, or 3) reducing the trigger value by 25% - 50% while maintaining today's implemented harvest rate of 0.5 all generated roughly the same yield in Ísafjarðardjúp. However, the probability that an annual catch will be set to 0 due to the survey index dropping below the index trigger value is 5% - 8% lower for option 3) than options 1) or 2), yielding an additional potential benefit (Figure 73). On the other hand, maintaining the current decision rule in option 1) yields the additional potential benefit of a reduced probability (0%) of SSB dropping below  $B_{lim}$ , down from the 5% upon which the other 2 options are based.

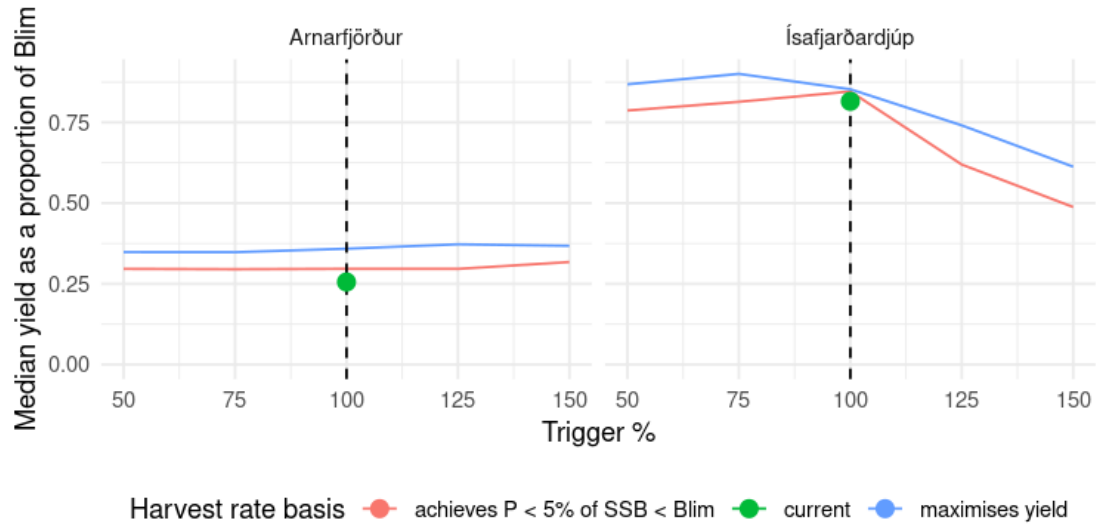


Figure 73: Relationship between index trigger level and median harvest rates that reflect the maximum harvest rate that can also achieve a spawning stock biomass that does not drop below a level with increased risk of recruitment impairment ( $B_{loss}$ ). Relationships are depicted by base model, 5 trigger scenarios set to 50%, 75%, 100%, 125%, and 150% of the current level. Vertical dashed lines show the status quo scenario values (100% predation level). Green dots represent currently implemented values.

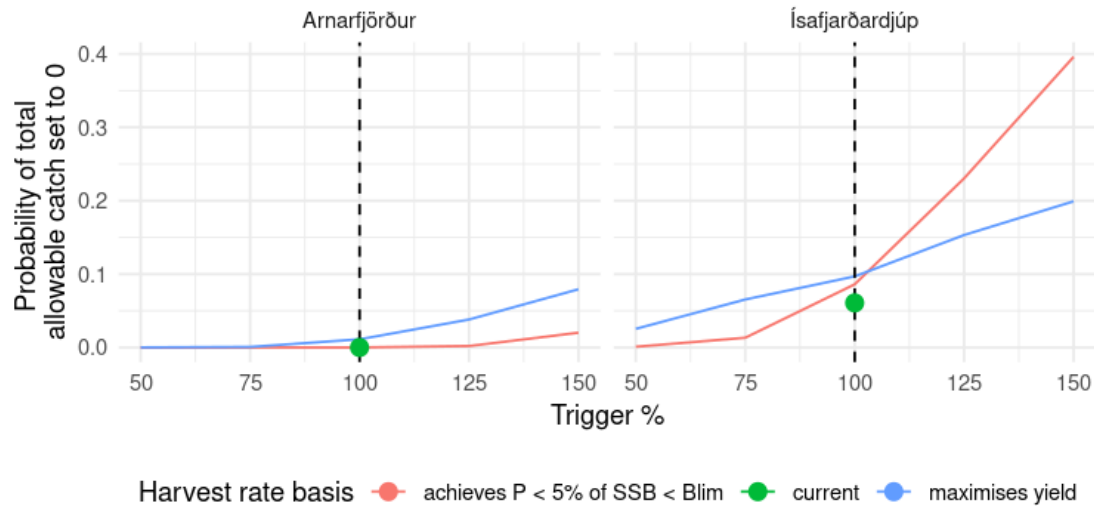


Figure 74: Relationship between index trigger level and probability of 0 catches resulting from the survey index falling below the trigger. Relationships are depicted by base model, 5 trigger scenarios set to 50%, 75%, 100%, 125%, and 150% of the current level. Vertical dashed lines show the status quo scenario values (100% predation level). Green dots represent currently implemented values.

## 8 Conclusions

Using analytical stock assessment models to assess invertebrate stocks is rarely done due to various problems (see *Introduction*), most notably those related to ageing invertebrates and accurately modeling somatic growth (molting). In this study, we used a length-based model to avoid the need for age data, and included extra flexibility in growth dynamics to allow the model to capture observed population dynamics. Although the models used were able to fit the data relatively well, they are nonetheless overparameterized, and therefore should not be taken as full statistical models. They do, however, present an opportunity to reflect on current management strategies used for fishing Northern shrimp in Arnarfjörður and Ísafjarðardjúp, support the choice of harvest rates in applied decision rules, and assess the impact of changing predation levels on management strategies.

According to these simulations, in Ísafjarðardjúp, the currently implemented harvest rate of 0.5 is slightly lower than that which would be chosen using ICES guidelines for defining  $H_{msy}$  (0.6) as the target harvest rate in a control rule as it is implemented currently with a pre-defined index trigger value of 604. Likewise, the currently implemented harvest rate of 0.346 is slightly lower than that which would be chosen using ICES guidelines for defining  $H_{msy}$  in Arnarfjörður (0.42) as the target harvest rate in a control rule as it is implemented currently with a pre-defined index trigger value of 390. However, these values are very sensitive to predation levels and, for Ísafjarðardjúp, also sensitive to the chosen index trigger value. A relatively small increase in predation (25%) causes an increase in the probability of spawning stock biomass dropping below a level expected to impair recruitment ( $B_{lim}$ ). This probability is a result of both predation, and naturally high variability in recruitment dynamics. As a result, an increase in future expected predation would require the definition of  $H_{msy}$  to decrease to (0.5), which is similar to the value implemented now (0.5). A similar value was also found to be appropriate for  $H_{msy}$  in the scenarios of considering different trigger values under status quo predation. In these cases,  $H_{msy}$  would be set to a value similar to the one implemented now if the implemented trigger value were either increased by 25% (to 0.51), or decreased by 25% (to 0.51). As yield levels were very similar between 0.6 and currently implemented harvest rates (Figure 73) there is little justification for considering an increase in harvest rate to 0.6 over the currently implemented harvest rate. That is, an increased harvest rate would increase the probability of SSB falling below  $B_{lim}$  and increase the probability of total catches being set to 0 due to the survey index dropping below the index trigger

value, with only a small long-term benefit in terms of yield. Reducing the trigger value to 75% its current value is a viable alternative to today’s implemented decision rule, as it would still satisfy ICES criteria for  $H_{msy}$  as a target, while reducing the probability of total catches being set to 0. This trigger value would also correspond with NAFO guidelines that indicated setting trigger index values as 15% of the mean of the highest 3 index values would be a sufficient strategy (04/12 [1]). The probability of SSB dropping below  $B_{lim}$  would increase in this case, but not enough to exceed ICES criteria of 5%.

In Arnarfjörður, results have little sensitivity to set trigger values, so there is little justification for considering an alternate trigger value. Harvest rates that satisfy ICES guidelines are generally higher at all trigger values than the implemented (Figure 72), but there is only a marginal increase in yield (Figure 73) and almost no difference in terms of the probability of the total allowable catch being set to 0 (Figure 74). Therefore, a slight increase in harvest rate could be considered as an alternative to the currently implemented decision rule, but there would be very little benefit in terms of yield, yet an increase in the probability of SSB dropping below  $B_{lim}$ , from (1.1%) to the ICES guidelines limit of 5%. Furthermore, a very small increase in predation was needed in Arnarfjörður to reduce the harvest rate deemed acceptable for defining  $H_{msy}$  to a level similar to the currently implemented harvest rate. Interpolating between the 100% and 125% predation levels, the increase is possibly closer to 10% than 25% as observed in Ísafjarðardjúp (Figure 63).

In conclusion, very little benefit was found for Arnarfjörður in terms of changing harvest rates or trigger values. The situation is slightly different for Ísafjarðardjúp, where there could be a benefit in terms of reduced probability of fishery closures if the trigger value is reduced by 25%. However, given that these ecological systems are highly uncertain and variable and there is a high amount of uncertainty in this modeling framework, it would be prudent to maintain a precautionary stance when choosing a decision rule. For example, simulations indicated that only a rather moderate increase in predation (to 125% current levels) resulted in a rather large decrease in  $H_{msy}$ . Past predation levels estimated by the models in both fjords have far surpassed those used in future projections (for example see Figures 54 and 62). In light of the high levels of predation and the linear relationship between predation levels and optimal harvest rates, it may be useful to be prepared for risks of future increases in predation levels, for example by designing decision rules that take into account an indicator of predation level (e.g., predator survey index) when setting the following fishing year’s TAC. Alternatively, harvest rates could be adjusted every few years according to recent mean predation levels experienced and the relationships given in Figure 63. Alternatively, multi-species and multi-step harvest control rules could be developed, as has been studied for a similar trophically linked system of cod, shrimp, and redbfish, as it was not possible to achieve the precautionary exploitation of all the stocks at the same time (Pérez-Rodríguez et al. [21]). At a minimum, this evaluation should be repeated in 5–7 year intervals to account for possible changes to the ecological system.

## 9 Acknowledgments

This study was partially funded by the Icelandic Research Fund under the grant titled “Fishing into the Future”, grant number 206967-052. We would also like to thank Dr. Guðmundur Þórðarson for generating the original inspiration for this project, and Dr. William Butler for reviewing the work and document.

## References

- [1] SCS Doc. 04/12. *Report of the NAFO Study Group on Limit Reference Points. Lorient, France, 15-20 April, 2004. Serial No. N4980.* Tech. rep. Northwest Atlantic Fisheries Organization, 2004, pp. 1–72.
- [2] Ástand nytjastofna sjávar og ráðgjöf 2022. *Shrimp in Arnarförður.* Tech. rep. Reykjavík, Iceland: Marine and Freshwater Research Institute, 2022.
- [3] Ástand nytjastofna sjávar og ráðgjöf 2022. *Shrimp in Ísafjörðurdjúp.* Tech. rep. Reykjavík, Iceland: Marine and Freshwater Research Institute, 2022.
- [4] Suman Barua, Gudmundur Thordarson, and Ingibjörg G Jónsdóttir. “Comparison of Catch and Survey Data for Assessing Northern Shrimp (*Pandalus borealis*) from Arnarfjörður (NW-Iceland) Using a Stock Production Model”. In: *Turkish Journal of Fisheries and Aquatic Sciences* 18.3 (2018), pp. 359–366.
- [5] Björn Björnsson et al. “Effects of cod and haddock abundance on the distribution and abundance of northern shrimp”. In: *Marine Ecology Progress Series* 572 (2017), pp. 209–221.
- [6] Haraldar Arnar Einarsson et al. *Bycatch in Icelandic offshore shrimp fishery.* Tech. rep. HV 2018-45. Reykjavík, Iceland: Marine and Freshwater Research Institute, 2018.
- [7] ICES ICES. *ICES fisheries management reference points for category 1 and 2 stocks. Technical Guidelines. In Report of the ICES Advisory Committee, ICES Advice 2021, Section 16.4.3.1.* Tech. rep. International Council for the Exploration of the Seas, 2021, pp. 1–19. DOI: <https://doi.org/10.17895/ices.advice.7891>.
- [8] ICES ICES. “ICES technical guidance for harvest control rules and stock assessments for stocks in categories 2 and 3”. In: (May 2022). DOI: 10.17895/ices.advice.19801564.v1. URL: [https://ices-library.figshare.com/articles/report%20ICES\\_technical\\_guidance\\_for\\_harvest\\_control\\_rules\\_and\\_stock\\_assessments\\_for\\_stocks\\_in\\_categories\\_2\\_and\\_3/19801564](https://ices-library.figshare.com/articles/report%20ICES_technical_guidance_for_harvest_control_rules_and_stock_assessments_for_stocks_in_categories_2_and_3/19801564).
- [9] Ingibjörg G Jónsdóttir. “Effects of changes in female size on relative egg production of northern shrimp stocks (*Pandalus borealis*)”. In: *Regional studies in marine science* 24 (2018), pp. 270–277.
- [10] Ingibjörg G Jónsdóttir. “Predation on northern shrimp (*Pandalus borealis*) by three gadoid species”. In: *Marine Biology Research* 13.4 (2017), pp. 447–455.
- [11] Ingibjörg G Jónsdóttir, Haakon Bakka, and Bjarki T Elvarsson. “Groundfish and invertebrate community shift in coastal areas off Iceland”. In: *Estuarine, Coastal and Shelf Science* 219 (2019), pp. 45–55.
- [12] Ingibjörg G Jónsdóttir, Höskuldur Björnsson, and Unnur Skúladóttir. “Predation by Atlantic cod *Gadus morhua* on northern shrimp *Pandalus borealis* in inshore and offshore areas of Iceland”. In: *Marine Ecology Progress Series* 469 (2012), pp. 223–232.
- [13] Ingibjörg G Jónsdóttir, Árni Magnússon, and Unnur Skúladóttir. “Influence of increased cod abundance and temperature on recruitment of northern shrimp (*Pandalus borealis*)”. In: *Marine biology* 160.5 (2013), pp. 1203–1211.
- [14] Ingibjörg G Jónsdóttir, Guðrún G Thórarinsdóttir, and Jónas P Jonasson. “Influence of decreased biomass on the ogive of sex change of northern shrimp (*Pandalus borealis*)”. In: *ICES Journal of Marine Science* 75.3 (2018), pp. 1054–1062.
- [15] Ingibjörg G Jónsdóttir et al. *Growth of shrimp in Arnarförður and Ísafjörðurdjúp.* Tech. rep. HV 2019-01. Reykjavík, Iceland: Marine and Freshwater Research Institute, 2019.
- [16] Ingibjörg G Jónsdóttir et al. *Northern shrimp research in Icelandic waters, 1988-2015.* Tech. rep. HV 2017-007. Reykjavík, Iceland: Marine and Freshwater Research Institute, 2017.
- [17] M Jørgensen et al. “Introducing time-varying natural mortality in the length-based assessment model for the *Pandalus Borealis* stock in ICES Div. IIIa and IVa east”. In: *Scientific Council Research Meeting NAFO.* 14/066. Northwest Atlantic Fisheries Organization. 2014.
- [18] Raouf Kilada et al. “Feasibility of using growth band counts in age determination of four crustacean species in the northern Atlantic”. In: *Journal of Crustacean Biology* 35.4 (2015), pp. 499–503.

- [19] Assessment Reports MFRI. *Shrimp in Arnarfjörður*. Tech. rep. Reykjavík, Iceland: Marine and Freshwater Research Institute, 2022.
- [20] Assessment Reports MFRI. *Shrimp in Ísaförjörðurdjúp*. Tech. rep. Reykjavík, Iceland: Marine and Freshwater Research Institute, 2022.
- [21] Alfonso Pérez-Rodríguez et al. “Evaluation of harvest control rules for a group of interacting commercial stocks using a multispecies MSE framework”. In: *Canadian Journal of Fisheries and Aquatic Sciences* 79.8 (2022), pp. 1302–1320.
- [22] André E Punt, Malcolm Haddon, and Richard McGarvey. “Estimating growth within size-structured fishery stock assessments: What is the state of the art and what does the future look like?” In: *Fisheries Research* 180 (2016), pp. 147–160.
- [23] Andre E. Punt, TzuChuan Huang, and Mark N. Maunder. “Review of integrated size-structured models for stock assessment of hard-to-age crustacean and mollusc species”. In: *ICES Journal of Marine Science* 70.1 (Jan. 2013), pp. 16–33. ISSN: 1054-3139. DOI: 10.1093/icesjms/fss185. eprint: <http://oup.prod.sis.lan/icesjms/article-pdf/70/1/16/29147323/fss185.pdf>. URL: <https://doi.org/10.1093/icesjms/fss185>.
- [24] Petrún Sigurðardóttir and Ingibjörg G Jónsdóttir. *A summary of shrimp surveys in inshore areas from 1961*. Tech. rep. HV 2017-032. Reykjavík, Iceland: Marine and Freshwater Research Institute, 2017.
- [25] Unnur Skúladóttir. “Comparing several methods of assessing the maximum sustainable yield of *Pandalus borealis* in Arnarfjörður [Iceland]”. In: *Rapports et Proces-Verbaux des Reunions* (1979).
- [26] G. Stefánsson. “Growth models in population simulations”. In: *Final Report:  $dst^2$ : Development of structurally detailed statistically testable models of marine populations*. Vol. 118. Technical Report. Marine Research Institute, Reykjavik, 2005, pp. 73–83.
- [27] Gunnar Stefánsson. “Issues in multispecies models”. In: *Natural Resource Modeling* 16.4 (2003), pp. 415–437. ISSN: 1939-7445.
- [28] Gunnar Stefánsson and Ólafur K Pálsson. “Statistical evaluation and modelling of the stomach contents of Icelandic cod (*Gadus morhua*)”. In: *Canadian Journal of Fisheries and Aquatic Sciences* 54.1 (1997), pp. 169–181.
- [29] L. Taylor et al. “A simple implementation of the statistical modelling framework Gadget for cod in Icelandic waters”. In: *African Journal of Marine Science* 29.2 (2007), pp. 223–245.